1973

Excitation Of Nitrogen By Alkali Ions

Robert Ernest Mickle

NATIONAL LIBRARY OF CANADA

CANADIAN THESES ON MICROFILM

BIBLIOTHÈQUE NATIONALE DU CANADA

THÈSES CANADIENNES SUR MICROFILM

NL-101(1/66)

EXCITATION OF NITROGEN BY ALKALI IONS

by

Robert Ernest Mickle

Department of Physics

Submitted in partial fulfillment
of the requirements for the degree of
Doctor of Philosophy

Faculty of Graduate Studies
The University of Western Ontario
London, Canada

February 1973

ABSTRACT

Studies of the phenomena produced by the passage of a beam of energetic particles through a gas have contributed significantly to determining the fundamental interactions which occur between the target and incident particles. If in inelastic collisions, excitation processes are frequent, a detailed study of the resulting luminosity can be useful in determining the final states of the excited particles and thereby obtain an insight into the interactions involved. For molecular targets, part of the kinetic energy lost can be transferred to vibrational and rotational energy of the molecule as well as producing ionization and dissociation.

This thesis reports on the spectroscopic study of the excitation processes in nitrogen due to the passage of alkali ions at energies between 0.58 and 25 keV through the gas. Processes involving simple excitation, charge transfer, dissociation and vibrational and rotational excitation of the molecular ion have been studied.

Survey spectra of the luminosity produced in alkali ion - nitrogen collisions indicate that simple excitation of the ion becomes more significant as the mass of the ion increases. Dissociation of the molecule was prominent for all alkalis. Relative emission cross-section measurements normalized to previous electron on nitrogen data were made for several spectral features.

All cross-sections were found to increase monotonically in the energy range of 1-10 keV except the ^2P-nd^2D series of the alkalis which displayed a distinct structure over the same energy range.

Rotational and vibrational excitation of the molecular ion was studied by measuring the relative intensities of the rotational lines in the (0,0) and (1,1) bands of the First Negative System. Rotational excitation was found to be extensive at all energies investigated, to increase as the energy of incident ion decreased and to be ion dependent. Similar non-Boltzmann distributions were observed in both the zeroth and first vibrational levels of the molecular ion. In the same energy range, the vibrational excitation of the molecular ion increased monotonically as the energy decreased.

ACKNOWLEDGEMENTS

The author wishes to thank the Physics Department for making available the facilities of the department for this work.

He is indebted to the members of his Advisory Committee, and in particular to Dr. H.I.S. Ferguson and Dr. R.P. Lowe for their supervision and expert advice on the many experimental and theoretical problems encountered throughout.

A special thanks to Mr. I. Schmidt and Mr. E. Gaze who helped at several stages in refinements of the existing apparatus.

The writer wishes to express his gratitude to the National Research Council for the scholarship held by him during the period from 1969 to 1971. He is also thankful for the Ontario Graduate Fellowship held from 1971-1972.

TABLE OF CONTENTS

LIST OF ILLUSTRATIONS

LIST OF TABLES

CHAPTER I

INTRODUCTION

Collisions between charged particles and gas molecules play an important role in many natural phenomena; well known examples being aurora and meteor trails. Knowledge of the atomic and molecular interactions involved has come from both scattering experiments and optical spectroscopic studies. Various types of scattering experiments have been used to study intermolecular forces, energy exchange and particle transfer during collisions. Spectroscopic studies have been used to determine energies, angular momenta and other characteristics of the system. Because some form of interaction is required to produce an excited state, spectroscopy can also be a very useful approach to the study of inelastic scattering reactions which lead to photon emission from one or more of the reaction products.

Emission sources used for the spectroscopic study of collision processes include flames, discharges, flowing afterglows, shock tubes and beams. Of these, beam experiments such as the one reported here are the easiest to interpret since both the identity and physical parameters of the beam and its target can be determined. In particular, the target pressure can be kept low enough

that the excited species will emit before undergoing a collision so that the initial energy levels can be determined directly. With all other sources, the nature of the excitation mechanism is more difficult to determine since many species are present. An additional complication is that the pressures in these sources are usually such that the excited species undergo at least a few and in some cases many collisions before emitting so that it may become virtually impossible to determine the initial energy levels populated by the collision.

Two distinct processes can occur between a beam and target gas - elastic and inelastic collisions. In the former kinetic energy is conserved with the ion being scattered from its original path with an appropriate recoil by the target. In inelastic collisions, there is an interchange of translational and internal energy of the target and projectile which can lead to electronic, vibrational or rotational excitation of the target gas molecule or ionization or dissociation with simultaneous excitation. The purpose of the present study has been to investigate the rotational and vibrational excitation of the molecular nitrogen ion resulting from charge transfer or ionizing collisions with alkali ions.

Recent technological advances have made possible several sophisticated experiments from which detailed information of inelastic processes has been obtained.

Monoenergetic beams have been used in energy loss measurements of the incident beam to obtain relative cross-sections for inelastic processes as a function of laboratory scattering angle. However, with the energy resolution available, rotational excitation has not been clearly observed. Energy distributions of dissociation products have been used to infer particular channels through which dissociation occurs (Fournier et al (1971)). Photon - particle coincidence measurements (Wehrenberg and Clark (1971)) have clarified the dominant mechanism in certain excitation collisions. Much of the present experimental information on rotational excitation of molecules during collisions has been obtained from spectroscopic methods. Unlike the previous techniques, sufficient resolution is usually available to deduce the rotational and vibrational distributions directly.

During the past decade, rotational and vibrational excitation of N_2^+ has received considerable study. The most extensively studied collisions are those in which the projectiles are electrons. More recent experiments have included inert gas ions and atoms and alkali ions. Of the heavier ions, the alkalis are particularly suited to both experimental and theoretical study. Their electronic structure is such that they have the lowest first ionization potentials of all the elements so that beams of singly-ionized particles can be easily obtained

Monoenergetic beams have been used in energy loss measurements of the incident beam to obtain relative cross-sections for inelastic processes as a function of laboratory scattering angle. However, with the energy resolution available, rotational excitation has not been clearly observed. Energy distributions of dissociation products have been used to infer particular channels through which dissociation occurs (Fournier et al (1971)). Photon - particle coincidence measurements (Wehrenberg and Clark (1971)) have clarified the dominant mechanism in certain excitation collisions. Much of the present experimental information on rotational excitation of molecules during collisions has been obtained from spectroscopic methods. Unlike the previous techniques, sufficient resolution is usually available to deduce the rotational and vibrational distributions directly.

During the past decade, rotational and vibrational excitation of N_2^+ has received considerable study. The most extensively studied collisions are those in which the projectiles are electrons. More recent experiments have included inert gas ions and atoms and alkali ions. Of the heavier ions, the alkalis are particularly suited to both experimental and theoretical study. Their electronic structure is such that they have the lowest first ionization potentials of all the elements so that beams of singly-ionized particles can be easily obtained

from thermionic sources. Since the electronic structure of the singly-ionized atom has the same closed shell structure as the noble gases, the high second ionization potential makes the presence of double-charged ions in the beam unlikely (Maurer (1939)). Of the projectiles listed above, the alkali ions have consistently produced greater rotational excitation of the molecular nitrogen ion. However, considerable disagreement exists as to the final distribution of the rotational states.

At the University of Western Ontario, the first controlled beam studies of the luminosity produced in alkali ion-nitrogen collisions were those of Pleiter (1956). Pleiter's work was extended by Reeves (1957, 1959) who by increasing the beam current was able to make initial measurements on the rotational excitation of N_2^+ by alkali ions. An improved accelerator delivering beam currents up to 100 μa. enabled Lowe (1966) to observe the rotational states of N_2^+ in 3-10 keV alkali ion collisons. Boltzmann distributions were found to exist to the fortieth level of the upper state with the rotational temperature increasing above 900°K with decreasing ion energy. Wink (1970) extended Lowe's work to higher rotational levels observing a non-Boltzmann distribution. He also obtained a relation whereby the rotational state populations could be determined directly without assuming a particular distribution as had been previously necessary (Wink et al (1971)).

Improved sensitivity now permits analysis to the hundredth level of the upper state. In this investigation, which forms the principal contribution of this thesis, the populations of the rotational states of the N_2^+ ion are determined for incident 0.6 - 10 keV Li^+ ions, 2.5 - 25 keV Na^+ ions and 4. - 7. keV K^+ ions. Simultaneous vibrational and rotational excitation of the first vibrational level by 4. - 10 keV Li^+ ions is also presented. In other experiments survey spectra of the luminosity from nitrogen excited by alkali ions were taken. Relative emission cross-sections of various spectral features normalized to electron on nitrogen data (Borst and Zipf (1970)) are also presented. Chapter II includes a brief examination of the theoretical treatment of vibrational and rotational excitation and a discussion of the factors which must be considered in controlled beam experiments. However the major part of this chapter reviews the results of previous experimenters indicating the conflicting results which exist in the reported data. Succeeding chapters cover the design and operation of the accelerator (Chapter III), survey spectra and emission cross-sections (Chapter IV) and rotational and vibrational studies involving nitrogen (Chapter V). General conclusions and recommendations are presented in the final chapter.

CHAPTER II

GENERAL THEORY AND HISTORICAL SURVEY

The principal concern of this thesis is the vibrational and rotational excitation of nitrogen during collisions with alkali ions. Since only spectroscopic techniques are used definite conclusions cannot be drawn as to the dominant mechanism of excitation. However, from recent experiments which are summarized in this chapter, trends emerge suggesting the more important processes involved. Factors which govern beam composition and luminosity produced by the passage of the beam through the gas are also discussed.

2.1 General Theory of Total Cross-sections.

In non-resonant inelastic collisions, the total excitation cross-section is characterized by three separate velocity regimes. Under gas-kinetic conditions when the colliding particles approach each other with a velocity (v) very small compared to the atomic electron velocity (u), a correspondence principle can be employed to show that the cross-section will be small unless ΔE, the energy defect, is also small. Because of the gradual character of the collision, the atomic electrons have sufficient time to readjust themselves to the slowly changing conditions without a transition taking place. In this case the impact

will be nearly adiabatic.

In the high velocity region, the behaviour of the cross-section for heavy particle excitation is similar to that for electrons of the same velocity. The Born approximation can be employed to show that ionization cross-sections decrease as v^{-2} while charge exchange cross-sections decrease very rapidly as v^{-12}. (Hasted (1964))

The third region, the velocity range in which this work was carried out, is the near adiabatic region. The most suitable theoretical method for calculating cross-sections in the near adiabatic region is the perturbed stationary state method. This method makes allowance for the gradual nature of the collision by treating the kinetic energy of relative motion as a perturbation and calculating the wave functions for a particular nuclear separation by regarding the nuclei at rest at that separation. During an infinitely slow collision, the atomic electrons adjust themselves in such a manner that no transition occurs, while a finite collision time leads to a finite probability of transition. However, the complexity of multi-electron colliding systems makes accurate wave functions unattainable so that cross-sections must be estimated using general approximations.

Despite the lack of quantitative theoretical calculations, some qualitative rules have enjoyed considerable success. Of particular importance is the adiabatic

criterion of Massey (1949). For a particular process, it is argued that the cross-section should rise, as ($a\Delta E/hv$) decreases, up to a maximum of the order of gas-kinetic cross-section when

$$\frac{a|\Delta E|}{hv} \simeq 1 \qquad (2.1)$$

where ΔE is the energy change in the collision and the duration of the collision is given by $^{a}/_{v}$ where a is the interaction distance for the reaction. At the velocity of maximum cross-section, the velocity of relative motion (v) is then comparable to the velocity of the atomic electrons concerned in the transition. Although the detailed variation of the cross-section in the near adiabatic region cannot be predicted, it is expected to increase as $\exp(^{-Ca|\Delta E|}/_{hv})$ with increasing velocity. The adiabatic theory therefore predicts that charge exchange reactions will have maxima at lower energies than ionization cross-sections due to the lower energy defect (ΔE).

Experimental verification of the exponential behaviour in charge exchange and ionization cross-sections was given by Hasted (1962). It was found that the peak cross-section occurred at a velocity corresponding to a value "a", the interaction range, of 7 angstroms. At lower velocities, the cross-section was found to have the form (Hasted and Bates (1962))

$$\sigma = C \exp\left(- \frac{a|\Delta E|}{4hv}\right) \qquad (2.2)$$

Similar features to those noted above are also observed in collision reactions leading to excitation (Dufay et al (1966)), with the probability of transition being greatest for those collisions in which total spin is conserved.

Due to the non resonant nature of the alkali-nitrogen collisions and the relatively small ionization potential of the alkalis, both

1) charge exchange with excitation

$$A^+ + N_2 \rightarrow A^{(*)} + N_2^{+(*)}(B^2\Sigma_u^+)$$

and 2) ionization with excitation

$$A^+ + N_2 \rightarrow A^{+(*)} + N_2^{+(*)}(B^2\Sigma_u^+) + e^-$$

may be significant in primary collision processes. Flaks, Kikiani and Ogurtsov (1966) have found in general that the ionization cross-section of N_2 by 1-30 keV alkali ions is about twice the charge exchange cross-section. However, the ionization cross-sections were suspected to be too high due to dissociative ionization which could not be discriminated against. Recent experiments (Latimer et al (1971)) have confirmed this suspicion for the ionization of N_2 by 5-42 keV Na^+ ions. Using a mass spectrometric analysis, the secondary ionic products were found to be

formed mainly by dissociative rather than by ionization processes. Ionization was found to be a factor of six lower than the total cross-section for the production of secondary ions. Normalizing the total cross-section of Flaks et al to that of Latimer for 10 keV Na^+ ions indicates that the ionization cross-section is a factor of three less than the charge exchange cross-section. To date no work has been undertaken to determine the relative significance of these two processes in forming the $N_2^+(B^2\Sigma_u^+)$ state in alkali ion processes. However, an indication of their importance may be otained from photon-particle coincidence measurements of charge transfer excitation of the $N_2^+(3914A^o)$ by protons (Wehrenberg and Clark (1971)). Previous work by de Heer et al (1966, 1970) has shown that the charge transfer (σ_c) and ionization (σ_i) cross-sections are about equal for 30 keV proton excitation ($\sigma_c = 53.4 \times 10^{-17} cm^2$, $\sigma_i = 53.4 \times 10^{-17} cm^2$). Coincidence measurements indicate that 66% of the excitations by 30 keV protons arise from charge transfer with the remainder from impact ionization.

The N_2^+B state can also be produced by the collision of secondary particles with the target gas. These may involve

1) ionization by fast neutrals

$$A + N_2 \rightarrow A + N_2^{+(*)}(B^2\Sigma_u^+) + e^-$$

2) ionization by secondary electrons

$$e^- + N_2 \rightarrow N_2^{+(*)}(B^2\Sigma_u^+) + 2e^-$$

Kikiani et al (1966) have found the total ionization cross-section of fast neutral alkalis on N_2 to be about twice the charge changing cross-section at the same energy. Charge changing cross-sections (Ogurtsov et al (1966)) and neutral stripping cross-sections (Kikiani et al (1966)) indicate an equilibrium fraction of 85% ions for 10 keV lithium ions so that neutral excitation may be an important factor in the excitation of N_2^+.

Work by Lowe (1966) has suggested that electrons are one of the main sources of secondary excitation. Cross-sections for electron impact excitation of the N_2^+ First Negative (0,0) band (Borst and Zipf (1970)) indicate a maximum of $1.7 \times 10^{-17} cm^2$ for 100 eV electrons. The cross-section falls quickly to half maximum at 30 eV in the low energy range and falls slowly according to the Bethe-Oppenheimer relation at higher velocities. In comparison, the emission cross-section of $N_2^+(0,0)$ for 2 keV Na^+ and K^+ ions is two orders of magnitude less being typically $5 - 10. \times 10^{-20} cm^2$ (Neff (1963)). To date, no experiments involving the energy of ejected secondary electrons from alkali ion-nitrogen collisions have been reported.

2.2 Vibrational Excitation

The laws governing the transfer of relative trans-

lational energy into vibrational energy of the nuclei of the target molecule has been the subject of many investigations.

Several experimenters (Philpot and Hughes (1964), Moore and Doering (1969)) have found that the vibrational population distributions of nitrogen ions formed in high velocity charge exchange interactions agree with those predicted from the application of the Franck-Condon principle. However, significant enhancement of higher vibrational states has been found for collisions of ions with velocities below 10^8cm/sec. At these lower velocities the strong interaction between the two colliding particles may last for times comparable to a vibrational period of the molecule. The perturbation is no longer applied "suddenly" as in the previous case so that the Franck-Condon principle is not expected to hold. A simple model has been proposed by Lipeles (1969) to explain the enhanced populations at the lower velocities. In it, the incoming ion is considered to polarize the neutral molecule, but after exchange the fast neutral atom has little effect on the molecular ion. By calculating the effect of this initial polarization on the ground state vibrational wave function and then taking the overlap integral with the unperturbed wave functions of the molecular ion, Lipeles has obtained reasonable agreement with observed distributions.

The adiabatic criterion of Massey for maximum cross-sections has been applied to the vibrational excitation of N_2^+ by Polyakova et al (1968, 1969). They have found maxima in the population ratio of the first to zeroth vibrational levels when the time of the interaction of the colliding particles becomes comparable to the vibrational period of the nitrogen molecule. From the maximum, the radius of action ($35A^o$) of the forces causing vibrational excitation of the N_2^+ ion was found to be much larger than the corresponding value ($7-8A^o$) for the forces acting in charge exchange processes.

A brief review given below of the experiments on vibrational excitation (Table 2.1) indicates the differences which still persist in this field. Measurements of the relative populations of v'= 0 and v'= 1 levels of the $N_2^+B^2\Sigma$ state excited by protons at energies greater than 10 keV (Philpot and Hughes (1964), Dufay et al (1966), Thomas et al (1968)) indicate that the ratio of the populations (N_1/N_0) is equal to the ratio of the Franck-Condon factors connecting the N_2 ground state with the N_2^+B state (Nicholls (1962)). However Fan (1956) reported a normal band intensity distribution in the First Negative system excited by 450 keV He^+, 205 keV H^+ and 120 eV electrons but an abnormal vibrational excitation by 150 keV He^+, 20 keV H^+ and 23 eV electrons. Polyakova et al (1967) found 30 keV H^+ gave an abnormal distribution while 10 keV H^+ gave a normal

TABLE 2.1

INVESTIGATIONS OF VIBRATIONAL EXCITATION OF N_2^+

Experimenters	Ion	Energy Range	Observed Band Sequence of N_2^+	Level Populations Calculated
Fan (1956)	$e^- + N_2$ $H^+ + N_2$ $He^+ + N_2$	23, 120 eV 20, 205 keV 150, 450 keV	$\Delta v = -2$ " "	v'=0,1,2
Philpot and Hughes (1964)	$H^+ + N_2$	5-130 keV	$\Delta v = 0, \pm 1, -2, -3$	v'=0,1
Sheridan and Clark (1965)	H^+, D^+, He^+ $Ne^+, N^+ + N_2$	10-65 keV	$\Delta v = 0, -1$	v'=0,1
Dufay et al (1966)	$H^+ + N_2$	0.15-1.0 MeV	$\Delta v = 0, \pm 1, -2, -3$	v'=0,1
Polyakova et al (1967)	H^+, H_2^+, He^+, C^+, N^+, O^+, Ne^+, N_2^+, $CO^+, Ar^+ + N_2$	5-30 keV	$\Delta v = 0, -1, -2$	v'=0,1
Polyakova et al (1968)	He^+, Li^+, Ne^+, Na^+, $Ar^+, K^+ + N_2$	0.7-30 keV	$\Delta v = -1$	v'=0,1
Thomas et al (1968)	$H^+ + N_2$	20-600 keV	$\Delta v = 0, \pm 1, -2, -3$	v'=0,1
Polyakova et al (1969)	He, Ne, Ar, Kr, Xe + N_2	5-30 keV	$\Delta v = -1$	v'=0,1
Moore and Doering (1969)	H^+, H_2^+, He^+, N^+, $Ne^+, e^- + N_2$	100 eV-13.5 keV	$\Delta v = -1$	v'=0,1,2,3
Haugh and Bayes (1970)	Ar^+, Kr^+ + HBr, HCl	2.5 keV	v'=i → v"=0 of HCl^+, HBr^+	v'=0,1,2,3,4

distribution.

For ion velocities less than 10^8cm/sec. all investigators have found ratios greater than those predicted by the Franck-Condon principle. For 5-30 keV He^+, C^+, O^+, N^+, Ne^+, Ar^+, Polyakova et al (1967) found a general increase in the ratio as the velocity of the ion decreased. Abnormal ratios were also observed for 0.7-30 keV Li^+, Na^+, K^+, He^+, Ne^+ and Ar^+ on nitrogen (Polyakova et al (1968)). He^+, Li^+, Na^+ and K^+ displayed maxima in the ratio at velocities of 2.5×10^7cm/sec. while Ne^+ and Ar^+ suggested a maximum shifted towards lower velocities. The vibrational excitation was also found to be ion dependent. Haugh and Bayes (1970) have obtained a similar result for 2.5 keV Ar^+ and Kr^+ ions on HCl and HBr with the vibrational excitation being a function of the energy defect as well. 5-30 keV inert gas atoms indicated that greater vibrational excitation of the N_2^+ molecule occurred for atomic collisions than for ionic impacts (Polyakova et al (1969)). Different results were obtained by Moore and Doering (1969) for 100 eV - 13.5 keV H^+, He^+, H_2^+, N^+, Ne^+ and electrons on N_2. At ion velocities greater than 10^8cm/sec., the relative band intensities were found to agree with those predicted by the Franck-Condon principle. Below this velocity, the relative populations of the $v'=0$ levels increased monotonically. The vibrational excitation was found to be solely dependent on the projectile laboratory velocity and independent of its chemical identity.

2.3 Rotational Excitation

Little theoretical work has been attempted to determine the rotational excitation of diatomic molecules by ions and atoms at velocities greater than gas-kinetic.

Using conservation of energy, momentum and angular momentum arguments, Lowe (1966, 1971) and Liu (1970) have shown that classically the angular momentum (ΔL) transferred to a molecule in "grazing" collisions is

$$\Delta L = \frac{b\Delta E}{v} \qquad (2.3)$$

where b is the impact parameter, ΔE the energy defect of the process and v the velocity of the approaching ion. An extension to this work by Lowe (1966) indicates that if the upper state is produced in a Boltzmann distribution, the rotational temperature of the distribution is given by

$$T=\left\{\frac{2\pi^2 cB}{hk}\right\} \frac{m\bar{b}^2(\Delta E)^2}{E} + T' \qquad (2.4)$$

where E is the energy of the incident ion (mass, m), B is the rotational constant of the molecule and T' is the gas temperature of the initial state. Rotational excitation of N_2^+ by 3-10 keV Li^+ ions indicated the linear behaviour with reciprocal energy giving a mean impact parameter (b) of 2.4A^o (Lowe (1966)).

Theoretical models of the distribution of angular momentum changes for the different levels of the molecule have been unable to explain the observed rotational excita-

tion. Results of Moore and Doering (1969) indicate that the probability of a transition with $|\Delta K|>1$ decrease exponentially with increasing ΔK. Unsuccessful attempts to synthesize the observed spectra using this model have led them to suggest that the transition probability is a function of the initial rotational level in addition to being a function of the change in angular momentum (ΔK).

Several investigators (Table 2.2) have spectroscopically studied rotational energy transfer during ion molecule collisions. In most experiments, nitrogen was the target gas and the v'= 0 level of the N_2^+ First Negative system was studied. In reactions for which rotational excitation was observed, the degree of excitation increased as the energy of the incident ion decreased in agreement with the classical theory (Liu (1970), Lowe (1966)).Polyakova et al (1968) have found the amount of rotational energy transferred and its distribution amongst the various rotational energy levels to depend on the identity of the incident ion for He^+ and Ne^+ ions at the same velocity. Moore and Doering (1969) observed no rotational excitation of N_2^+ at ion velocities greater than 10^8cm/sec. However for velocities below 10^8cm/sec., they found the excitation to high rotational levels to be a function of projectile ion velocity only. A similar result was obtained for C^+, N^+, O^+, and Ne^+ ions having velocities of 4×10^7cm/sec. (Polyakova et al (1967)). Atoms were found to give greater deviations from a Boltzmann distribution than the ions at

TABLE 2.2

INVESTIGATIONS OF ROTATIONAL EXCITATION OF N_2^+

Experimenter	Ion	Energy Range	Band Observed	Maximum K"
Carleton (1957)	$H^+ + N_2$	1-5 keV	(0,1)	20
Reeves and Nicholls (1961)	H^+, H_2^+, H_3^+ $Li^+ + N_2$	0.5-1.5 MeV 1-3 keV	(0,0) (0,1)	17
Sheridan and Clark (1965)	$H^+, D^+, He^+,$ $Ne^+, N^+ + N_2$	10-65 keV	(0,0) (0,1)	21
Lowe and Ferguson (1965)	$Li^+ + N_2$	3 keV	(0,1)	44
Lowe (1966)	$Li^+, Na^+, K^+,$ $Rb^+, Cs^+ + N_2$	3-10 keV	(0,0)	37
Polyakova et al (1966)	$H^+, H + N_2$	30 keV	(0,0), (0,1)	21
Polyakova et al (1967)	$H^+, H_2^+, He^+,$ $C^+, N^+, O^+, Ne^+,$ $N_2^+, CO^+, Ar^+ + N_2$	5-30 keV	(0,1)	21
Culp and Stair (1967)	$e^- + N_2$	19-300 eV	(0,0)	21
Polyakova et al (1967)	$e^- + N_2$	25-600 eV	(0,1)	21
Moore and Doering (1968)	$e^- + N_2$	30-300 eV	(0,0)	21

TABLE 2.2 (cont'd)

Experimenter	Ion	Energy Range	Band Observed	Maximum K"
Polyakova et al (1968)	He^+, Li^+, Ne^+, Na^+, Ar^+, K^+ + N_2	0.7-25 keV	(0,1)	21
Moore and Doering (1968)	H_2^+ + N_2	0.4-3 keV	(0,0), (0,1)	50
Moore and Doering (1969)	H^+, D^+, He^+, Ne^+, H_2^+, D_2^+, + N_2	0.6-10 keV	(0,0)	29
Polyakova et al (1969)	He, Ne, Ar, Kr, Xe + N_2	5-30 keV	(0,1)	21
Moran et al (1971)	CO^+ + Ar	5.5-13.5 eV	energy loss spectra for rotational excitation alone.	35
Lowe and Ferguson (1971)	Li^+ + N_2	3-10 keV	(0,0)	36

the same velocity (Polyakova et at (1969)).

Experimental observations using electron excitation have also been somewhat contradictory on the rotational distribution in the N_2^+B state. Boltzmann distributions at elevated temperatures were observed for electrons at energies less than 100 eV (Culp and Stair (1967)). The rotational temperature was found to increase non-monotonically below 100 eV with an apparent maximum near 50 eV, followed by a minimum near 25 eV and then rising to 350°K at 19 eV. Sheridan (1964) had previously observed a Boltzmann distribution for 40 eV electrons at a rotational temperature of 426°K. On the other hand, Moore and Doering (1969) found that from 30 eV upwards there was no significant departure from a Boltzmann distribution at ambient temperature. These latter experiments were carried out in a cooled collision chamber so that the slope of the Boltzmann plot to determine the rotational temperature was more sensitive to rotational temperature changes. Polyakova and co-workers (1967) found that the distribution deviated from Boltzmann at electron energies less than 100 eV. The degree of deviation increased as the electron energy decreased. Improved experimental technique was suggested as the reason for observing deviations in reactions for which previous observers had detected none. A correlation was also observed between the deviation from the Boltzmann distribution and the degree of deviation of the relative

population of the first vibrational level from the value computed from the Franck-Condon principle.

Disagreement has also appeared for collisions involving the heavier ions. Boltzmann distributions with rotational temperatures approximately equal to ambient have been reported by Carleton (1957), Sheridan and Clark (1965) and Reeves and Nicholls (1961) for H^+ at laboratory energies of 3 keV, 10-65 keV and 0.5-1. MeV respectively. On the other hand, Polyakova et al (1966, 1967) using H^+ in the energy range of 5-30 keV found that the intensities of the lines corresponding to higher K' values were greater than those corresponding to a Boltzmann distribution at gas temperature. Non-Boltzmann distributions in the N_2^+B state have been found for 0.4-3.0 keV H_2^+ ion excitation (Moore and Doering (1968)), for 0.6-10. keV H^+, D^+, He^+ and D_2^+ excitation (Moore and Doering (1969)) and for 5-30 keV H^+, H_2^+, He^+, C^+, N^+, O^+, Ne^+, N_2^+, CO^+ and Ar^+ bombardment (Polyakova et al (1967)). Both groups observed an increased deviation from a Boltzmann distribution as the ion energy decreased. Moore and Doering (1968) reported that the high rotational levels had a population distribution characterized by a temperature greater than 3000°K.

Room temperature Boltzmann distributions were observed for the bombardment of N_2 by D^+, He^+, Ne^+ and N^+ with laboratory energies from 10 to 65 keV (Sheridan and Clark (1965)), and by 1.5 MeV H_3^+ (Reeves and Nicholls

(1961)). Doering (1964, 1968) studying the reaction of He^+, N_2^+ and Ar^+ with N_2 found that for projectile velocities less than 2×10^8cm/sec., the rotational temperature increased from ambient to 650°K at ion velocities of 1×10^7cm/sec. This effect was independent of the nature of the ion, depending only on its velocity. Elevated rotational temperatures have also been observed in the reaction $Li^+ + N_2$ (Reeves and Nicholls(1961), Lowe and Ferguson (1965, 1971)). Using an improved analysis technique (Wink et al (1971)), Lowe and Ferguson (1971) found the rotational temperature to increase from 960 - 2500°K as the Li^+ laboratory energy decreased from 10 to 3 keV. Lowe (1966) also studied the effect of Na^+, K^+, Rb^+ and Cs^+ bombardment on N_2. As the Na^+ energy decreased from 10 to 6 keV, the rotational temperature increased from 2270°K to 3050°K. K^+ in the energy range 5-10 keV, and Rb^+ and Cs^+ in the energy range 6-10 keV produced temperatures only slightly higher than room temperature. However from a study of the intensity variation with target pressure secondary processes, suggested to be secondary electrons, were the dominant excitation processes in the K^+, Rb^+ and Cs^+ reactions. The observed rotational temperatures were therefore not characteristic of direct excitation by the primary ion.

2.4 Beam Content

As a beam of ions ($I^+(1)$) passes through a gas,

the beam will be partially neutralized by charge exchange (σ_c) and some of the neutralized atoms ($I^\circ(l)$) will be re-ionized (σ_i). The change of the ion content in the beam per unit length is

$$\frac{dI^+(l)}{dl} = -\sigma_c I^+(l)[N] + \sigma_i I^\circ(l)[N] \qquad (2.5)$$

where [N] is the number density of the target gas. Assuming the total beam content remains constant

$$I^+(0) = I^+(l) + I^\circ(l) \qquad (2.6)$$

equation (2.5) can be solved using (2.6) to give

$$I^+(l) = I^+(0)\left[\frac{\sigma_i}{\sigma_i + \sigma_c}\right]\left\{1 + \frac{\sigma_c}{\sigma_i}\exp(-(\sigma_i + \sigma_c)[N]l)\right\} \qquad (2.7)$$

In order that the beam consist mainly of ions, measurements are made close to the entrance of the collision chamber and at low pressures so that

$$(\sigma_i + \sigma_c)[N]l \ll 1 \qquad (2.8)$$

2.5 Excitation and Emission Cross-Sections

2.5.1 Target Molecules

Excitation of target molecules can be produced in primary collisions with beam ions or in secondary collisions with atoms. At pressures less than a few tens of millitorr, collisional de-excitation is negligible and

the processes of excitation and decay can be considered to take place in the same observation region. Neglecting cascading, the number of photons emitted per second in a beam element dl is

$$d\mathcal{J} = [N]\, I^{+}(l)\sigma_{+}(i)dl + [N]\, I^{\circ}(l)\,\sigma_{N}(i)\,dl \qquad (2.9)$$

where $\sigma_{+}(i)$ is the excitation cross-section to state (i) for primary processes and $\sigma_{n}(i)$ is the excitation cross-section for secondary processes. Neglecting the effect of re-ionization, the total number of photons emitted along a path of length (L) is

$$\mathcal{J} = I^{+}(0)\left\{\frac{\sigma_{+}(i)}{\sigma_{c}}\left(1-\exp(-\sigma_{c}[N]L)\right)\right\} + I^{+}(0)\sigma_{N}(i)\left\{[N]L - \frac{1-\exp(-\sigma_{c}[N]L)}{\sigma_{c}}\right\} \qquad (2.10)$$

When σ_{c} is small

$$\mathcal{J} = \sigma_{+}(i)I^{+}(0)[N]L + (\sigma_{N}(i)-\sigma_{+}(i))\left[\frac{I^{+}(0)\sigma_{c}[N]^{2}L^{2}}{2}\right] \qquad (2.11)$$

For primary collisions, therefore, the intensity is expected to vary with pressure in two distinct ways, depending upon the value of σ_{c}. For σ_{c} large, the emission intensity should be linear at low pressure and monotonically decrease at higher pressures according to the first term in equation (2.10). For σ_{c} small, the emission will be linear with pressure in accordance with the first term in equation (2.11). When both primary and secondary collisions are responsible for excitation of the particular

state, the emission versus pressure graph should have a monotonically increasing slope. When $\sigma_c[N]L$ is small, the behaviour will be a linear plus a quadratic curve as indicated by equation (2.11).

A careful distinction must be made between excitation and emission cross-sections. The former, usually derived in theoretical calculations, refers to the probability that one of the products of the collision is left in a certain excited state. The latter, usually obtained from experiment, refers to the probability that a collision produces the emission of a photon at a certain wavelength and is defined by (de Heer (1966))

$$\phi_{ij} = \sigma(ij)[N]IL \qquad (2.12)$$

where ϕ_{ij} is the number of photons of wavelength λ_{ij} emitted per second along the path length (L). If cascading is neglected, the two cross-sections can be related by

$$\sigma(ij) = \frac{A_{ij}}{\sum_{l<i} A_{il}} \sigma(i) \qquad (2.13)$$

where A_{ij} is the transition probability from state i to state j.

2.5.2 Beam Particles

When dealing with fast beam particles, the rate of emission at a position 1 in the collision chamber does not equal the rate of excitation at that point since the excited particles move relatively large distances before

emitting. Collisional deactivation (σ_d) must also be considered due to the distance travelled prior to emitting. Once again neglecting cascading effects, the total number of photons emitted per second along a distance 1 to 1 + L inside the collision chamber becomes

$$\mathcal{F} = \frac{A_{ij}[N] I^{+} L \sigma(i)}{v a} \left[1 - \frac{\exp(-a l)}{a L} (1 - \exp(-a L)) \right] \qquad (2.14)$$

where

$$a = \frac{\sum_{j<i} A_{ij}}{v} + \sigma_d[N]$$

and for simplicity the beam current I^{+} has been assumed constant along distance L. The condition for insignificant deactivation is that the mean free path

$$\frac{1}{\sigma_d[N]} \gg v\tau, \qquad (2.15)$$

the average distance along which the atom will radiate where τ is the radiative lifetime of the state. It is also apparent that the number of photons emitted per second along the path length L will be less than the number of atoms created in state (i) by the factor in the square brackets in equation (2.14). This is the correction factor representing the loss of light by the escape of radiating fast particles out of the observation region and by deactivation of excited atoms. When L is large, this effect is negligible but in order to obtain only primary collisions L must be small as indicated in equation (2.7).

CHAPTER III

EXPERIMENTAL EQUIPMENT AND TECHNIQUES

The apparatus for this experiment is basically the same as that used by Lowe (1966) and consists of three distinct sections: the anode chamber in which the ions are produced and focused; the collision chamber with its pressure and beam current monitors; the monochromator and associated photon counting equipment. Each section will be discussed separately in the remainder of the chapter with typical experimental parameters being given where applicable.

3.1 Ion Source

A thermionic source was used to produce the desired ions which were then accelerated and focused by an electrode configuration adapted from a design by Pierce (1940). A rectangular strip of platinum mesh (figure 3.1.a) precoated with an alkali carbonate, Al_2O_3-S_iO_2 mixture in the molecular proportions of 1:3:3 was mounted on high current high voltage vacuum lead-throughs in a slot of the hollow stainless steel lower cathode (figure 3.1.b). The upper electrode was mounted on three externally adjustable rods which were used to align the ion beam with respect to the entrance slit of the collision chamber and which were insulated from the lower electrode by sleeves of pyrex tubing. A slot of the same dimensions as the filament was

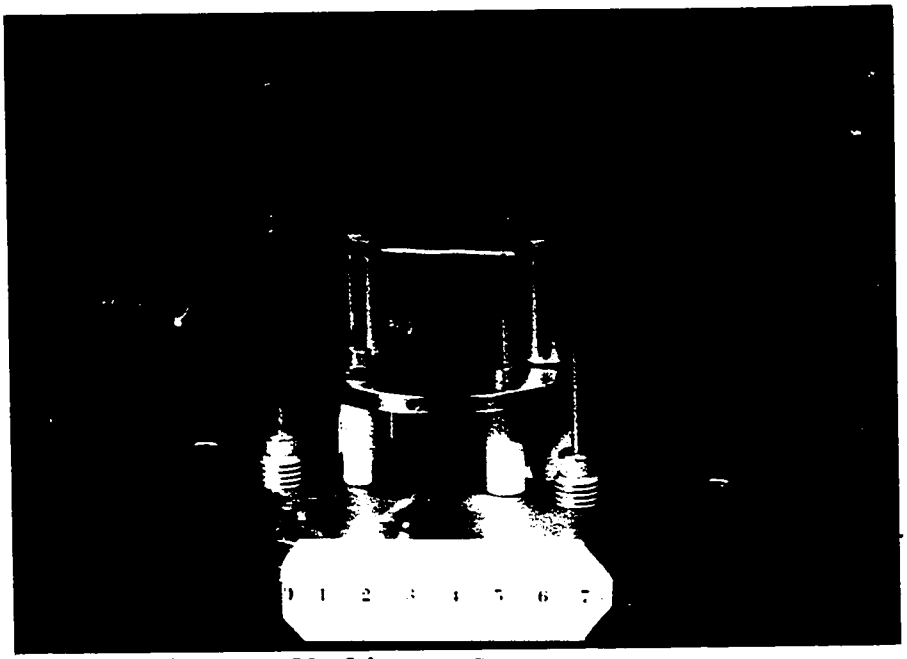

Figure 3.1.a. Alkali Ion Source
The filament can be seen clamped between two supports mounted on high-voltage feed-throughs.

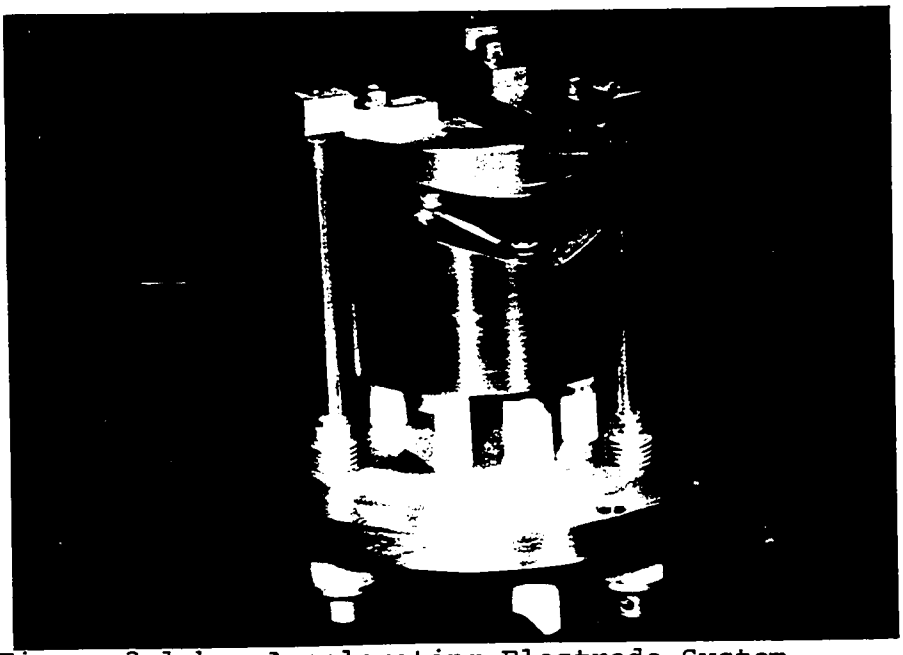

Figure 3.1.b. Accelerating Electrode System
The filament can be seen in the V-shape of the lower electrode. The upper electrode at ground potential is mounted on three externally adjustable rods.

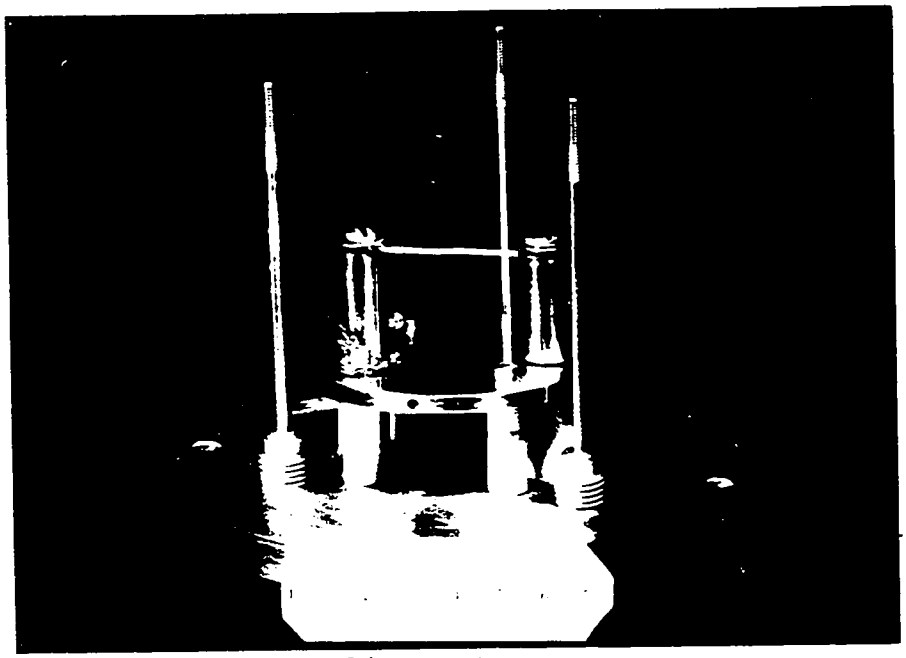

Figure 3.1.a. Alkali Ion Source
The filament can be seen clamped between two supports mounted on high-voltage feed-throughs.

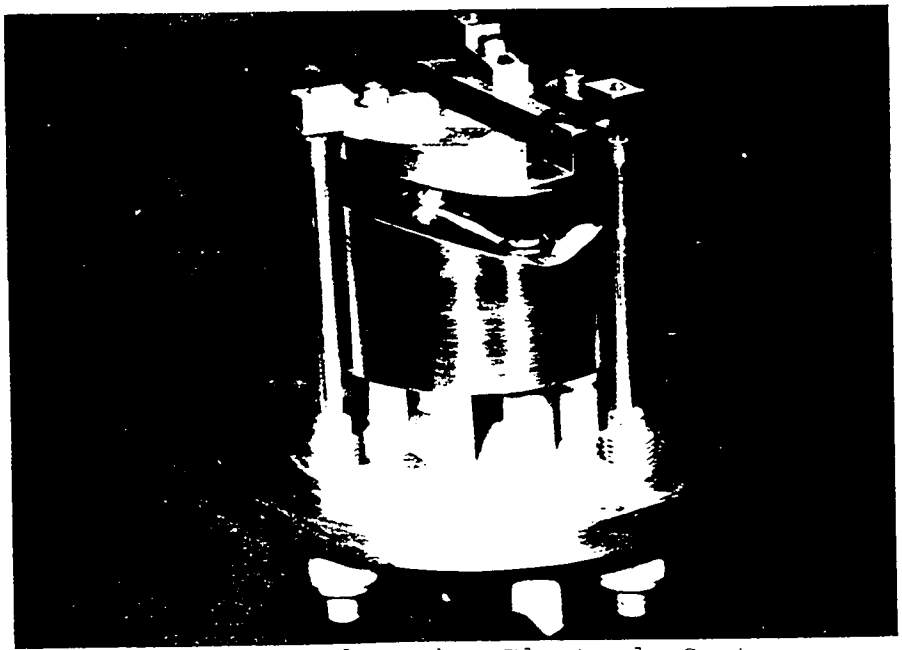

Figure 3.1.b. Accelerating Electrode System
The filament can be seen in the V-shape of the lower electrode. The upper electrode at ground potential is mounted on three externally adjustable rods.

provided in the upper electrode for the ions to pass through. The entire electrode system was attached to the base plate of the accelerator by standoffs.

In the accelerator (figure 3.2), the filament was heated with current from a transformer capable of supplying 50 amps at 6 volts A.C. Isolation between the primary and secondary of the transformer permitted operation to 30 kV. The accelerating voltage applied to the lower electrode was supplied by a 1-10 kV (Sorensen) voltage supply rated at 8 milliamperes output current. Manufacturer standards indicated regulation to 0.1% and 0.1% ripple. Filament currents up to 40 amperes were required to obtain 1-3 milliamperes of the desired ion. Focusing efficiencies of 1-10% produced beam currents up to 100 microamperes in the collision chamber for all alkali ions used in the present investigation.

3.2 Collision Chamber and Vacuum System

The collimated ion beam passed through an intermediate pumped chamber which was separated from the collision and anode chambers by slits 4 cm. long and externally adjustable in width from 0 to 2.5 cm. The slits served to collimate the beam and to maintain a pressure differential between the chambers. Both the anode and intermediate chambers were evacuated by a 2 inch diameter diffusion pump which was in turn backed by a single-stage-gas-ballasted rotary pump with a capacity of 450 litres per

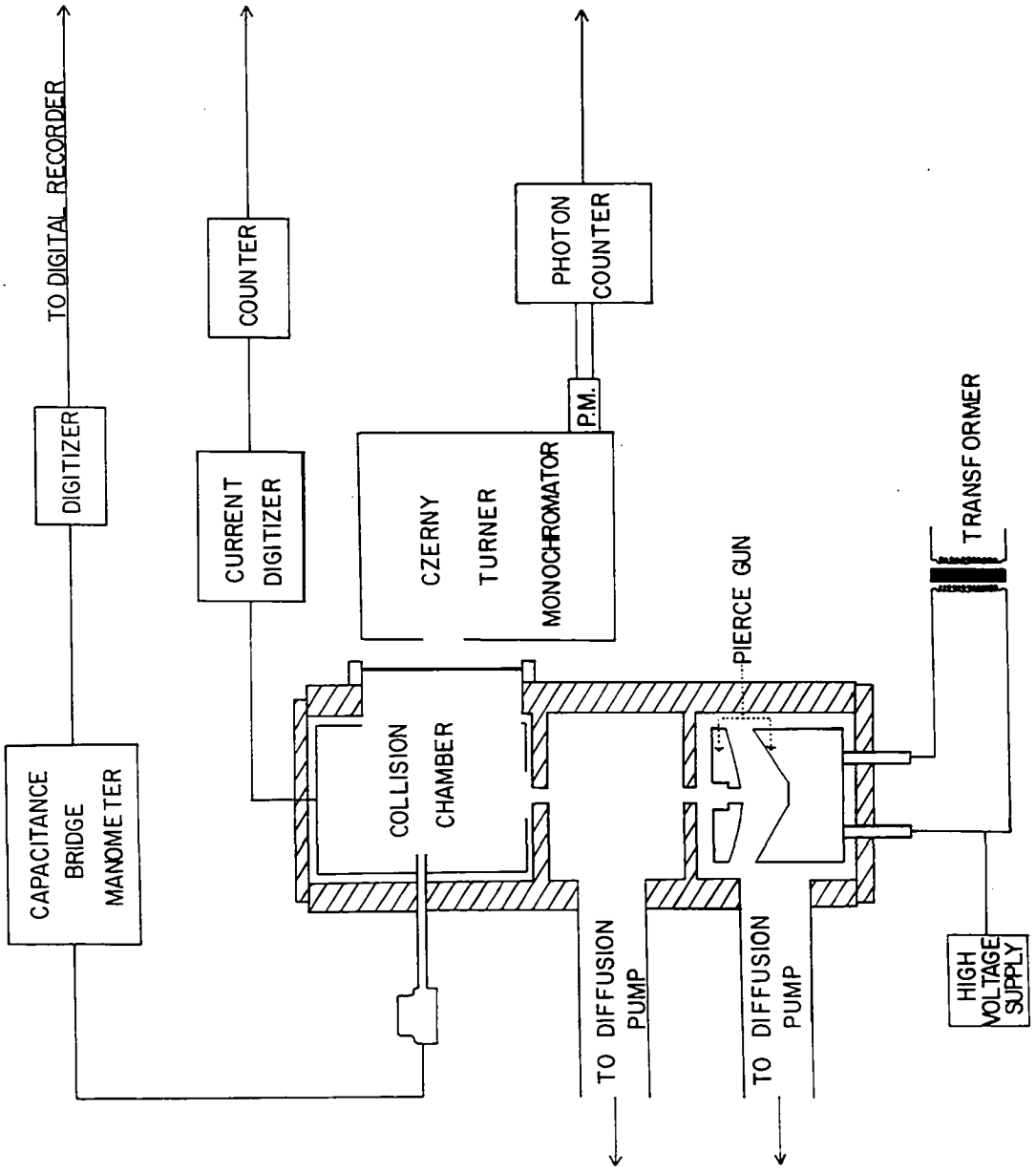

Figure 3.2 Schematic of accelerator and associated measuring equipment

minute. A pressure differential of 100:1 was usually maintained between the upper and lower chamber.

The observation chamber was completely isolated from ground so that all charge entering the chamber was collected, except that lost to the viewing port through which optical measurements were made. The beam current collected in the chamber was measured by a low input impedance current-digitizer capable of measuring currents from 1 nonoampere to milliamperes. The gas entered the collision chamber through a Hoke leak-valve. The pressure in the collision chamber, at the position where the optical measurements were made, was measured by a capacitance manometer (MKS Baratron - differential pressure head) capable of measurements from 0.1 millitorr to 1 torr. Experiments reported in this thesis were carried out at collision chamber pressures of 1-20 millitorr.

3.3 Optical Measurements

The first 5 cm. of the beam in the collision chamber were viewed through a quartz window and focused by a quartz lens onto the entrance slit of a $^3/_4$ - metre Czerny Turner double monochromator of aperture~f7. The monochromator was equipped with Bausch and Lomb replica gratings having 1200 lines per millimetre and blazed for 7200 A° in the first order. The lens was mounted a distance $2f$ from both the slit and the beam so as to give a 1:1 image at the slit entrance. Most optical measurements were

made in the second order where the instrument's dispersion is 2.7A° per millimetre. The photomultiplier of S-20Q spectral response (EMI 9558 QB) was cooled by nitrogen gas boiled from a liquid nitrogen dewar to reduce the dark counting rate. Typical dark count rates of 5 per second were observed in the cooled state. The voltage for the photomultiplier was obtained from a regulated 0 -2.5 kV voltage supply (Fluke). The photomultiplier pulses were shaped and amplified, the resulting signal being counted or integrated by a ratemeter. The analogue signal from the ratemeter was recorded on one channel of a ten inch dual channel chart recorder with the beam current as measured by the current digitizer on the other channel. When scanning a particular spectrum, the time constant of the ratemeter was set so as to give four time constants per time interval to cover one slit width.

CHAPTER IV

EXCITATION OF NITROGEN BY ALKALI IONS

In this chapter survey spectra of the optical emissions produced in alkali ion collisions with nitrogen are presented. In addition the changes in intensity of various spectral features with pressure and beam current are discussed. Finally relative emission cross-sections normalized to previous work are presented for various dissociation products and alkali lines. Their behaviour in the near adiabatic region is also discussed.

4.1 Survey Spectra

Survey spectra from 3500A° to 7000A° were taken for Li^+, Na^+ and K^+ ions incident on nitrogen. The spectra from 7000A°-5500A° were scanned at a rate of 15A° per minute in the first order and at 30A° per minute from 5500A°-3500A° in the second order. Filters were used to prevent overlapping from other spectral regions. The spectral slit width in both cases was 1A° with an appropriate change in recorder time constant to maintain the four time constants per slit width. The beam current was simultaneously recorded and varied by less than 10% during any particular spectrum. All survey spectra were taken at an ion energy of 8 keV and a target pressure of 5 millitorr. The line spectra were identified using Multiplet Tables (Moore (1959))

the M.I.T. Wavelength Tables (1939), and the wavelength tables in the Handbook of Chemistry and Physics (1961). The molecular bands were identified using the Identification of Molecular Spectra (Pearse and Gaydon (1963)).

4.1.1 $Li^+ \rightarrow N_2$

The spectrum observed for 8.0 keV Li^+ excitation of N_2 is given in figures 4.1.a and 4.1.b. Table 4.1 is an identification list for the spectrum with the multiplet numbers being those of Moore (1959).

The strongest features other than the $(0,0)N_2^+$ band are the Li I lines. As indicated by the energy level diagram in figure 4.2 the resonance line is observed as well as the ^2P-^2S and ^2P-^2D series. Although Li I 3915A° was not observed directly, the intensities of Li I 4132A° and Li I 3794.7A° indicate that Li I 3915A° would be sufficiently intense to affect any measurements made on the band head of the $N_2^+(0,0)$ band. As expected, no Li II lines are observed due to their high excitation potentials.

Many of the multiplets listed by Moore (1959) for N II are apparent. Lines with excitation potentials as high as 26 eV have been identified. On the other hand few N I lines are observed even though their excitation potentials of 14 eV are considerably lower than those for the N II lines.

The remaining strong features are those of the First Negative system of N_2^+. Sequences of $\Delta v=-1$ at

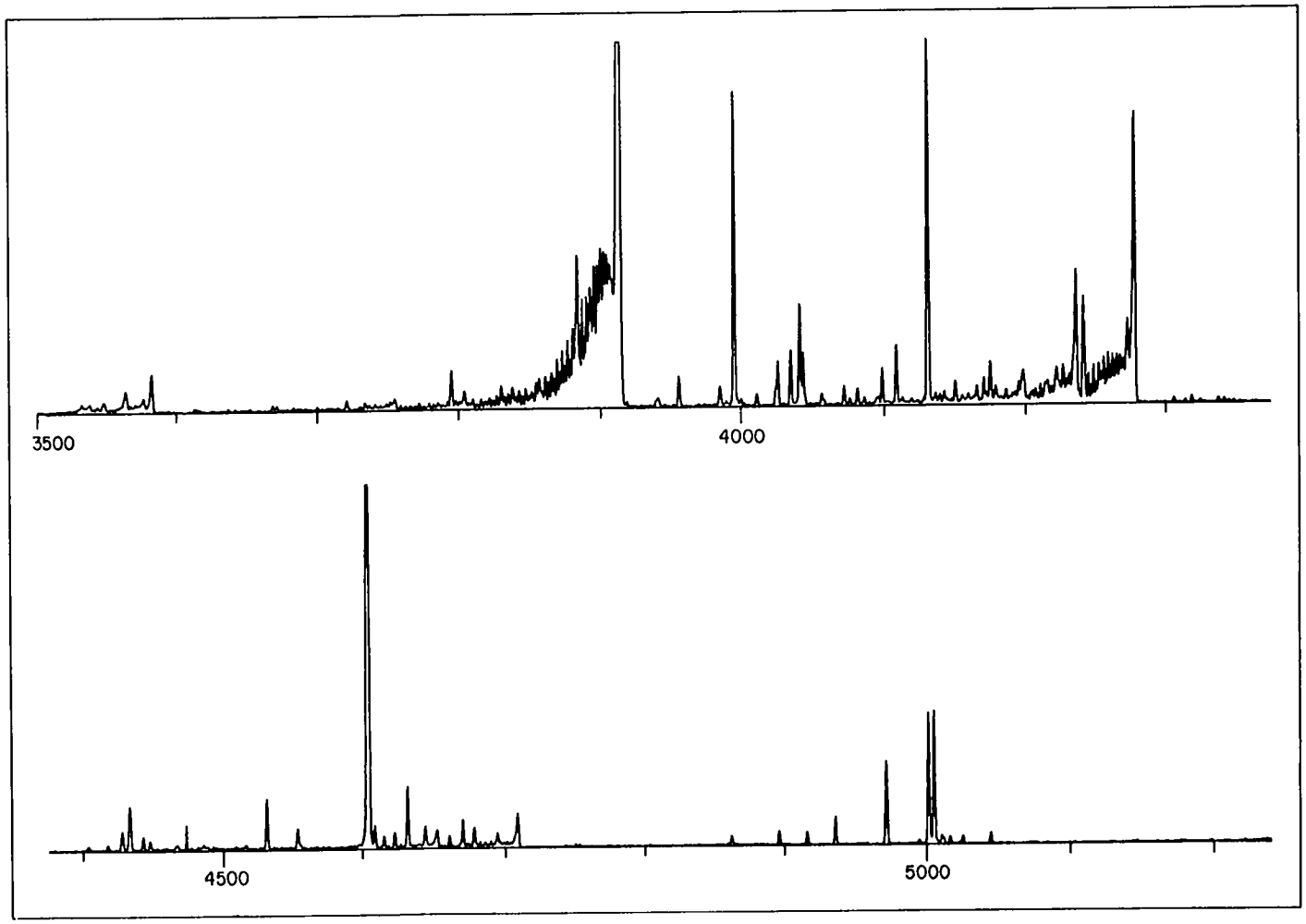

Figure 4.1.a Survey Spectrum, 3500A^{o} to 5200A^{o} for 8.0 keV Li^{+} excitation of N_2

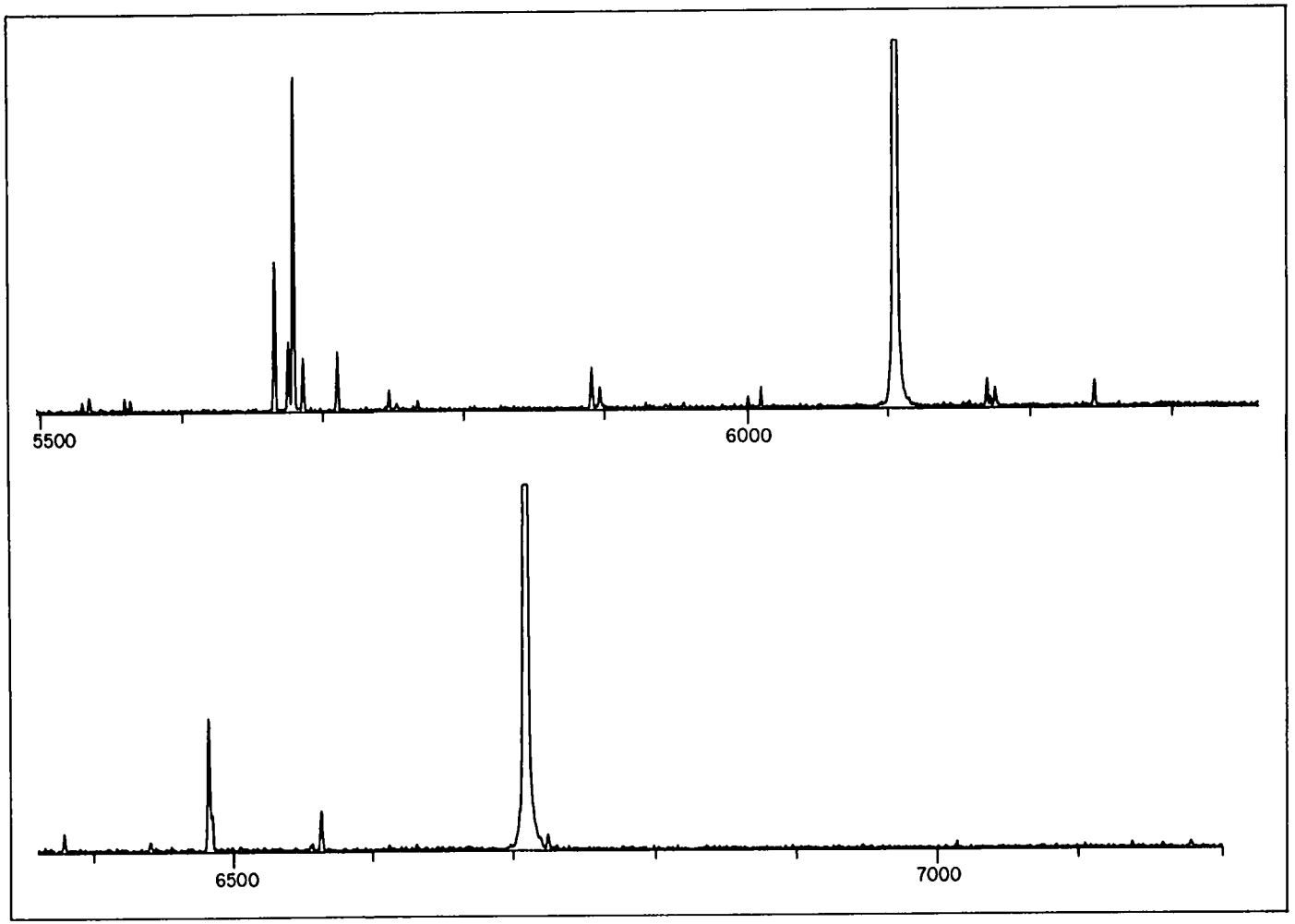

Figure 4.1.b Survey spectrum, 5500A° to 7200A° for 8.0 keV Li^+ excitation of N_2

TABLE 4.1

IDENTIFICATION LIST

SPECTRUM OF $Li^+ + N_2$

Emitting Species	Wavelength (Angstroms)	Multiplet Number	Emitting Species	Wavelength (Angstroms)	Multiplet Number
$N_2^+(1,0)$	3582.1		N II	4860.4	(67)
				4887	(24)
Li I	3718.7				
			N I	4914	
Li I	3794.7			4935.0	(9)
$N_2^+(1,1)$	3884.3		Li I	4971.9	
$N_2^+(0,0)$	3914		N II	5005	(19)
N II	3955	(12)		5666.6	
				5670.0	
Li I	3985.5			5679.6	(3)
				5686.2	
N II	3995	(6)		5710.8	
N II	4026.1	(40)	Na I	5889	
				5896	
N II	4035.1				
	4043.5	(39)	Li I	6103	
	4041.3				
			N II	6482.1	(8)
N I	4099.9	(10)			
	4110		H	6562.8	
Li I	4132.3		Li I	6707	
N II	4176.2	(42)			
	4237.0	(48)			
Li I	4273.3				
$N_2^+(0,1)$	4278.1				
N II	4432.7	(55)			
	4530.4	(59)			
Li I	4603				
N II	4630.5	(5)			
$N_2^+(0,2)$	4709.2				

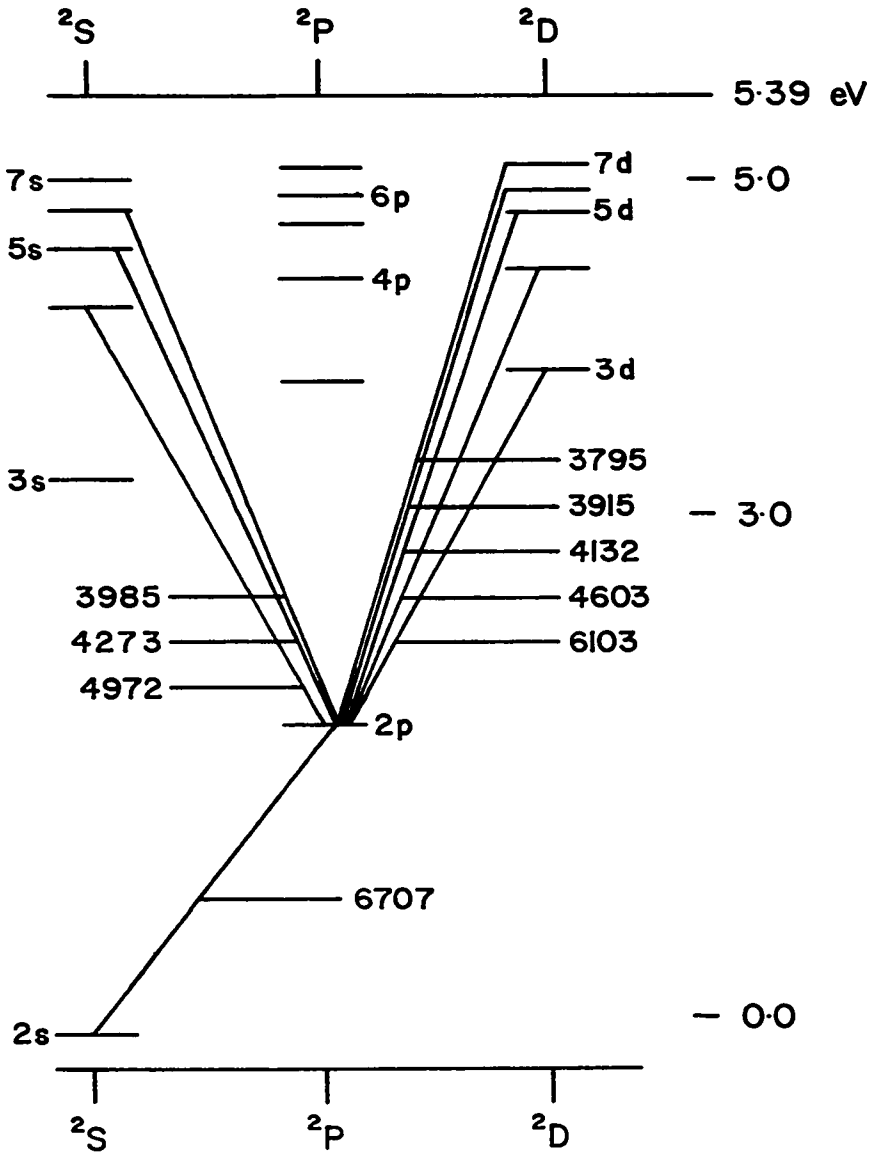

Figure 4.2 Energy Diagram for Li I
Observed transitions are indicated

4278.1A°, $\Delta v = 0$ at 3914A° and $\Delta v = +1$ at 3582.1 are observed. Due to the lack of momentum analysis, impurities such as Na are observed with the resonance lines at 5889A° being apparent. The only other feature of interest is the H line at 6562.8A° probably due to the dissociation of water vapour in the system.

4.1.2 $Na^+ N_2$

The spectrum observed for 8.0 keV Na^+ excitation of nitrogen is given in figures 4.3.a and 4.3.b with the identification list given in Table 4.2. As in the Li^+ excitation, the dominant feature is the NaD doublet. The ^2P-^2S and ^2P-^2D series are again observed as indicated in figure 4.4 but only from the 5 s level and up to the 5d level respectively. The lines below 3800A° are tentatively identified as Na II lines having excitation potentials greater than 36 eV.

Once again the same N II lines and N I lines obtained in Li^+ excitation are observed. Besides the lines indicated in figure 4.5 additional N II lines were observed as indicated by the dashed lines. The remaining features are N_2^+ bands of the $\Delta v = 0, \pm 1$ sequences. The increased rotational development of $N_2^+(0,0)$ from the 8.0 keV Li^+ case is apparent. Weak bands of the Second Positive system of N_2 at 3805A° and 3755A° suggest excitation by secondary processes.

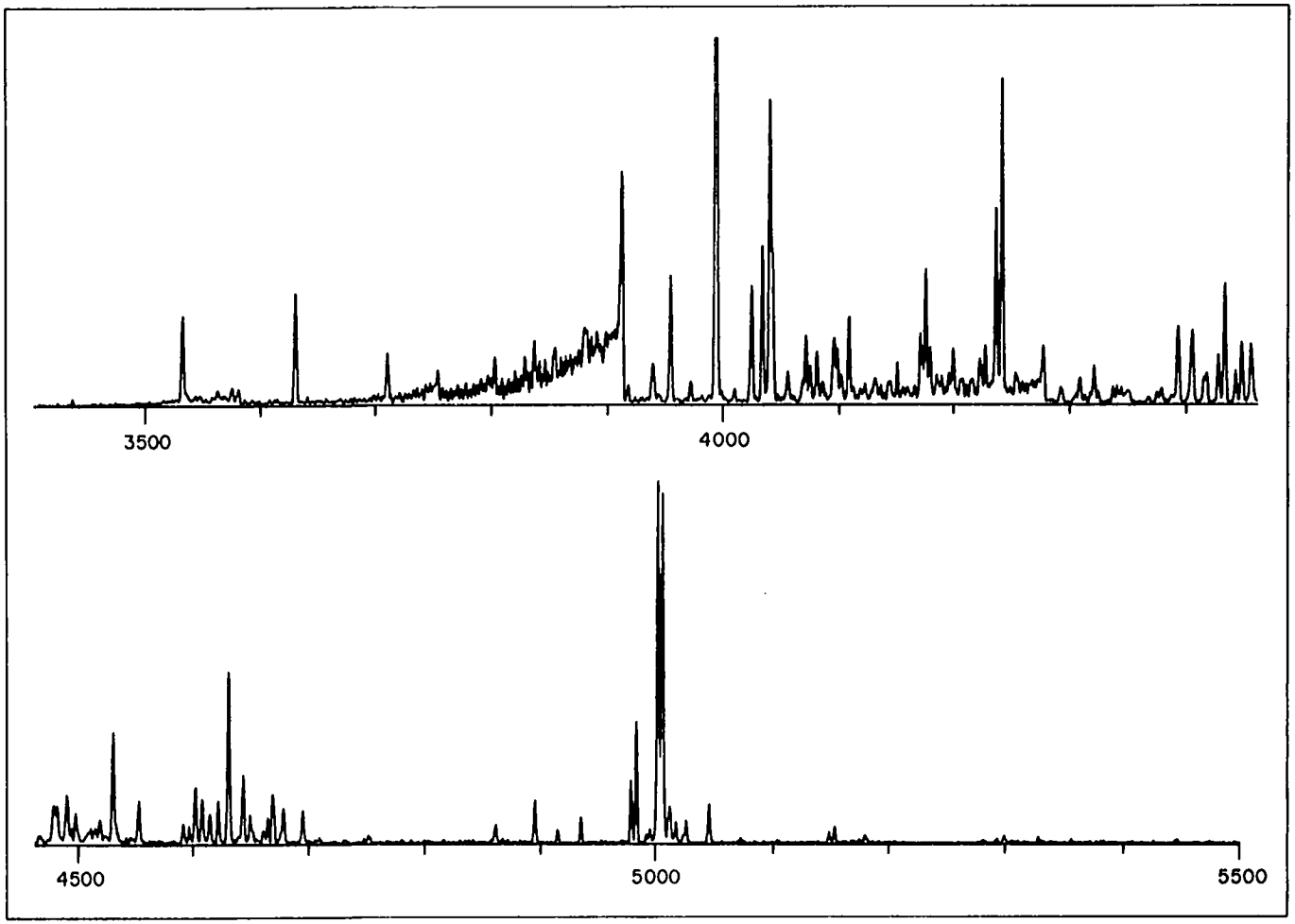

Figure 4.3.a Survey spectrum, 3500A^{o} to 5500A^{o} for 8.0 keV Na^{+} excitation of N_2

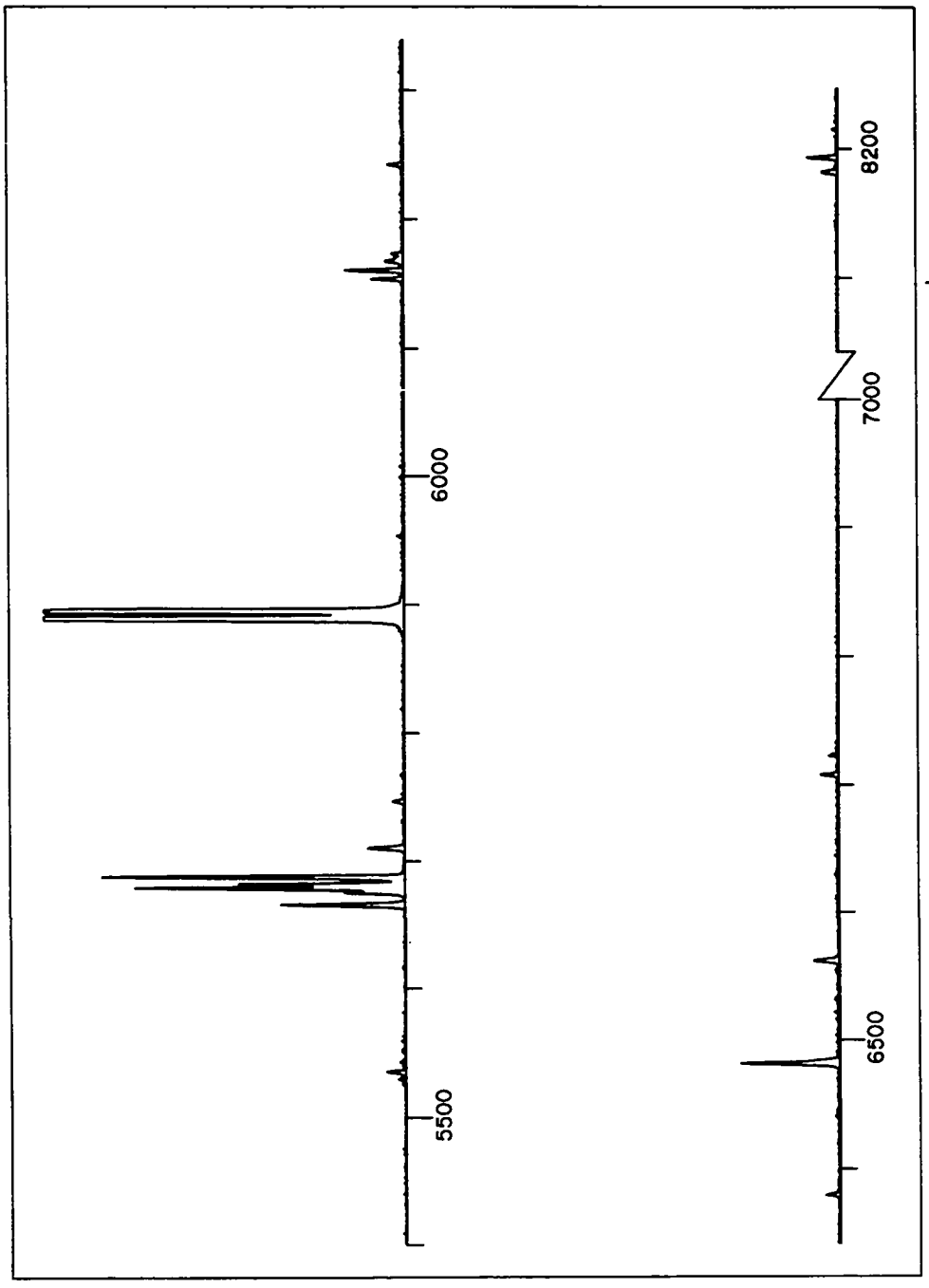

Figure 4.3.b Survey spectrum, 5400A° to 8200A° for 8.0 keV Na^+ excitation of N_2

TABLE 4.2

IDENTIFICATION LIST

SPECTRUM OF $Na^+ + N_2$

Emitting Species	Wavelength (Angstroms)	Multiplet Number	Emitting Species	Wavelength (Angstroms)	Multiplet Number
Na II	3533		N II	4552.5	(58)
	3631.3			4601.5	
	3711.1			4607.2	
				4613.9	(5)
N_2(1,3)	3755			4621.4	
				4630.5	
N_2 (0,2)	3804			4643.1	
				4654.6	(11)
N_2^+(1,1)	3884.3				
			Na I	4662.6	
N_2^+(0,0)	3914			4664.8	
N II	3919	(17)	N II	4667.3	(11)
	3955	(6)		4675.0	
	3995	(12)		4860.9	(67)
	4026.1	(40)		4887	(24)
	4035.1				
	4041.3	(39)	N I	4914	(9)
	4043.5			4935	
	4073				
	4076.8	(38)	Na I	4978.6	
	4082			4982.9	
	4095				
			N II	5001	(19)
N I	4099.9	(10)		5005	
	4109.9				
				5666.6	
				5670.0	
N II	4171.6	(43)		5679.6	(3)
	4176.2	(42)		5686.2	
	4237.0	(47)		5710.8	
	4241.8	(47)			
			Na I	5682.6	
N I	4253.3	(4)		5688.4	
N_2^+(0,1)	4278.1		Na I	5889	
				5896	
N II	4432.7	(55)			
	4447.0	(15)	Li I	6103	
	4477	(21)			
	4530.4	(59)	Na I	6160.7	
				6154.2	

TABLE 4.2 (cont'd)

Emitting Species	Wavelength (Angstroms)	Multiplet Number
N II	6242.5	(57)
	6379.6	(2)
	6482.1	(8)
H	6562.8	
Li I	6707	

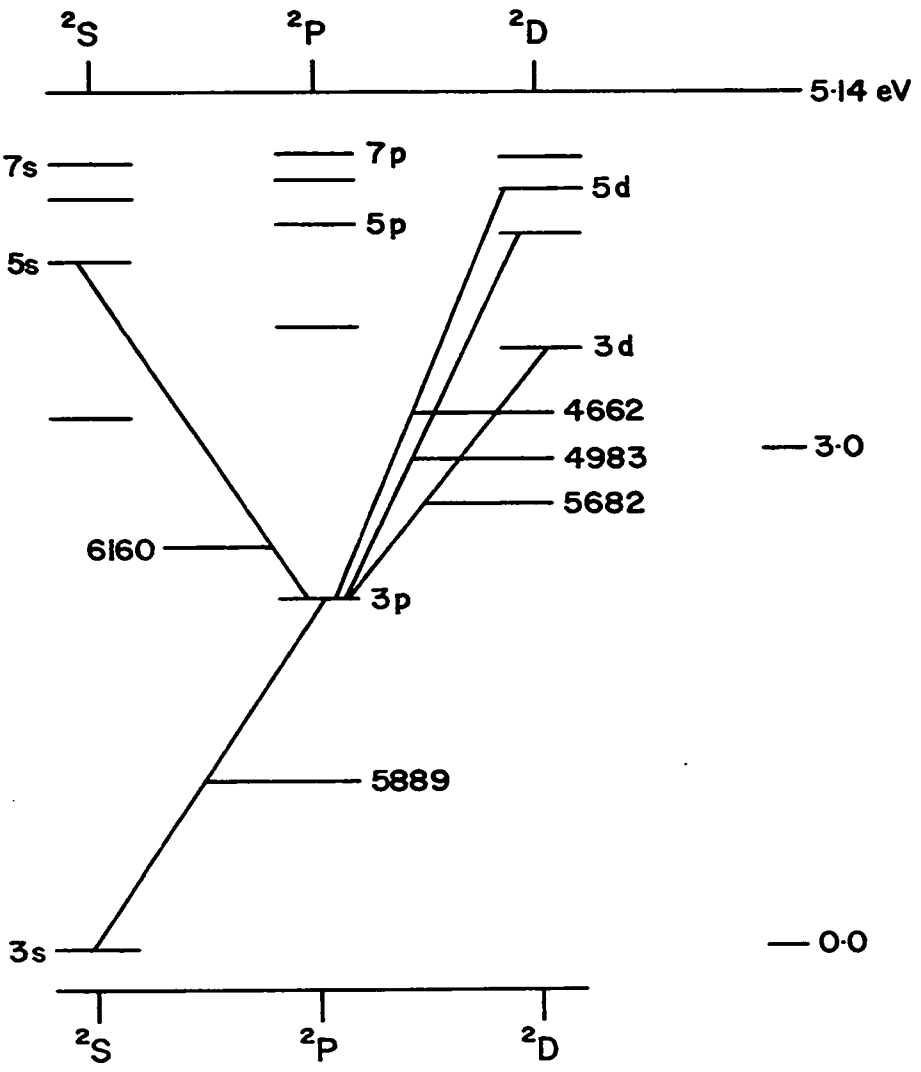

Figure 4.4 Energy Diagram for Na I
Observed transitions are indicated

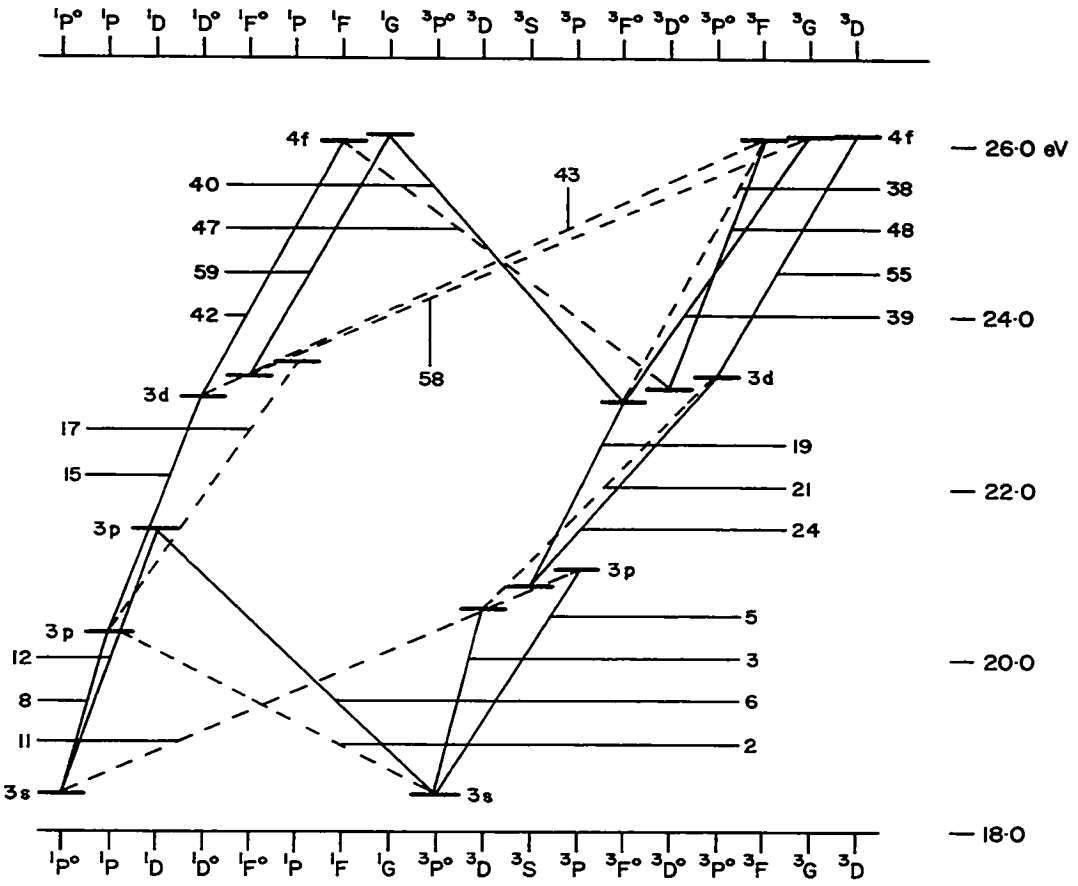

Figure 4.5 Energy Diagram for N II

Observed transitions are indicated. Multiplet numbers of transitions are given. (Moore (1959))

(——) observed in Li^+ and Na^+ excitation.
(---) observed in Na^+ excitation only.

4.1.3 $K^+ \rightarrow N_2$

The spectrum observed for 8.0 keV K^+ excitation of nitrogen is given in figures 4.6.a and 4.6.b with the identification list given in Table 4.3. The main features are the K II lines with excitation potentials in excess of 23 eV. The only lines due to K I are the doublets of the resonance series (4^2S-4^2P, 4^2S-5^2P). The ^2P-^2S transition is no longer observable while only one line of the ^2P-^2D series was observed.

The remainder of the lines are due to N II and N I but with intensities substantially less than the K II lines. The $N_2^+(0,0)$ band is apparent at 3914A° however the rotational development is significantly less than in the case of Na^+ excitation. The (0,2) and (1,3) bands of the Second Positive system of N_2 are observed as in the previous case suggesting secondary excitation processes.

4.2 Discussion of Survey Spectra

In the spectrum of N_2 excited by Li^+ ions, Li II lines were not observed while in the case of K^+ excitation, the spectrum was predominantly K II lines. According to Massey's adiabatic criterion, the observed K II lines requiring only 23 eV for their excitation in comparison to the Li II lines which require about 60 eV should be more prominent. In the case of Na^+ excitation, the long wavelength members of the first three Na II multiplets listed

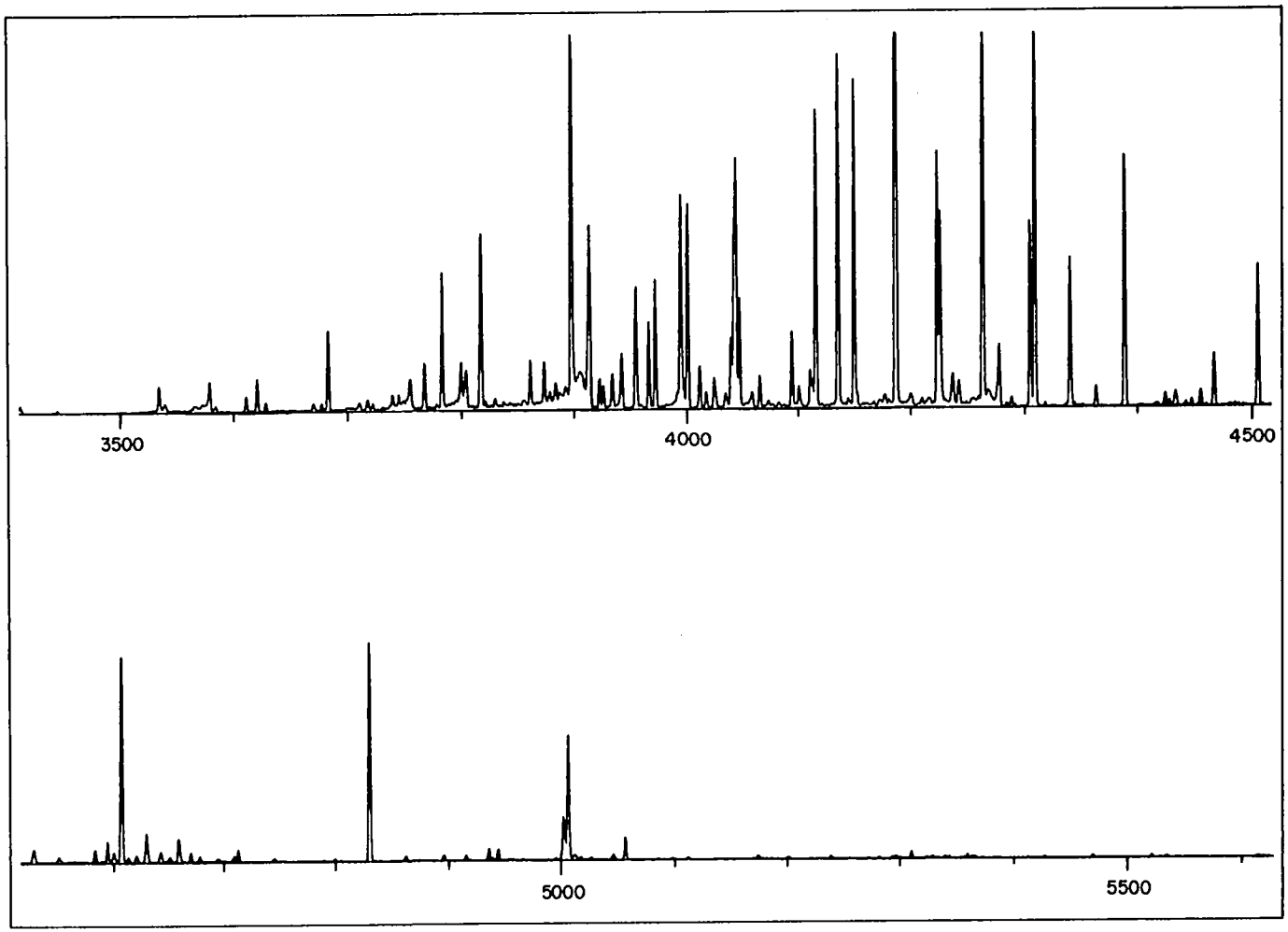

Figure 4.6.a Survey spectrum, 3500A^{o} to 5600A^{o} for 8.0 keV K^{+} excitation of N_2

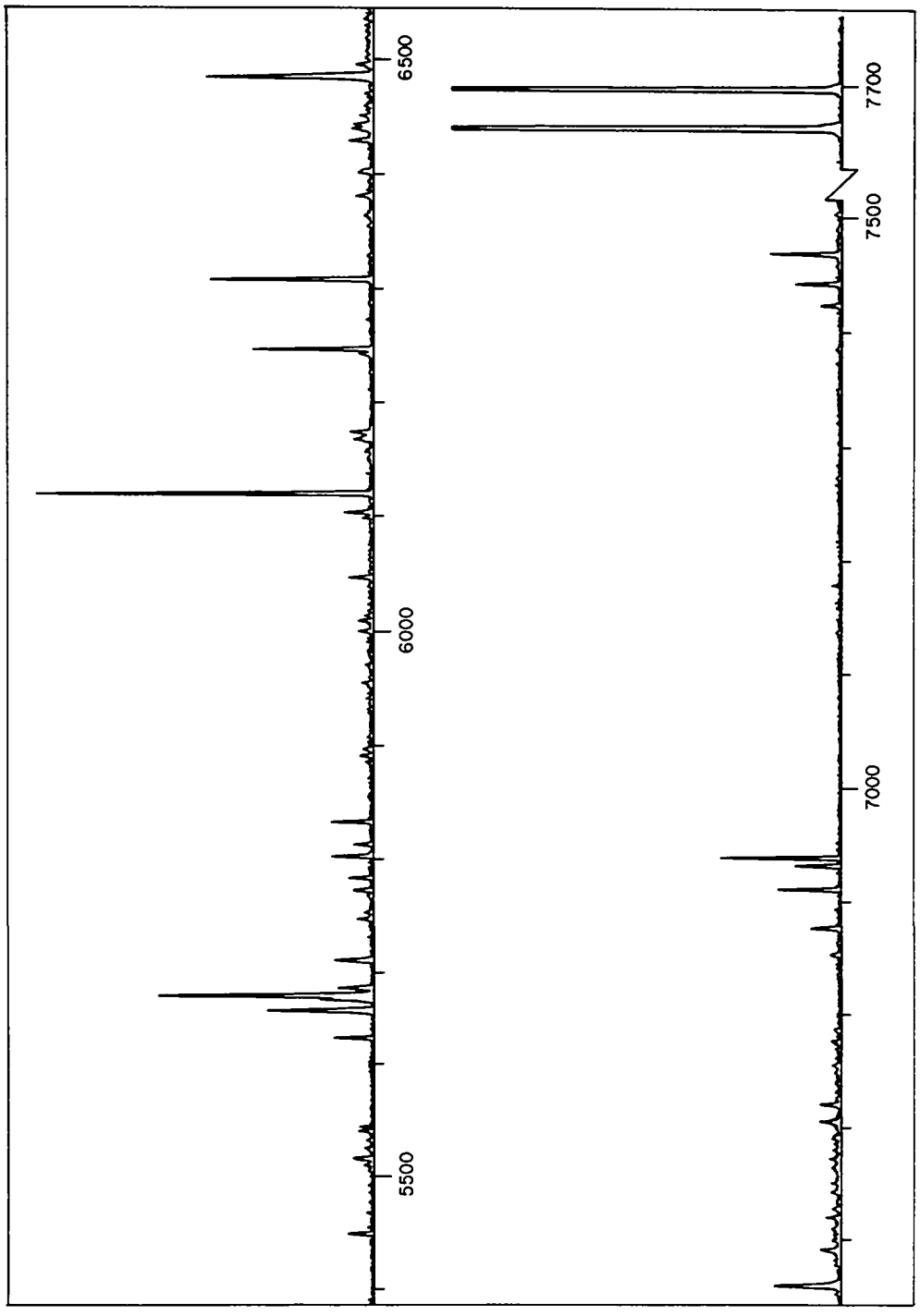

Figure 4.6.b Survey spectrum, 5400A° to 7700A° for 8.0 keV K^+ excitation of N_2

TABLE 4.3

IDENTIFICATION LIST

SPECTRUM OF $K^+ + N_2$

Emitting Species	Wavelength (Angstroms)	Multiplet Number	Emitting Species	Wavelength (Angstroms)	Multiplet Number
K II	3530.7			4223.9	
	3618.5				
	3681.5		K II	4225.6	
N_2(1,3)	3755		N II	4237.0	(48)
				4241.8	(47)
K II	3767.4				
	3783.2		K II	4263.3	
	3800.1				
			N_2^+(0,1)	4278.1	
N_2(0,2)	3804				
			K II	4304.9	
K II	3817.5			4309.1	
	3861.4			4339.9	
	3873.8			4362.9	
	3897.9			4388.1	
N_2^+(0,0)	3914		N II	4432.7	(55)
K II	3955		K II	4466.7	
				4505.3	
N II	3955	(6)			
			N II	4530.4	(59)
K II	4001.2				
	4012.1		K II	4608.4	
	4024.4				
			N II	4630.5	(5)
N II	4041.3	(39)			
	4043.5		K II	4659.6	
				4829.2	
K I	4044.1				
	4047.2		N II	5001	(19)
				5005	
K II	4065.2			5666.6	
	4093.7			5676.0	(3)
				5679.6	
N I	4109.9	(10)		5710.7	
K II	4114.9		Na I	5889	
	4134.7			5896	
	4149.2				
	4186.2		K II	6246.5	
				6307.2	

TABLE 4.3 (cont'd)

Emitting Species	Wavelength (Angstroms)	Multiplet Number
N II	6482.1	(8)
H	6562.8	
Li I	6707	
K I	6911.3	
	6938.4	
N I	7423.9	(3)
	7442.6	
	7468.8	
K I	7664.9	
	7699.98	

by Moore (1959) were observed indicating excitation to levels in excess of 36 eV. The (^2S-^2P) resonance transition was the main atomic feature observed for all alkalis. For the heavier alkalis, the intensities for the (^2P-^2S) and (^2P-^2D) transitions decreased. Whereas with Li^+ excitation the (^2P-4s$\rightarrow$6s^2S) and (^2P-3d$\rightarrow$8d^2D) transitions are observed with K^+ excitation only the (^2P-4d^2D) transition was found.

In all cases, the dominant molecular features are the N_2^+ bands in particular the (0,0) band. The increased rotational development of the (0,0) band in the case of Na^+ excitation is apparent when compared to Li^+ excitation, but the band shows a reversal towards a lower rotational temperature with the still heavier K^+ ion. This may in fact be due to secondary electron excitation as discussed later in this chapter supported by the fact that with increased sensitivity, the N_2(0,2) and (1,3) bands are observed. The probability that this system is excited in primary collisions is very small since the excitation requires a multiplicity change, whereas it is easily excited by electrons.

Dissociation of the target molecule also appears to be an important process as indicated by the numerous N I and N II lines observed. As the mass of the alkali ion is increased the probability of dissociation increases as suggested by the greater number of N II lines for Na^+

excitation than for Li^+ excitation. The N II lines are found to be more intense than the N I lines even though the excitation potentials are greater (26 eV) than the N I lines (14 eV).

4.3 Variation of Intensity with Pressure

Single collision conditions are usually assumed to be indicated by a linear variation of intensity with pressure and beam current. However as indicated in Chapter II, there are times when secondary processes are linear with beam current and pressure whereas primary processes may be non-linear.

In making intensity measurements with the monochromator slit parallel to the beam, it is important that the full width of the beam be viewed so that changes in density across the beam do not interfere with the measurements. In the following experiments involving pressure variation of intensity and cross-section measurements, the beam was narrowed and the monochromator slits widened so that the beam was the effective slit of the instrument. This was ascertained by measuring the half width of an atomic line and comparing it with the spectral slit width as given by the slit geometry of the monochromator.

In all this work, a region of the beam 2.2cm. in length extending from a point 1.5cm. above the collision chamber entrance, was focused on the entrance slit.

Intensity measurements were made at a beam energy of 10 keV for all spectral features for which cross-section measurements are reported in the next section. Total cross-sections for the production of free electrons (Kikiani et al (1966)) and charge exchange cross-sections (Ogurtsov et al (1966)) indicate that the probability of secondary excitation processes increases with increasing energy.

For Li^+ excitation of N_2, all features except the Li I lines were found to be linear with pressure up to 20 millitorr. Typical results are illustrated in figure 4.7 for N I 4109, for N II 3995 and for the N_2^+(0,0) band. Due to overlapping of the Li I 3915A° line with the head of the N_2^+(0,0) band, intensity versus pressure measurements were made on the R branch part of the band. Overlapping of N I and N II lines, resulted in only sections of the band, indicated by the K values for the R branch lines, being observed. This also ensured that all sections of the band were excited in primary collisions. For the Li I lines, the intensities deviated from linear with the decrease in intensity probably due to collisional deactivation of the fast particles.

In the case of Na^+ and K^+ excitation, significant deviation from linearity was observed in the first thirteen lines of the N_2^+(0,0) band. This nonlinear effect is probably due to excitation of the band by secondary elec-

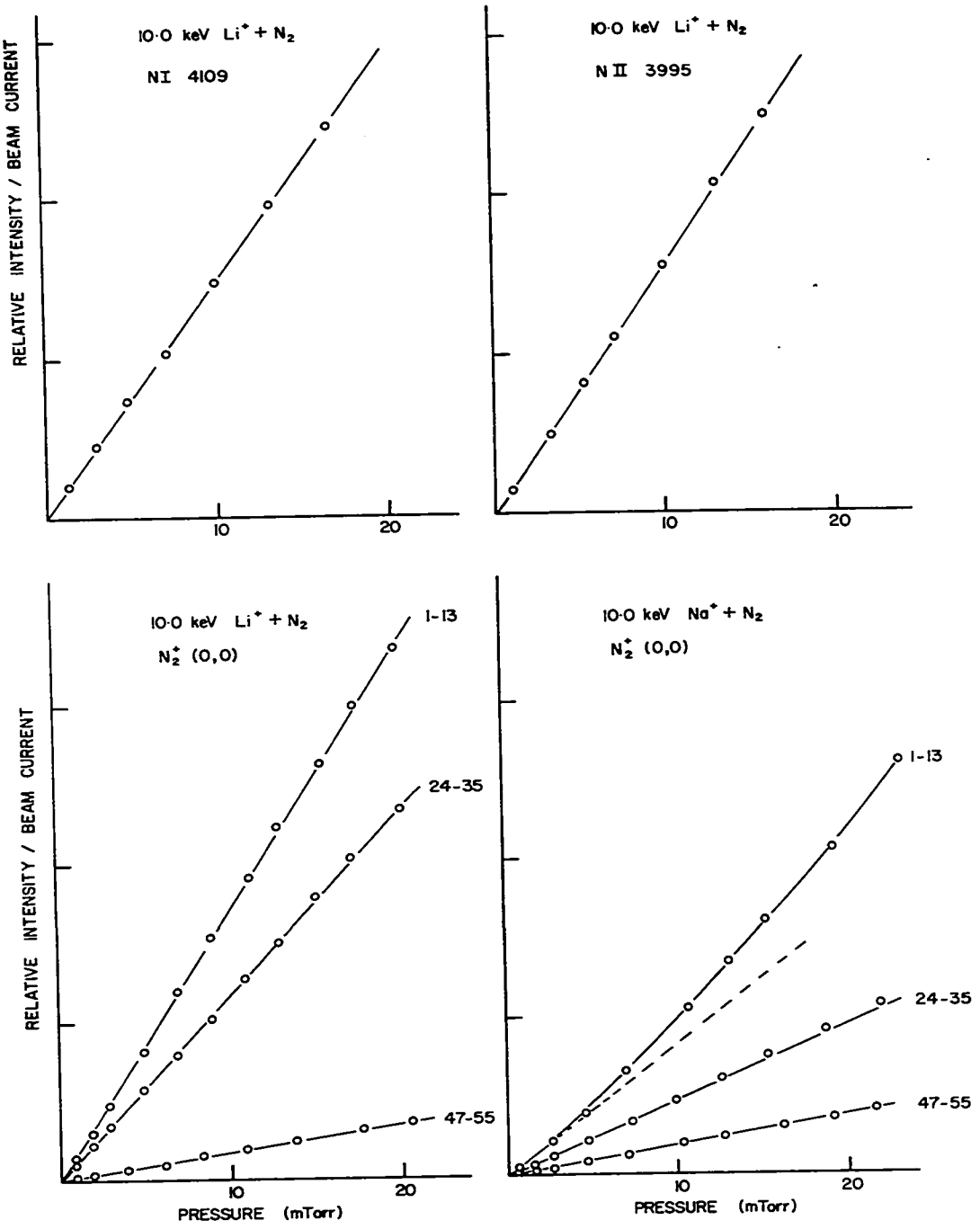

Figure 4.7 Variation of intensity with pressure. Series of lines observed in $N_2^+(0,0)$ band are indicated.

trons as indicated by a marked increase in the intensity of the N_2 Second Positive bands ((0,2), (1,3)) in the same pressure range. In figure 4.7, the intensities of the higher K lines of the band excited by Na^+ ions remain linear with pressure over the entire pressure range. Such a behaviour suggests that the secondary process is producing a rotational distribution with significantly less rotational development than for the primary process. While atoms have been found to produce greater rotational excitation than the ions of the same energy (Polyakova et al (1969)), electron excitation produces distributions characteristic of the ambient gas temperature (Moore and Doering (1968)) suggesting that the secondary process is due to electrons.

4.4 Emission Cross-sections

The cross-sections in this section are relative emission cross-sections normalized to that of $N_2^+(0,0)$ excited by 1.0 keV electrons (Borst and Zipf (1970)). For the normalization, the rotational lines of the $N_2^+(0,0)$ band during electron excitation were integrated over the full band. In the energy range of 1 to 10 keV, the emission cross-sections obtained by this technique and using the normalization factor at 1 keV never deviated by more than 10% from the absolute values of Borst and Zipf.

Since intensity measurements were made perpendicular to the beam axis, polarization of the radiation

was studied. For the excitation of nitrogen by electrons, the polarization was found to be less that 4% for the (0,0) band of the N_2^+ First Negative system in good agreement with the results of Borst and Zipf. Similar results were obtained for alkali ion excitation of N_2, with all radiations for which cross-sections are given being polarized less than 5%. For the (0,0) band of N_2^+ excited by alkali ions, polarization of the radiation was found to be less than 4% over the entire band.

Again, the beam itself was made the effective slit of the optical system, but this time being set up for the lowest energy used where beam spreading would be greatest. All cross-sections were taken at collision chamber pressures of 1 millitorr with beam current, line intensity and collision chamber pressure being recorded. The relative sensitivity of the instrument over the wavelength range observed was calibrated by means of a NBS quartz iodine lamp. Using the electron calibration, absolute cross-sections were reproducible within 15%.

Only a limited number of emission cross-sections were measured. The strong resonance lines of the alkali atoms were selected as an indication of the probability of charge exchange with excitation of the alkali neutral, and to compare the calibration with the work of Neff (1963). The particular N II and N I lines were chosen as examples of target gas excitation and to determine if the exponential

form of the cross-section given by Hasted (1962) was applicable for collisions involving dissociative excitation of the target molecule. The K II line was chosen as an example of direct ion excitation and as a further check on the calibration used.

4.5 Discussion of Cross-section Data

The emission cross-sections for the various features observed in Li^+, Na^+ and K^+ excitation of N_2 are given in figures 4.8, 4.9 and 4.10. Total charge changing cross-sections (Ogurtsov et al (1966)) have also been plotted. Comparison to the absolute emission cross-sections of Na I 5889A° and N II 3995 (Neff (1963)) is indicated by the dash - dot curves in figure 4.9. Figure 4.10 gives the absolute cross-section of K II 4186 in K^++Ne collisions compared to the work of Pop et al (1970) indicated by the dashed line.

The shapes of the emission cross-section curves for the atomic alkali lines, which rise quickly to a flat plateau are clearly different from those for the other features studied. The similarity in the resonance lines of the alkali atoms indicates the similarity in the energy defects for the three cases. A distinct oscillatory structure in the ^2P-^2D transitions of Li I (6103, 4603, 4132A°) is apparent with the structure becoming more pronounced for the higher $2_p\,^2P$-$nd\,^2D$ transitions. For the

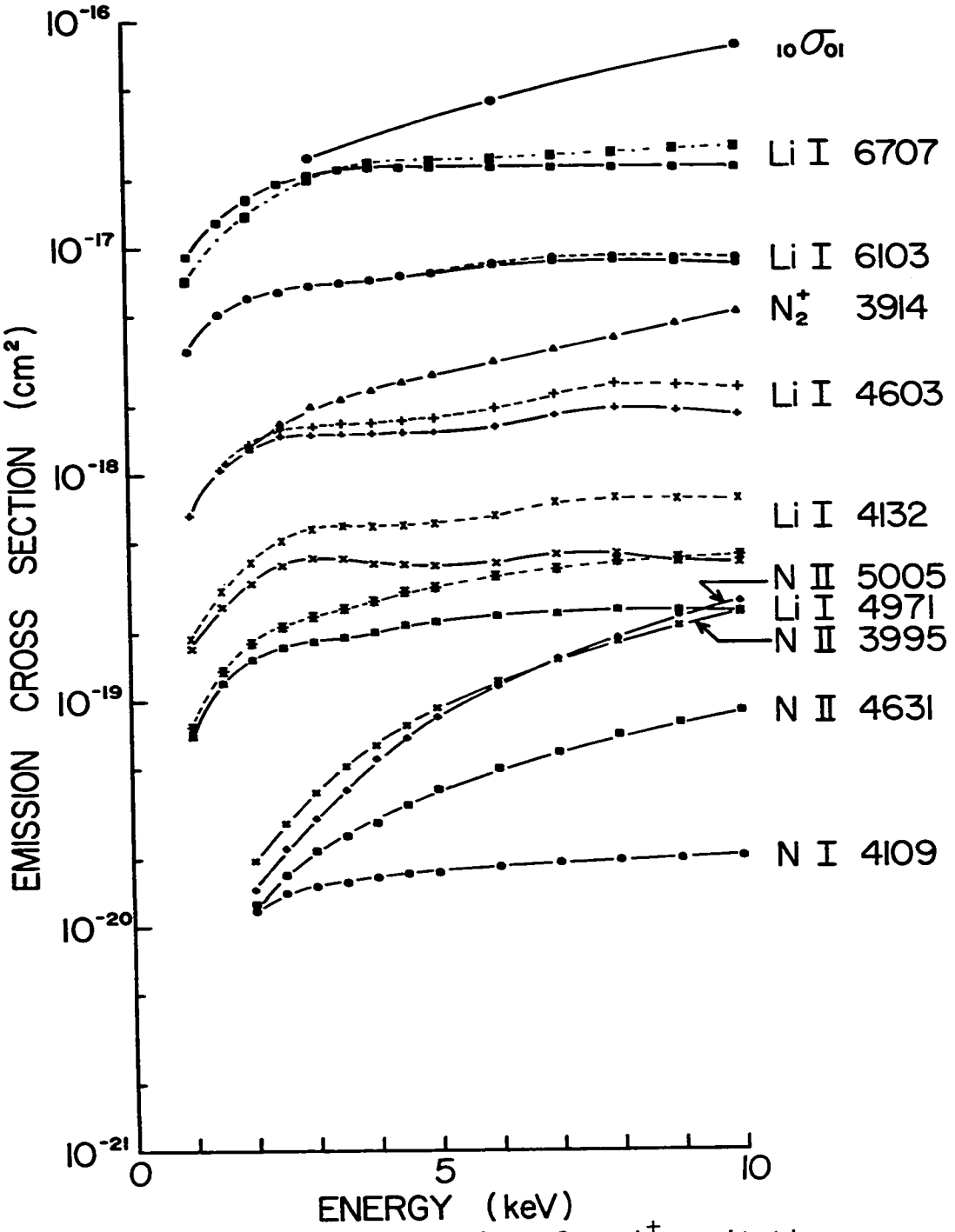

Figure 4.8 Emission cross-sections for Li^+ excitation. $_{10}\sigma_{01}$ Ogurtsov et al (1966). (---) lifetime and (-·-) cascade corrections applied.

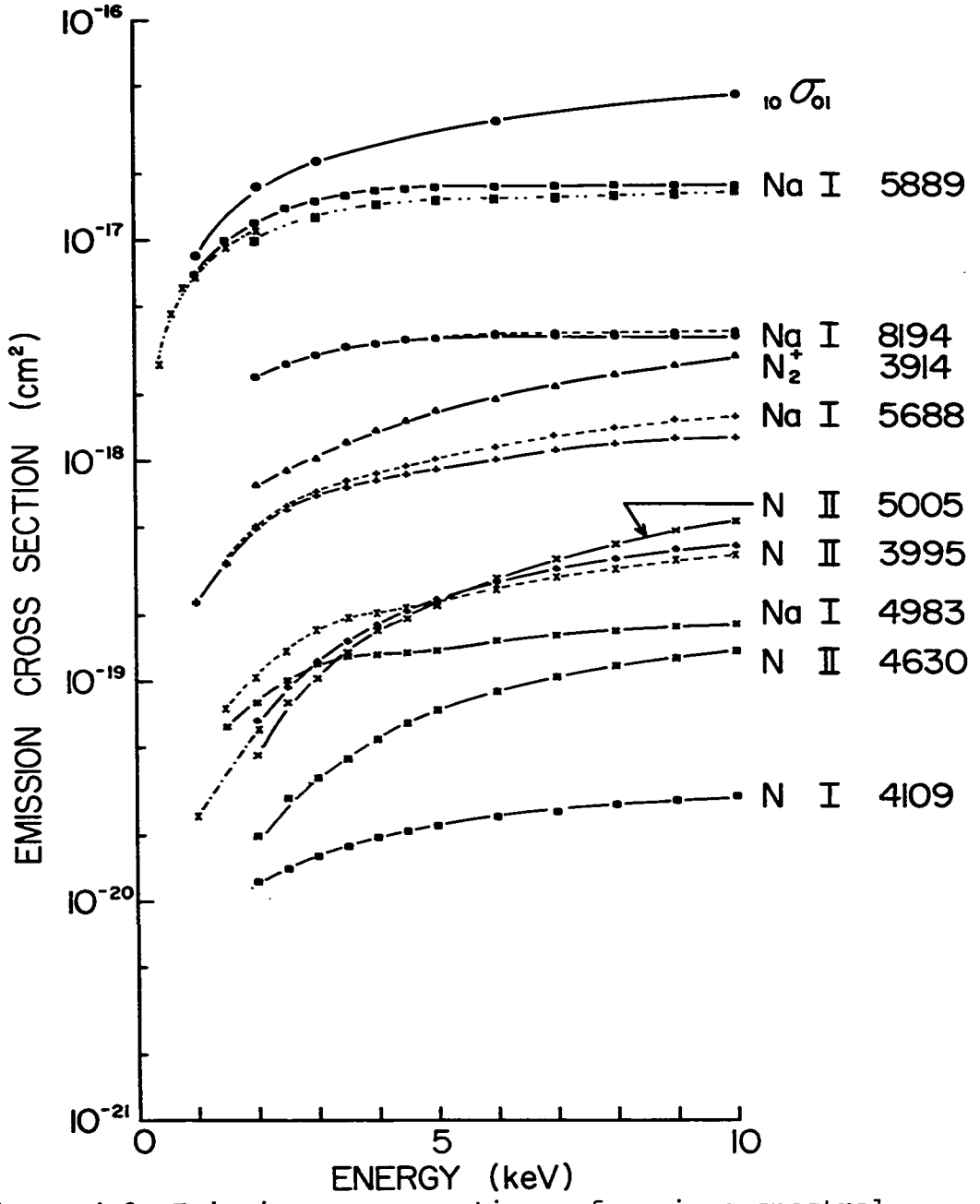

Figure 4.9 Emission cross-sections of various spectral features observed in the excitation of N_2 by Na^+ ions. $_{10}\sigma_{01}$ - Ogurtsov et al (1966). (-·-) ≙ Neff (1963). (---) - lifetime corrections applied. (-··-) - cascade and lifetime corrections applied.

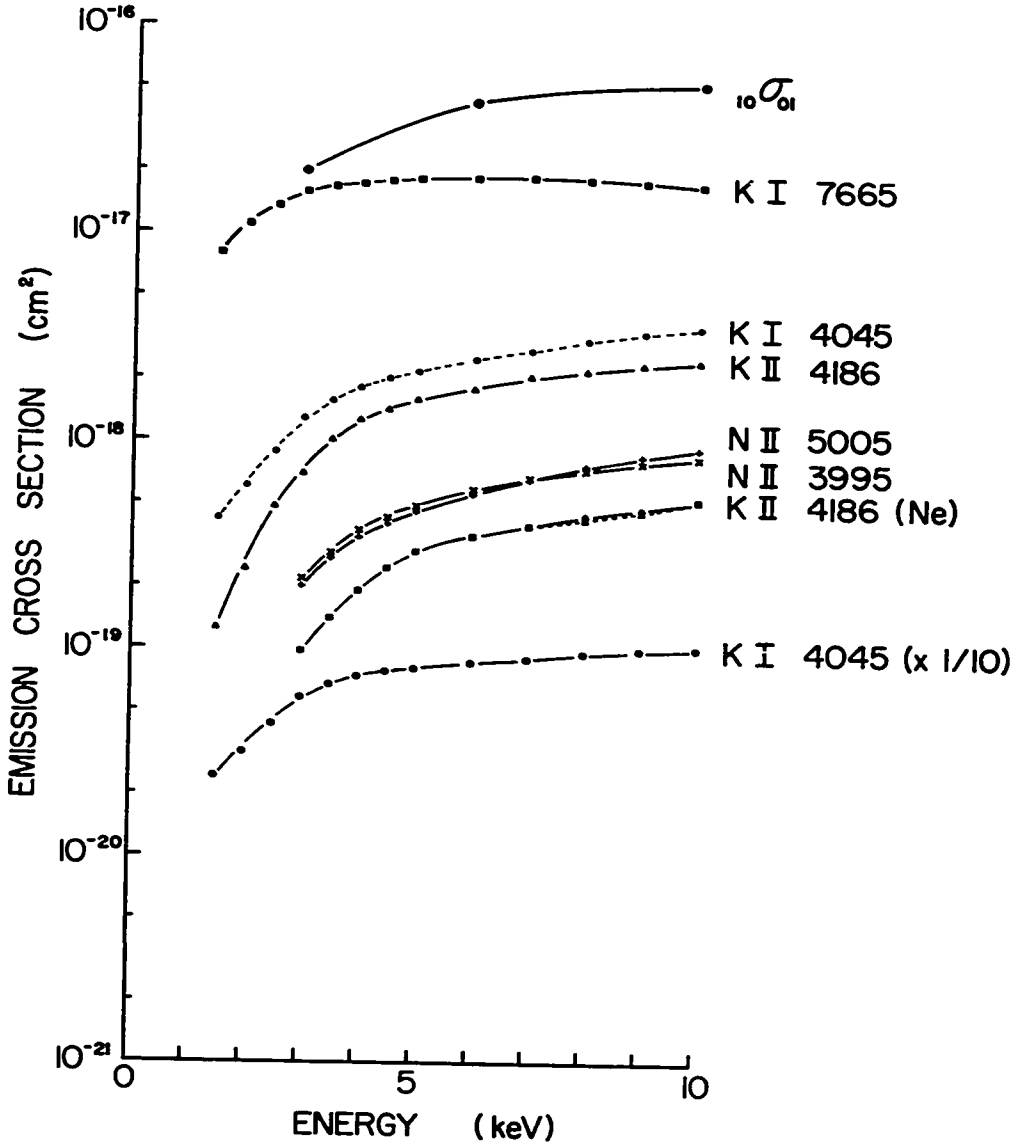

Figure 4.10 Emission cross-sections of various spectral features observed in the excitation of N_2 by K^+ ions. $_{10}\sigma_{01}$ - Ogurtsov et al (1966). (--) (Ne) - Pop et al (1970). (---) - lifetime corrections applied.

Na I lines of the ^2P-^2D series, a slight change of slope in the cross-section curves occurs in the same energy range. As discussed in chapter II, when dealing with radiating fast particles, a lifetime correction factor of

$$\left[1-\frac{x_i}{L}\exp\left(-\frac{L}{x_i}\right)\left\{1-\exp\left(-\frac{L}{x_i}\right)\right\}\right]^{-1} \qquad (4.1)$$

where x_i denotes $v\tau_i$ and τ_i is the mean lifetime of state i, must be applied in order to compensate for the loss of light by the escape of fast particles from the observation region before emission. de Heer (Bates (1966)) has shown that a first order cascade correction to equation (2.14) gives

$$\sigma_{ij} = \sigma(i)\,A_{ij}\,\tau_i\left[\left(1+\sum_{k>i}\frac{\sigma(k)}{\sigma(i)}\,A_{ki}\,\tau_k\right)(1-F(x_i)) - \sum_{k>i}\frac{\sigma(k)}{\sigma(i)}\,A_{ki}\,\tau_k x_k\,\frac{F(x_k)-F(x_i)}{x_k-x_i}\right] \qquad (4.2)$$

where $\left[1-F(x_i)\right]^{-1}$ represents the equation (4.1). For cascading from an upper state which is sufficiently long lived compared to state (i), equation (4.2) simplifies to

$$\sigma_{ij} = \sigma(i)A_{ij}\tau_i\left[1-F(x_i)+\sum_{k>i}\frac{\sigma(k)}{\sigma(i)}\,A_{ki}\tau_k\,(1-F(x_k))\right] \qquad (4.3)$$

so that lifetime corrections are accounted by the two states separately. Apparent maxima in emission cross-sections due to significant light loss at high energies have been observed previously (Lowe (1966)). Since cascade contributions to the levels showing structure in the emission

cross-sections could not be measured, an attempt to synthesize the emission cross-section for the 5d(Li I 4132A° emission) was made assuming cascade contributions from the 6p and 6 f levels whose excitation cross-section shapes were assumed similar to that of the 5d level. A structureless excitation cross-section for the 5d level was obtained only if the cross-sections for the levels from which cascade occurred were about two orders of magnitude greater than that for the 5d level. In view of this unlikely result being the cause, the oscillatory structure must arise from primary excitation processes. Recent work on charge exchange cross-sections in Na^+-Ne collisions (Latypov et al (1970)) has shown that oscillatory structure exists in the total cross-sections. Optical measurements on the same system (Tolk et al (1971)) have indicated structure in the Na I 5890A° and Ne I 6266A° emissions with the oscillations being 180° out of phase from each other corresponding to interference between charge exchange and direct excitation collision channels.

Assuming the Li I and Na I cross-sections are due to primary processes only, lifetime corrections can be made. Using equation (2.7) of Chapter II, it was determined that the beam upon reaching the observation region was less than 1% atoms. Assuming a beam consisting only of ions at the entrance slit to the collision chamber and using the lifetimes for the alkali states (Wiese et al (1966),

Weise et al (1969)), the correction factors listed in Table 4.4, using equation (4.1), were applied to the cross-sections from which the dashed curves were plotted in figures 4.8 and 4.9. With the correction applied, the separate maxima in the Li I cross-sections are removed with just a change in slope occuring as observed for the Na I cross-sections. The corrections to the Li I and Na I resonance lines were made using equation (4.2) thereby removing the cascading effects of the ^2P-^2D transitions. The resulting excitation (emission) cross-sections indicate that at 10 keV about one quarter of the charge transfer collisions leave the atom in its lowest ^2D state.

The dissimilar shapes of the N I and N II cross-sections indicate a difference in their excitation processes. According to the adiabatic criterion, the difference in shapes can be partially accounted for if the energy defect involved in the excitation of the N II lines is significantly greater than that for the N I excitation. Charge exchange collisions involving dissociative excitation may produce either N II or N I lines

$$Li^+ + N_2 \rightarrow Li + N^+(^3P)^* + N \qquad (\Delta E = 40.5 \text{ eV for N II 3995 transition})$$

or $$Li^+ + N_2 \rightarrow Li + N(^2D^o)^* + N^+ \qquad (\Delta E = 34.9 \text{ eV for N I 4109 transition})$$

while simple dissociative excitation can also produce the N I line through

TABLE 4.4

LIFETIME CORRECTION FACTORS

	A_{ij} x 10^7 sec^{-1}	ΣA_{ij} $_{j<i}$ x 10^7 sec^{-1}	Energy (keV) 10	8	6	4	2
Li I 6707	3.72	3.72	1.21	1.17	1.12	1.08	1.03
6103	7.16	7.16	1.04	1.03	1.02	1.01	1.00
4603	2.30	2.985	1.32	1.26	1.20	1.13	1.05
4132	1.06	1.59	1.87	1.74	1.60	1.44	1.23
4971	1.01	1.756	1.76	1.64	1.51	1.37	1.19
Na I 5889	6.30	6.30	1.01	1.01	1.00	1.00	1.00
8194	4.95	4.95	1.02	1.01	1.01	1.00	1.00
5688	1.31	1.98	1.23	1.18	1.13	1.08	1.03
4983	0.50	0.76	2.05	1.90	1.74	1.54	1.30
K I 7665	3.85	3.85	1.02	1.01	1.01	1.00	1.00
4045	0.124	0.284	3.57	3.25	2.90	2.48	1.94

$$Li^+ + N_2 \rightarrow Li^+ + N(^2D^o)^* + N \qquad (\Delta E = 25.8 \text{ eV for N I 4109 transition})$$

Definite conclusions regarding the excitation process of N I therefore cannot be made. However, the substantial difference in the shapes of the cross-section for N I 4109 and N II 3995 indicates a preference towards the second process. Comparison of the shapes of the cross-section curves for dissociation products to those for charge exchange excitation processes suggests that dissociation of the target molecule is more probable than the adiabatic criterion would indicate. Also the cross-sections for the N I and N II lines indicate that dissociation is more probable for the heavier alkalis at a common energy.

Hasted (Bates (1962)) has found in the near-adiabatic region, that charge transfer cross-sections have the form

$$\sigma = \sigma_o \exp\left(-\frac{a|\Delta E|}{4hv}\right) \qquad (4.4)$$

where "a" the interaction distance is approximately constant for a variety of processes. For charge exchange, ionization or excitation of the target by a positive ion projectile, the mean value is $7A^o$. To test whether this relation holds for dissociative excitation, the emission cross-sections for N I 4109 and N II 5005 were plotted as a function of reciprocal ion velocity for the different alkali ions (figure 4.11). All cross-sections gave straight

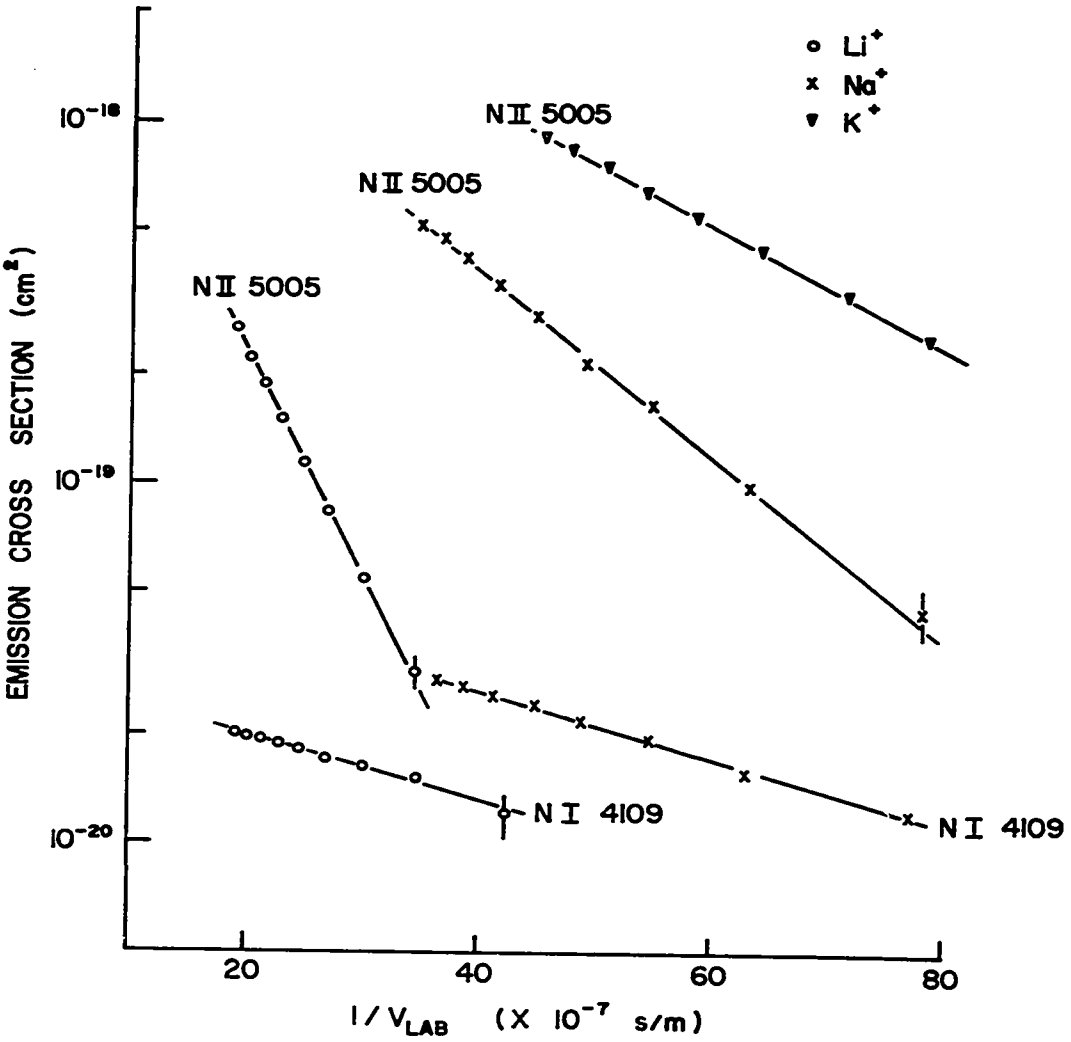

Figure 4.11 Effect of ion velocity on emission cross-sections for N II 5005 and N I 4109 for Li^+, Na^+ and K^+ excitation.

lines indicating the applicability of the general form for the cross-sections. In the case of dissociation with excitation (N I 4109), assuming ΔE determined the more likely reaction, the inverse velocity is the significant variable for describing the collision since both lines are parallel. However for charge exchange with dissociative excitation, the slopes of the N II 5005 cross-sections vary significantly indicating that the interaction distance is ion dependent since $|\Delta E|$ is equivalent for the three alkalis. The interaction distance was found to vary from $5A^{\circ}$ for Li^{+} to $2A^{\circ}$ for K^{+} excitation. Similar results have been obtained for 0.15-1 MeV proton excitation of nitrogen (Dufay et al (1966)). Maxima in the N II 5005 and N II 3995 emission cross-sections suggested interaction distances of $3A^{\circ}$ also much less than the $7A^{\circ}$ mean found applicable to charge exchange collisions.

The emission cross-sections for the $N_2^{+}(0,0)$ band, which closely resemble the total charge exchange cross-section, were obtained by integrating over the deduced rotational distributions of the band. Corrections for the branching ratio indicate that about one-tenth of the charge exchange collisions leave the molecular ion in the $v' = 0$ level of the B state assuming that charge exchange is the dominant process.

CHAPTER V

ROTATIONAL AND VIBRATIONAL EXCITATION

In inelastic collisions involving molecules, the energy loss can contribute to electronic, vibrational and rotational excitation of the molecule. In this chapter, the excitation of vibration and rotation will be discussed.

5.1 Measurement of Rotational Populations

In a given band, the intensity $I(J',J'')$ of the rotational lines arising from the $J'-J''$ transition is a function of the number of molecules in the upper state ($N(J')$), the line strength factor ($S(J',J'')$) and the frequency of the transition ($\nu(J',J'')$). If the gas is in thermal equilibrium at a temperature T, the intensity of a rotation line is

$$I(J',J'') = \frac{C_{em}\nu^4}{Q_r}(J'+J''+1)\exp\left(-\frac{F(J')hc}{kT}\right) \qquad (5.1)$$

where C_{em} is a constant dependent on the change of dipole moment and total number of molecules in the initial vibrational level; Q_r is the rotational state sum; $F(J')$ the term value of the rotational level in the upper state. Often, the intensity distribution has been found to follow equation (5.1) even though equilibrium did not exist among the degrees of freedom, in which case T is referred to as the rotational temperature. It is usual to

plot (log $I(J',J")/\nu^4 S(J',J")$) as a function of $J'(J' + 1)$ where $S(J',J")$ is the line strength factor. A straight line indicates a Boltzmann distribution exists at the particular rotational temperature deduced from the slope.

The rotational population measurements reported in this chapter were made on the (0,0) and (1,1) bands of the N_2^+ First Negative system with band heads at 3914A° and 3884A° respectively. These bands, which are degraded to the violet, arise from transitions between the $B^2\Sigma$ state and the $X^2\Sigma$ ground state and consist of a P branch (which forms the head of the band) and an R branch. The spin doublets are not resolved in the spectra taken and hence the band can be treated as a $^1\Sigma - ^1\Sigma$ transition with K replacing J. The appearance of the two bands at room temperature is illustrated in figure 5.1 obtained by the excitation of N_2^+ by 1.0 keV electrons. The numbering of the lines is according to the lower rotational level K". The 2:1 intensity alternation between adjacent rotational lines due to the nuclear spin degeneracy is clearly visible with the slight discrepancies being due to changes in beam current indicated by the line above the spectrum. Correcting for beam fluctuations, the intensity of the (0,0) band peaks at K"= 7 and quickly decreases towards higher K" values. The (1,1) band (at a gain of 14X) shows a similar rotational development with the anomalously strong lines near the band origin being due to overlapping of the

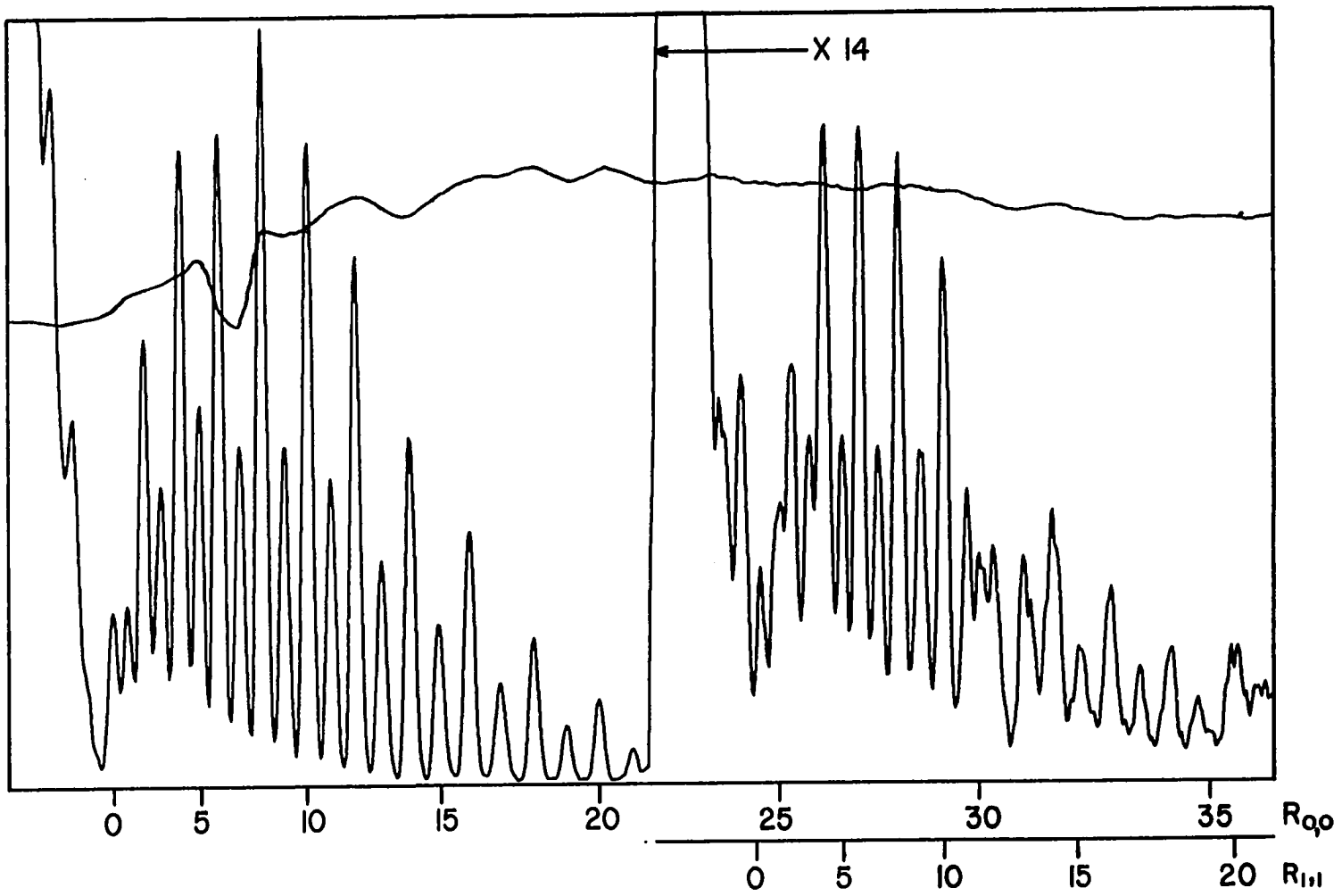

Figure 5.1 (0,0) and (1,1) Bands of N_2^+ excited by 1.0 keV electrons. Upper curve indicates electron beam current. Rotational lines numbered according to lower state rotational level.

(0,0) band.

At elevated temperatures when the higher K' levels become significantly populated with respect to the lower levels, the (0,0) band no longer displays the 2:1 intensity ratio of alternate lines due to the folded back P branch lines overlapping the R-branch lines. In the (0,0) band of N_2^+, the R(K") line differs in wavelength by about 0.15A° from the P(K" + 27) line (Childs (1932)) so that at low resolution a strong P branch line overlaps a weak R branch line. This feature is illustrated in figure 5.2 where the P and R branch contributions for a Boltzmann distribution at a rotational temperature of 7000°K have been calculated and plotted separately as a function of wavenumber. The resulting band, assuming the P and R branch lines exactly overlap, is plotted at the bottom with the lines numbered by K". It is immediately obvious that due to the overlapping of the P lines, which are of significant intensity, the 2:1 intensity ratio is lost at low K" values. In this particular example, a complete reversal of intensity alternation should be observed for the first few lines from the band origin. Such reversals have been observed for spectra excited by slow alkali ions, a typical example being given in figure 5.3 for 1.5 keV Li^+ ions. At this energy, extensive rotational excitation of the $B^2\Sigma$ state permits observations to be carried out to the one hundredth level. The

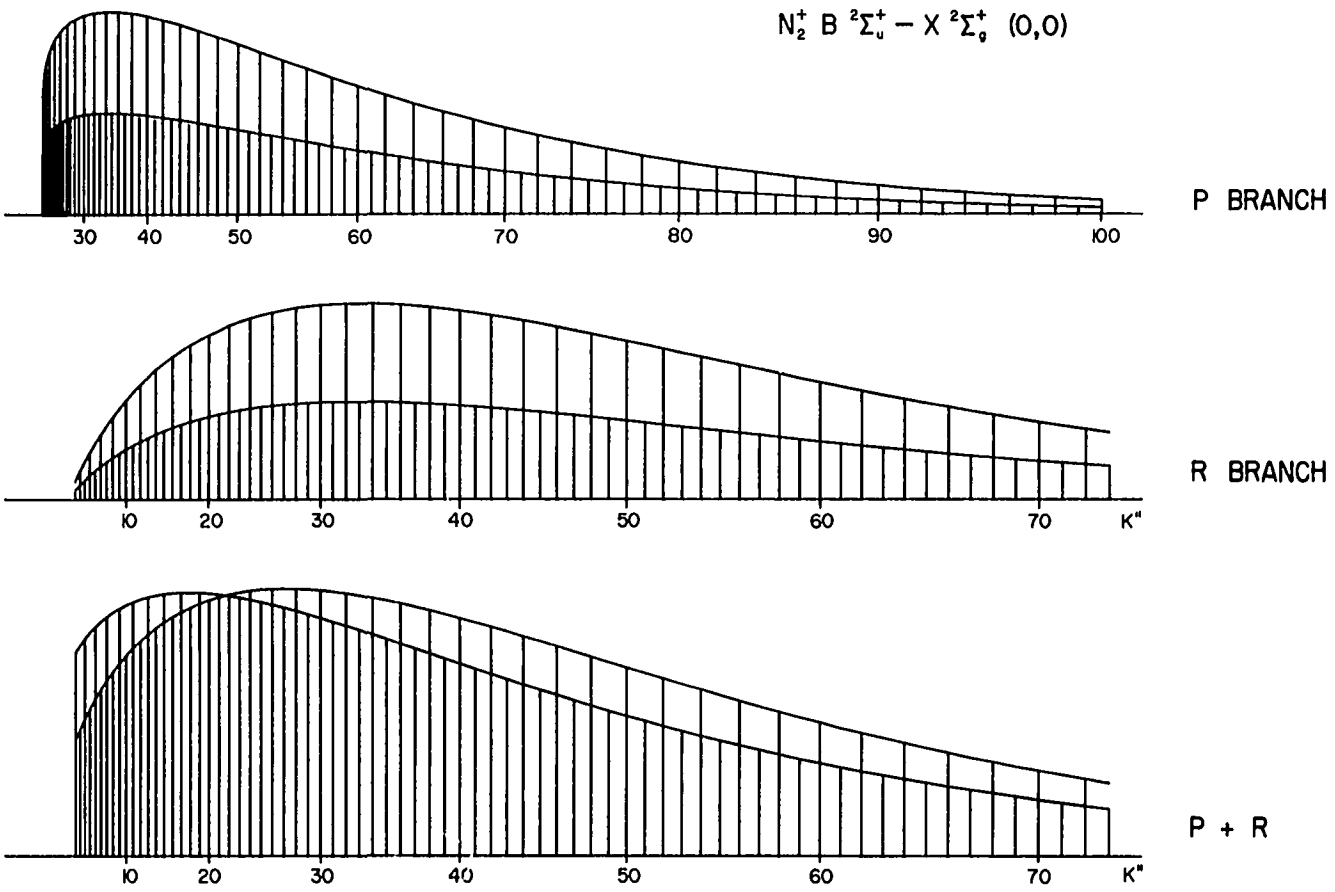

$$I_{em} = \frac{C_{em}\nu^4}{Q_r}(K'+K''+1)\exp-(B'K'(K'+1)hc/kT) \qquad T = 7000°K$$

Figure 5.2 Rotational line intensities of N_2^+(0,0) Band for 7000°K Boltzmann Distribution

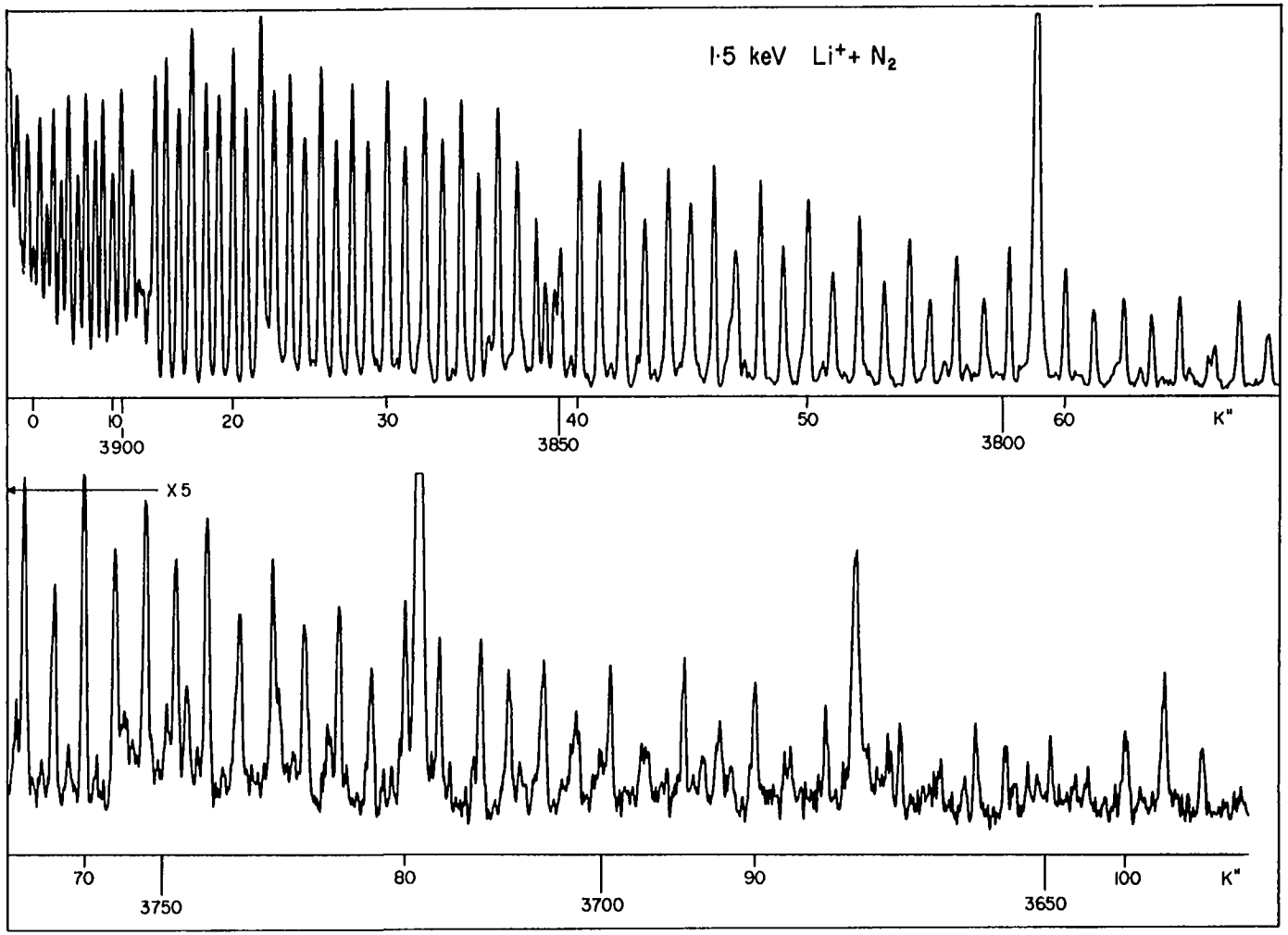

Figure 5.3 $N_2^+(0,0)$ Spectrum observed in the excitation of N_2 by 1.5 keV Li^+ ions

previously mentioned intensity reversal is clearly observed in the first eighteen lines of the R branch part of the spectrum. Beyond K"= 22, the even K" lines become the stronger indicating the dominant contribution is coming from the R branch. An approach to the normal 2:1 intensity alternation is observed towards the higher K" valued lines. Anomalies in the spectrum at K"= 13, 38 and 65 are due to perturbations of the rotational levels of the $B^2\Sigma$ state by the $A^2\Pi$ state (Childs (1932)). The anomalously weak line at K"= 13 results from a perturbation in the 39th rotational level of the B state (v'= 0) so that there is no overlapping of R(13) by the P(40) line. The same perturbation as well as a perturbation in the 66th level cause the weak lines at K"= 38. The perturbation in the 66th level also causes the splitting in the line at K"= 65.

Making use of the 2:1 intensity alternation in the R and P branch, Wink et al (1971) have shown that the intensity contributions of the R(K") and P(K" + 27) lines can be determined uniquely using a triplet method and assuming that the rotational population of the upper state varies slowly as a function of K'. Therefore the forms of the upper state distribution and the P branch contributions need not be assumed but are instead results of the analysis. This method was used to compare the results obtained from the analysis of the (0,0) band taken under low resolution (spectral slit width of 0.33A^o) with the

results of a high resolution (spectral slit width of $0.075A^{o}$) spectrum (figure 5.4) analysed using equation (5.1). The particular spectra analysed were produced in 4.0 keV $Li^{+} + N_2$ collisions. In the high resolution spectrum, the strong P branch lines are seen to precede the weak R branch lines. For the first few lines of the R branch, the even P branch lines are stronger than the odd R branch lines. It is this feature which leads to the previously mentioned intensity reversal when the spectra are taken at low resolution. The perturbation in the upper $^{2}\Sigma$ state is clearly visible leading to a splitting of the P(40) line into its separate components with no component overlapping R(13). The usual Boltzmann plots are presented in figure 5.5 with the low resolution analysis (using the method of Wink et al) plotted above the high resolution analysis (using equation (5.1)). The even and odd K" lines have been plotted separately for the high resolution analysis as an added check for the 2:1 intensity alternation. Relative populations for K'>26 levels were obtained from P branch contributions. The accuracy of this method is apparent and so all spectra were taken at low dispersion in order to obtain a better signal to noise ratio and therefore observe the band to higher K" values.

The (1,1) band had to be observed at high resolution in order to separate its rotational structure

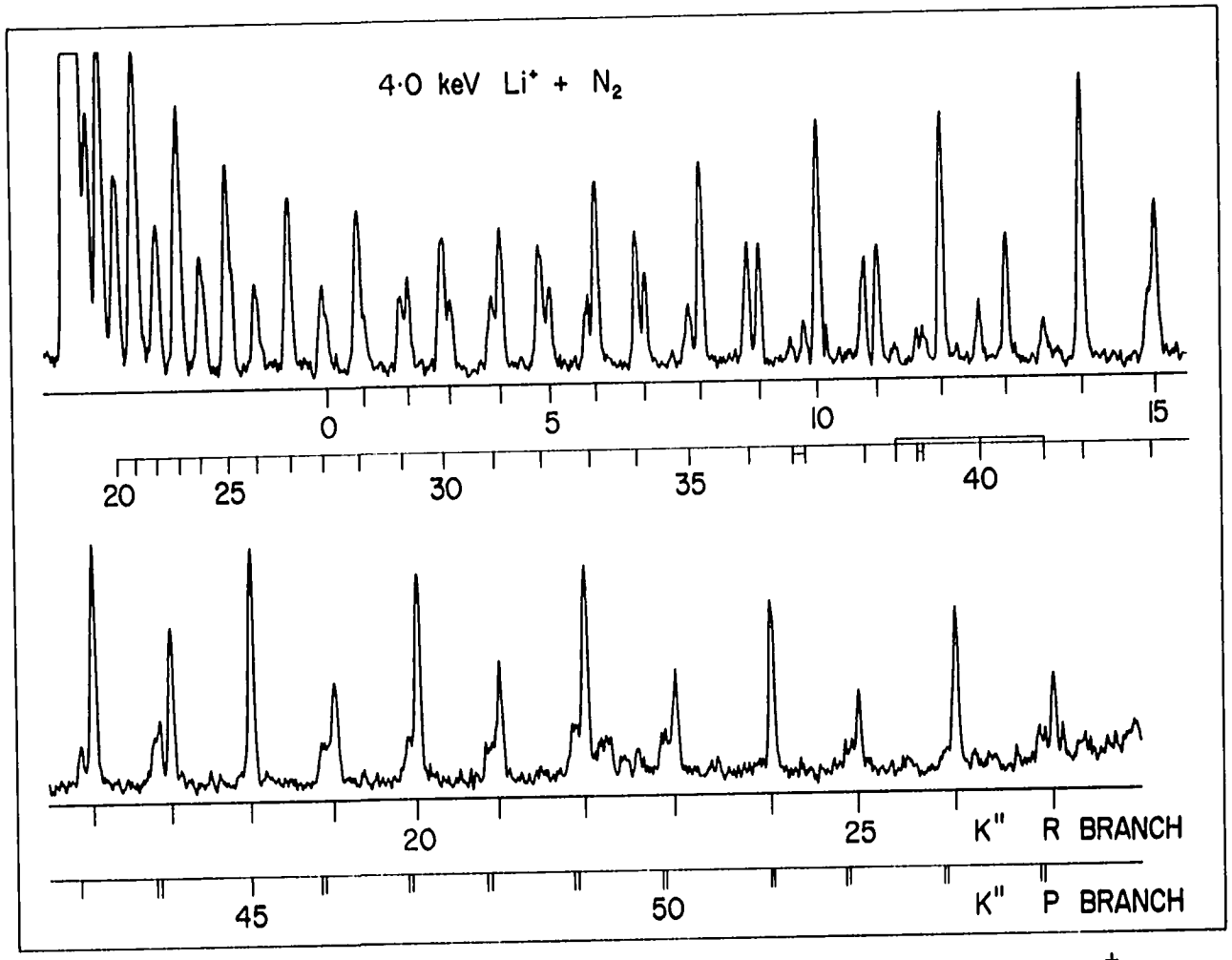

Figure 5.4 High resolution spectrum of $N_2^+(0,0)$ band for 4.0 keV Li^+ excitation of N_2. R- and P- branch lines are numbered separately.

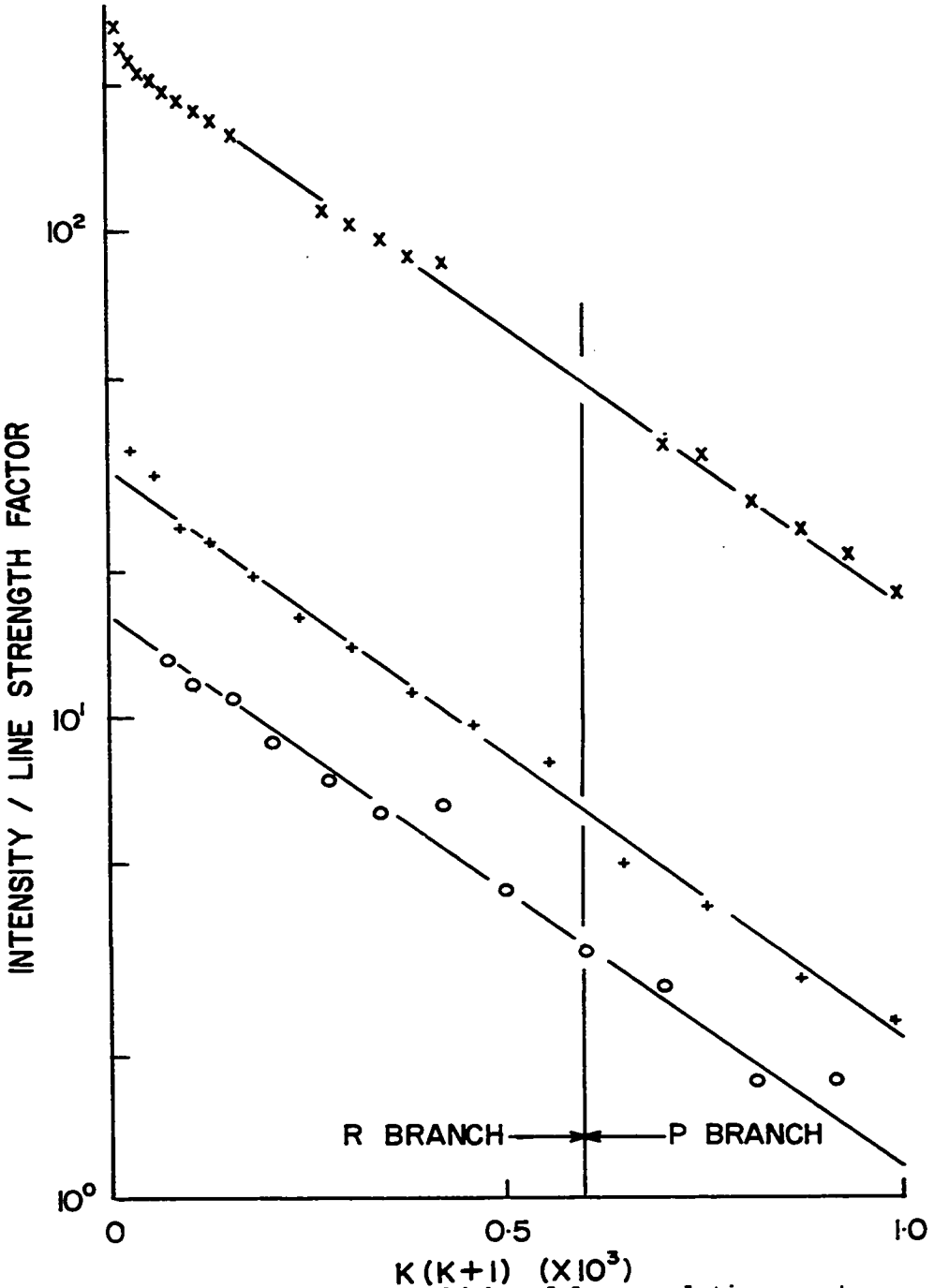

Figure 5.5. Boltzmann plots for high and low resolution spectra observed in 4.0 keV Li^+ excitation of N_2. (xxx) - using Wink's method. (++), (00) - using equation (5.1).

from that of the (0,0) band. Under these conditions, the folded back P branch was resolved from the R branch lines and direct calculations were made using equation (5.1). In this band, P(K" + 28) lies almost midway between R(K") and R(K" + 1) (Fassbender (1924)).

5.2 Rotational Excitation of v'= 0 State

5.2.1 $Li^+ + N_2$

Spectra of the (0,0) band of the N_2^+ First Negative system were obtained at ion energies ranging from 0.69 keV to 10 keV and were taken at collision chamber pressures of 15 millitorr with a spectral slit width of 0.33A°. Typical results are given in figure 5.6 with a 1.0 keV electron excitation spectrum for comparison. As the energy of the incident ion is decreased, the higher rotational levels of the upper state are increasingly populated with respect to the lower levels. The loss of the 2:1 intensity alternation at low K" values and the relative weakening of the 13th line indicate the significant contribution of the P branch lines to the observed spectrum at the lower energies. In analysing the spectra, only certain regions were used as indicated by the upper brackets in figure 5.6. The remainder of the spectrum was overlapped by N I, N II, Li I lines and N_2 Second Positive bands. Each spectrum was analysed separately and the deduced intensities(constituting a set of data)of

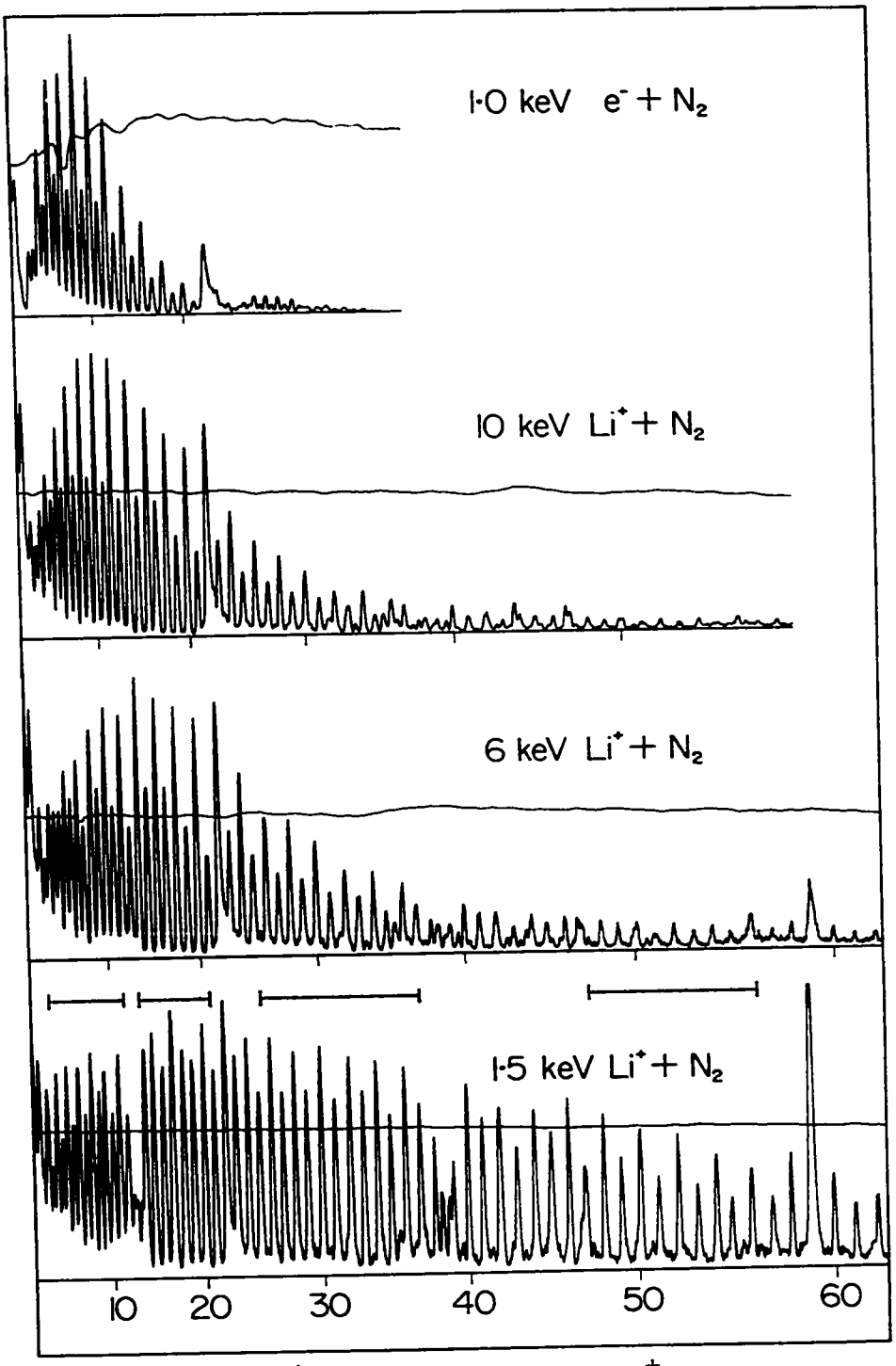

Figure 5.6 $N_2^+(0,0)$ Band due to Li^+ excitation. Lines used in analysis are indicated by brackets. Beam current indicated by smooth lines above spectra.

the P and R branches divided by the line strength factors were plotted as a function of K'(K' + 1) on semi-log graphs. The intensities of the odd lines were doubled in order to give a single curve describing the distribution. Four typical sets of raw data are given in figure 5.7 where the populations of the upper state determined from the R branch lines are indicated by the triangles and from the P branch lines are indicated by the plus signs. The good agreement for a common upper level from the R and P branch lines provides further support for the technique of Wink et al. The remaining graphs presented in figures 5.8 to 5.13 are plotted as the average of five sets of data with the error bars being one standard deviation. Overlapping of the (1,1) band was eliminated using the results discussed in section 5.3. Additional loss of data for low K" values at low ion energies resulted from the necessary increase of the spectral slit width in order to obtain a usable signal as a result of which the first few lines of the spectrum were not resolved.

At high energies, the plots indicate that the molecules are in rotational disequilibrium contrary to the results of Lowe and Ferguson (1971) whose analysis included only the first 36 lines of the spectrum. A room temperature Boltzmann distribution has been added to figure 5.8 to indicate the degree of rotational excitation. As the energy of the ion decreases, the upper levels

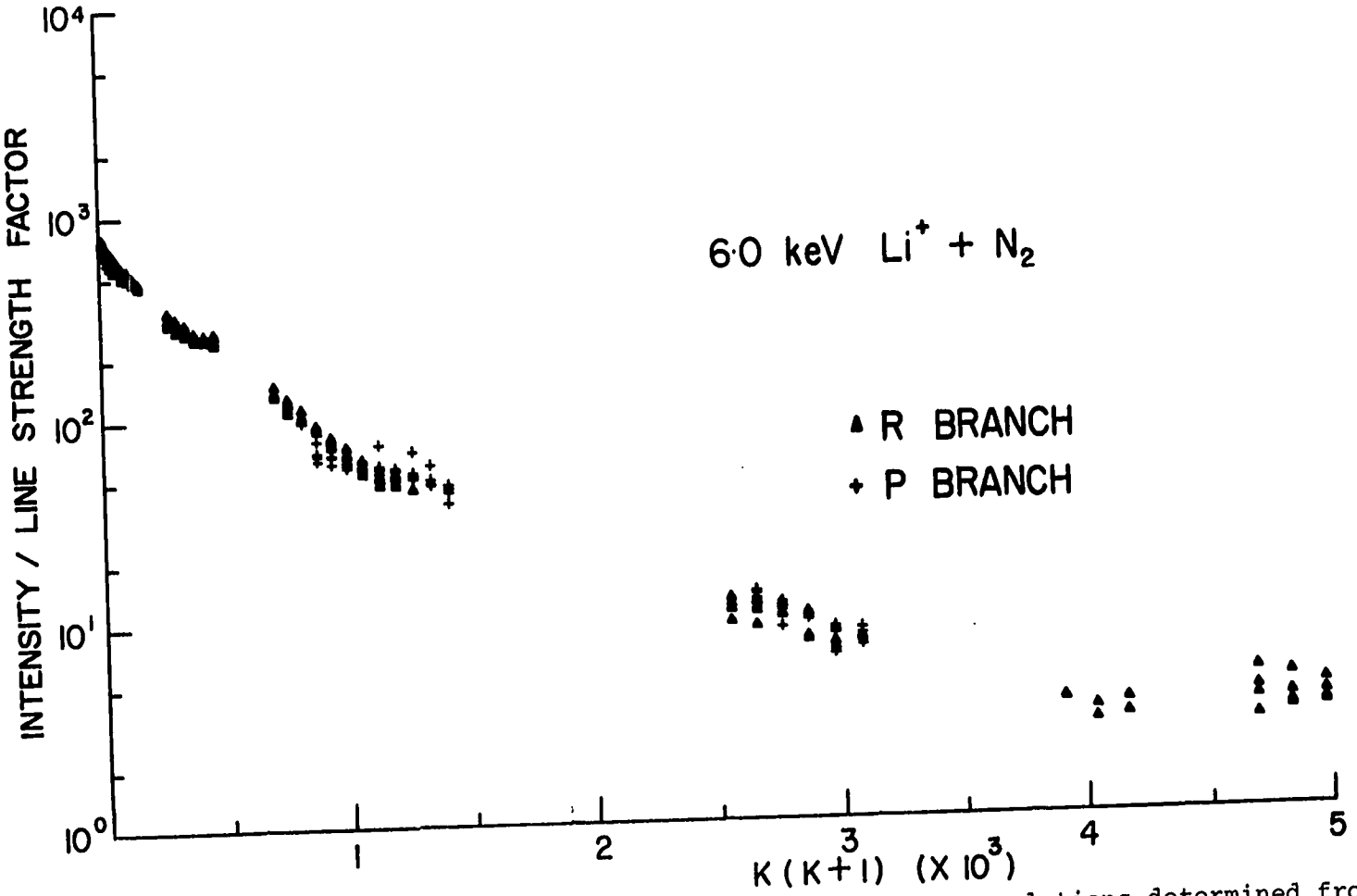

Figure 5.7 Boltzmann plots for four separate experiments. Populations determined from R- branch (▲) and P branch (+) have been plotted separately.

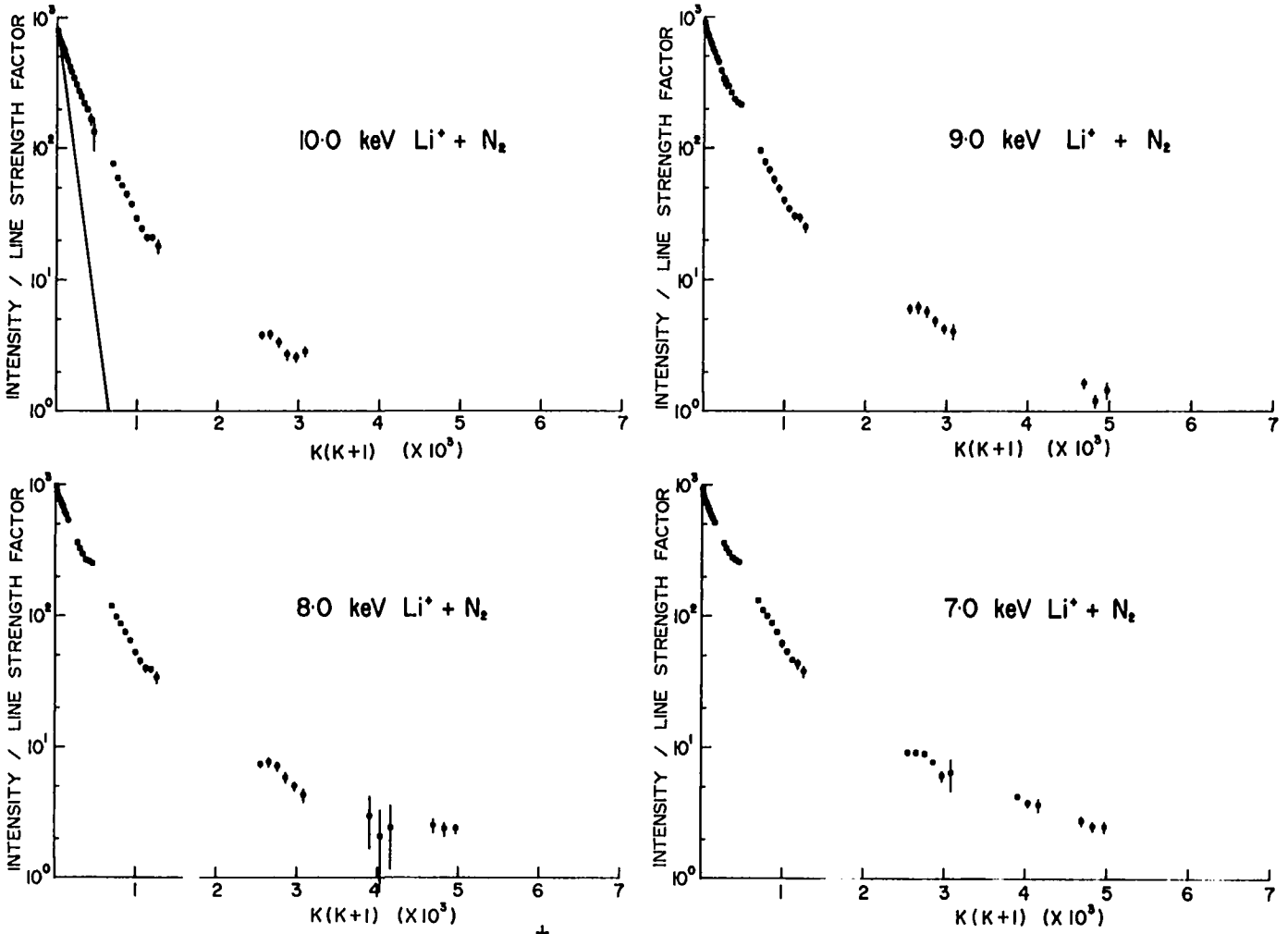

Figure 5.8. Boltzmann plots of N_2^+ rotational populations observed during 10.-7. keV Li^+ excitation. Boltzmann plot for 300 K distribution indicated by solid line in 10.0 keV $Li^+ + N_2$ graph.

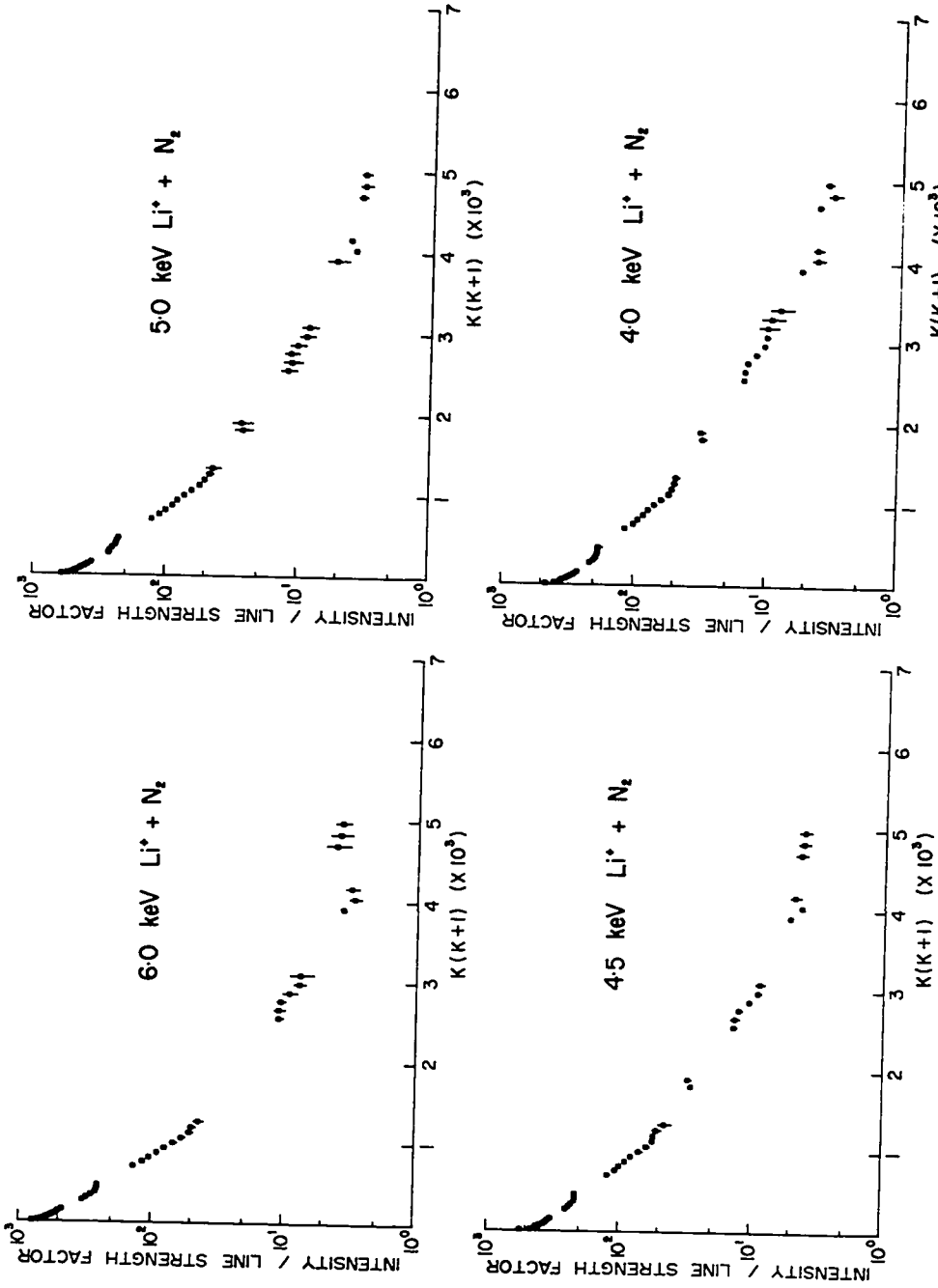

Figure 5.9 Boltzmann plots of N_2^+ rotational populations observed during 6.-4. keV Li^+ excitation.

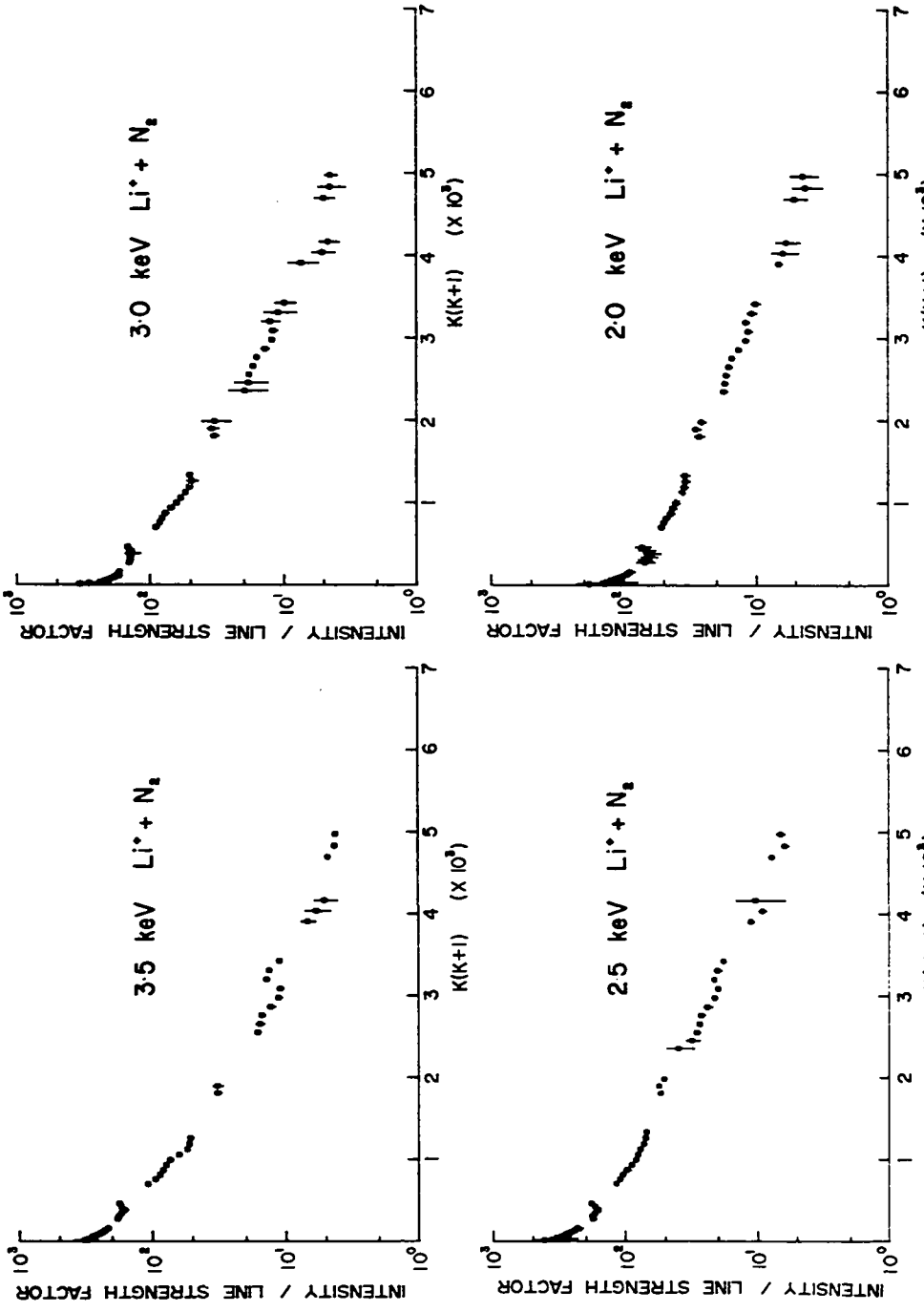

Figure 5.10 Boltzmann plots of N_2^+ rotational populations observed during 3.5-2. keV Li^+ excitation.

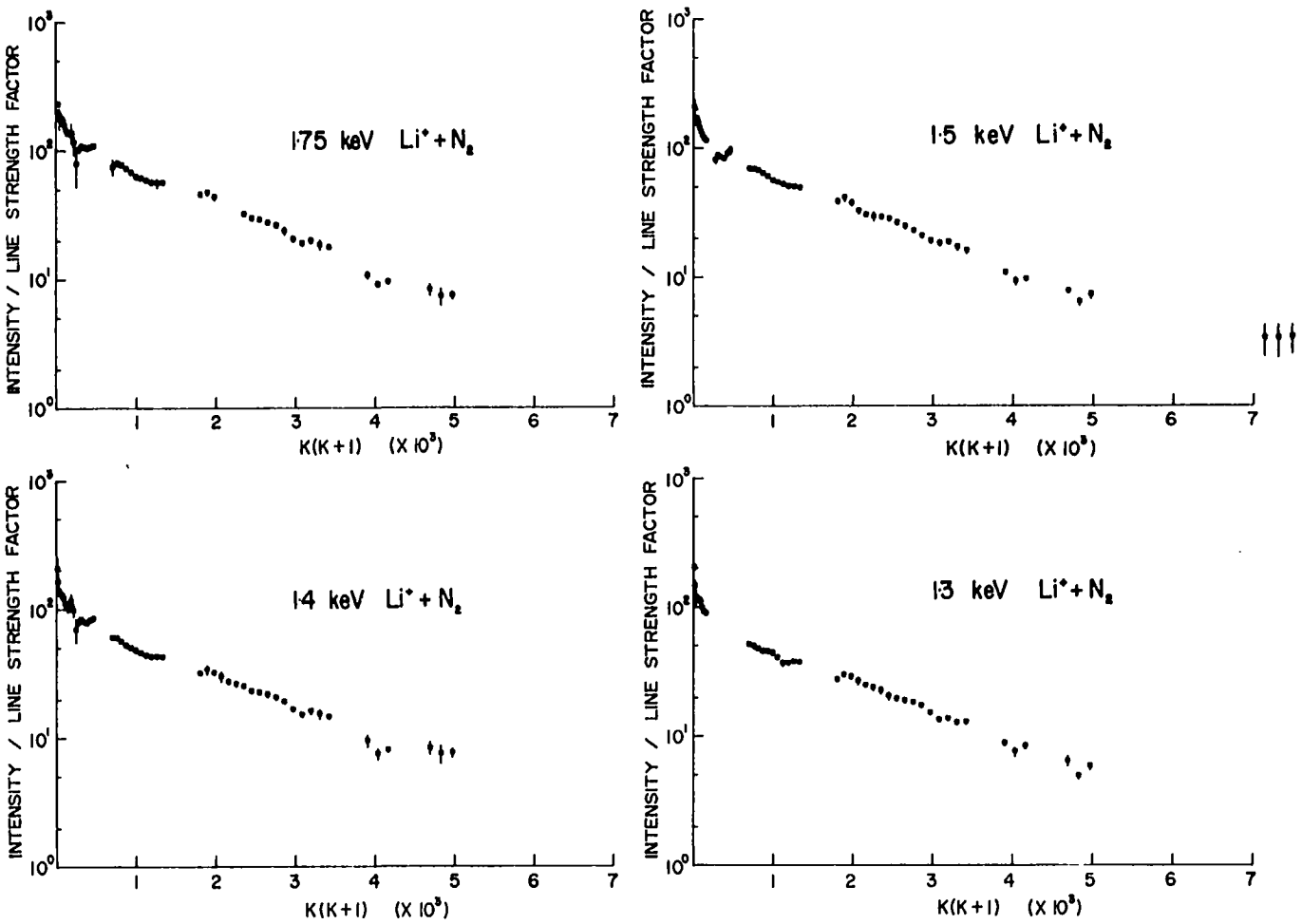

Figure 5.11 Boltzmann plots of N_2^+ rotational populations observed during 1.75-1.3 keV Li^+ excitation.

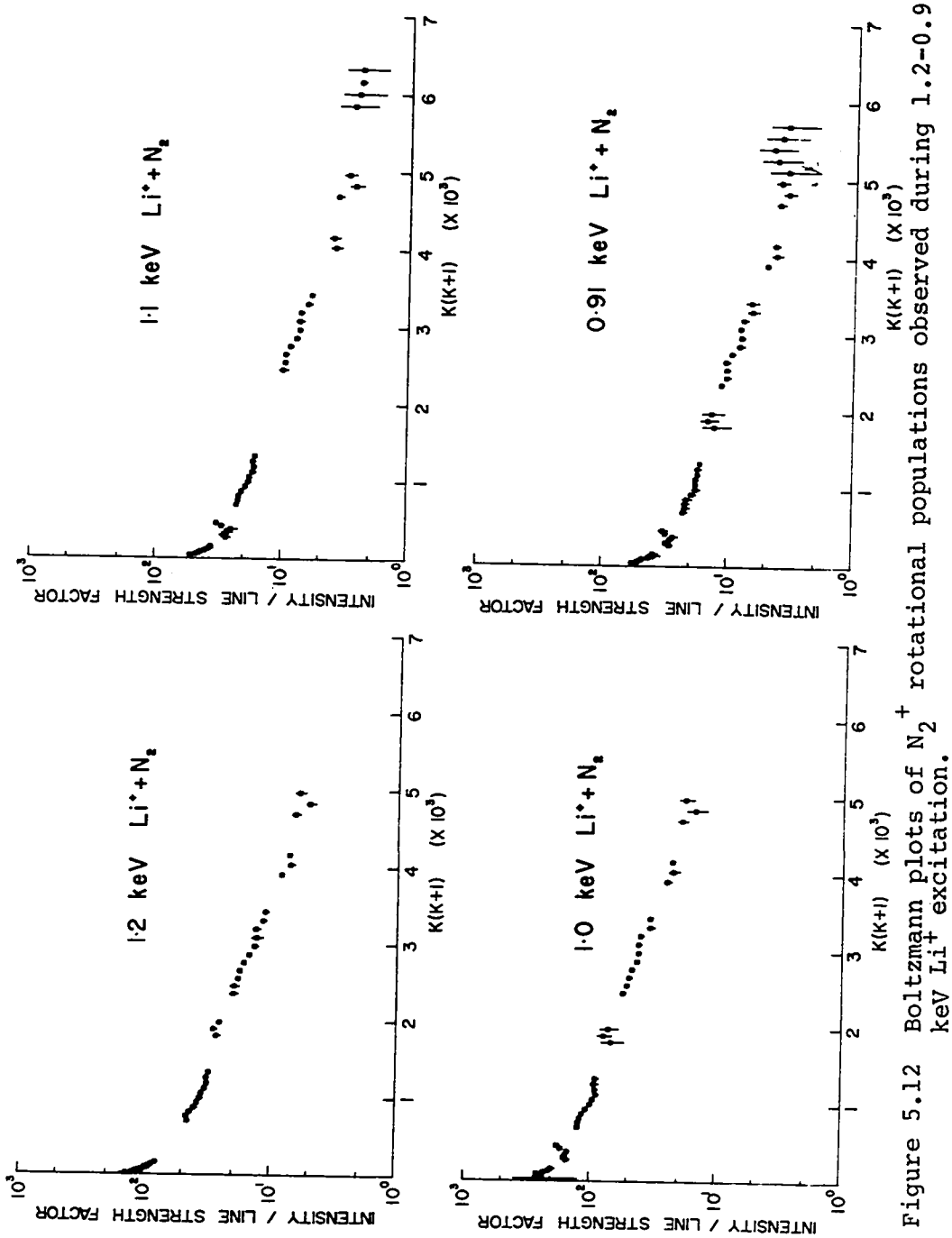

Figure 5.12 Boltzmann plots of N_2^+ rotational populations observed during 1.2-0.91 keV Li^+ excitation.

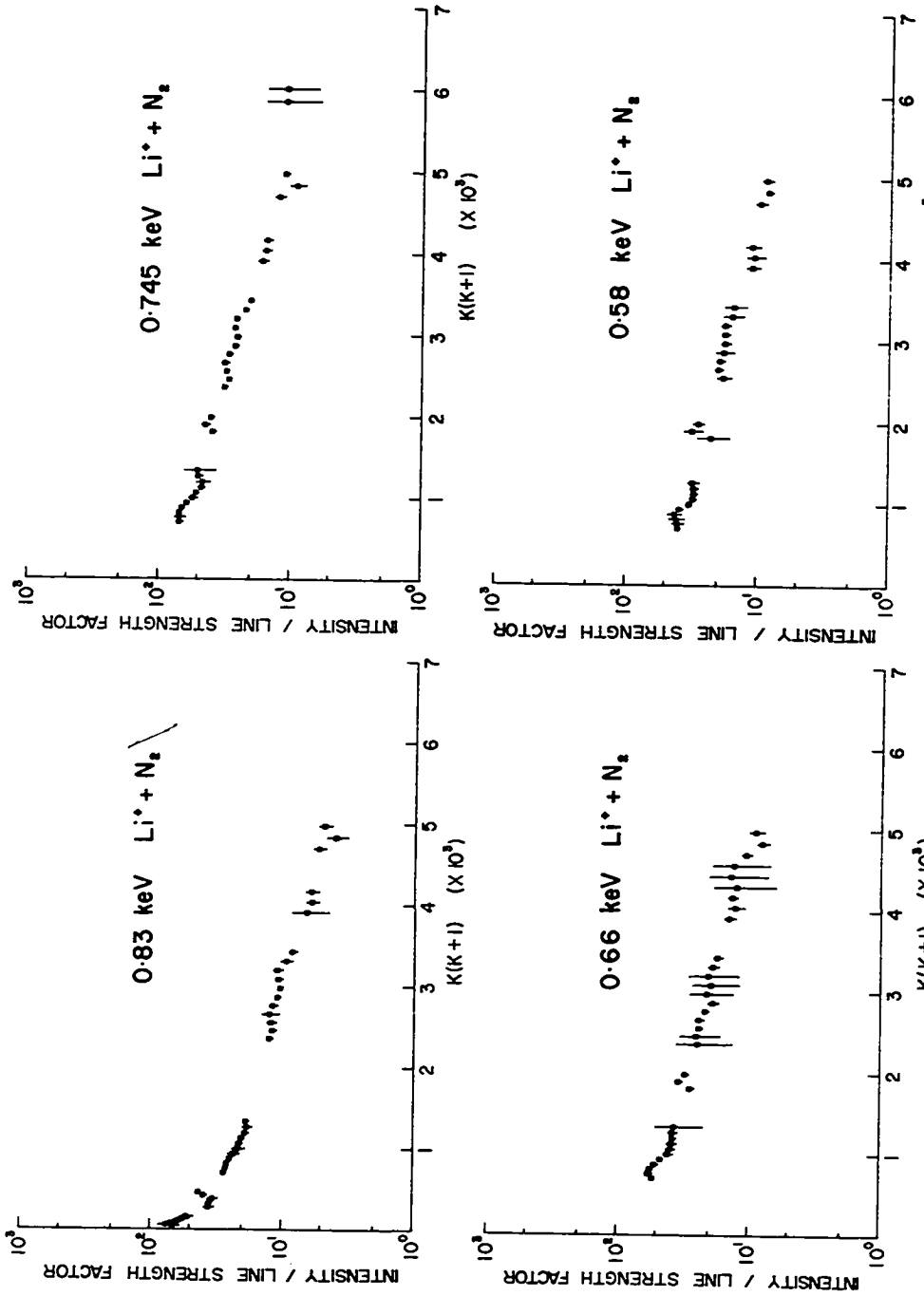

Figure 5.13 Boltzmann plots of N_2^+ rotational populations observed during 0.83-0.58 keV Li^+ excitation.

become significantly populated with respect to the lower levels. At these lower energies, the sharp increase of the populations of the lower levels is associated with excitation by secondary electrons. The distributions also tend towards linearity suggesting a possible approach to rotational equilibrium. A Boltzmann fit to the 0.58 keV Li^+ data gives a temperature close to 9000°K. However analysis of the 1.5 keV Li^+ spectrum in figure 5.3 suggests that even at low ion energies, rotational disequilibrium still exists. The results (figure 5.14) indicate that the non-Boltzmann "tail" observed in distributions produced by high energy collisions is still present but that its onset is at much higher rotational levels.

The information given in the previous "Boltzmann plots" is summarized in the contour plot presented in figure 5.15 where the rotational populations of the various rotational levels have been plotted as a function of inverse velocity squared. Data for all levels were obtained from a smooth curve representing the observed distribution at each energy so that no breaks occur in the plot. The contour lines give the relative population of each level referenced to the maximum population of the distribution observed for a given ion energy. At the higher energies, the rotational excitation of the molecule increases significantly as the velocity of the incident ion decreases. In the same energy range. the upper

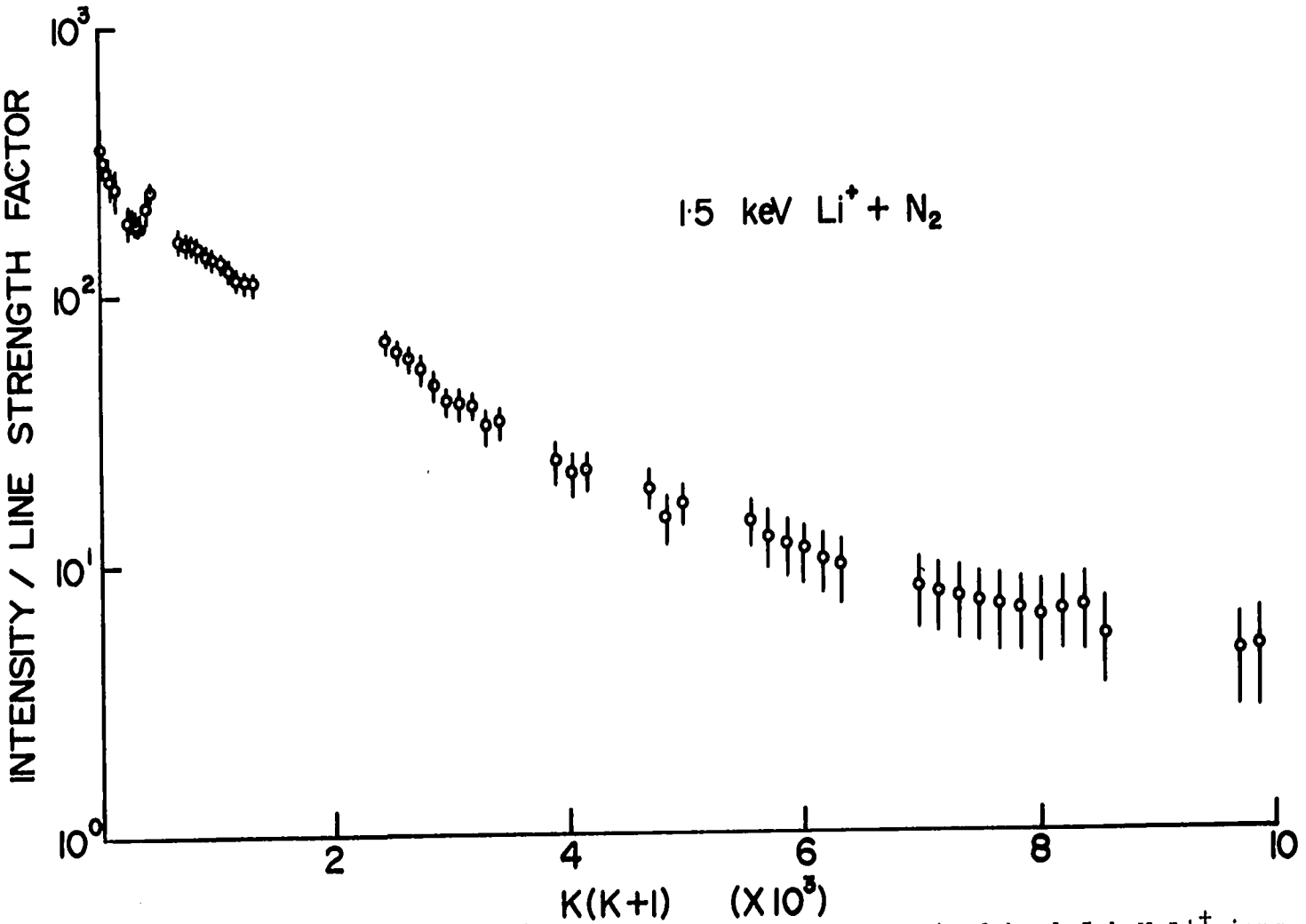

Figure 5.14. Boltzmann plot of N_2^+ rotational populations excited by 1.5 keV Li^+ ions Observations have been extended to K"= 100 of the (0,0) band.

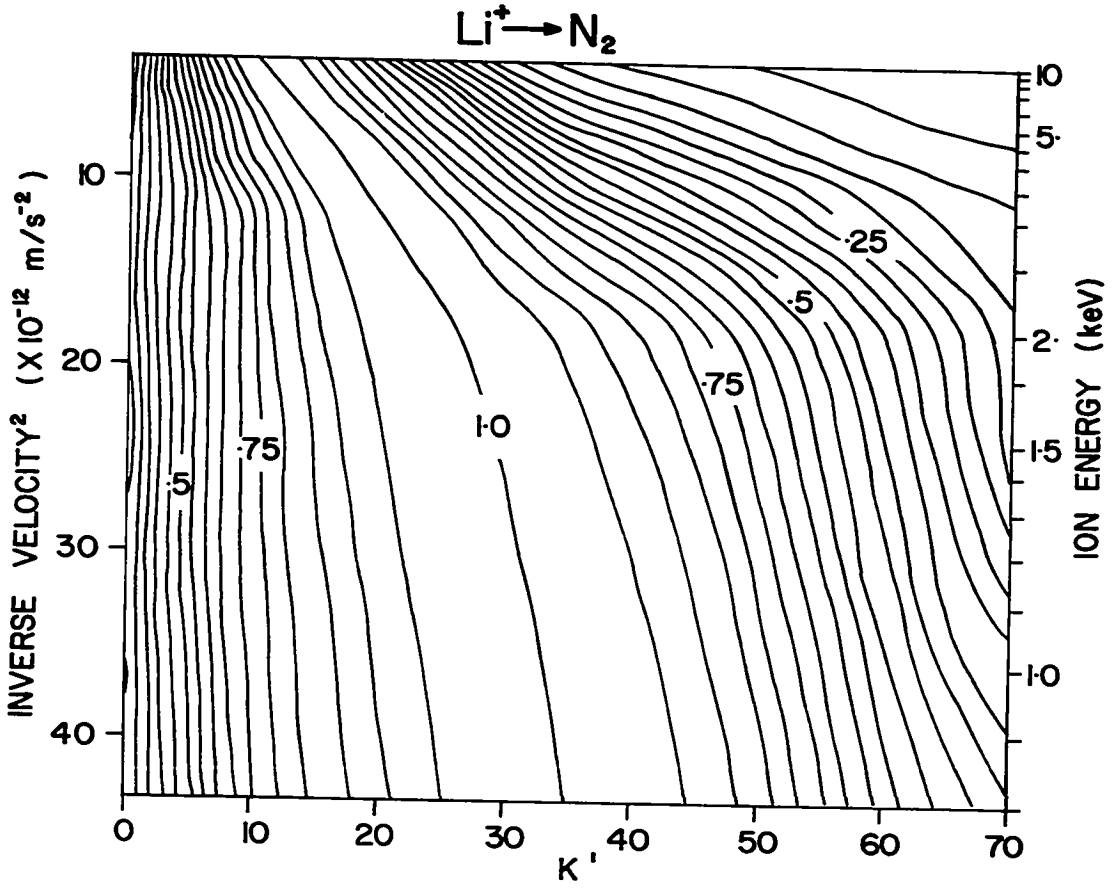

Figure 5.15. Rotational development of $N_2^+B(v'= 0)$ state as a function of reciprocal velocity for Li^+ excitation. The contour lines give the relative population of each level referenced to the maximum population of the distribution at each energy.

rotational states (K'>40) are populated more rapidly than suggested by the trend of the maximum. However below 2 keV there is a sharp change in the rate at which the relative populations of these upper states increase. Also in this lower energy range, the rate at which K' changes with inverse velocity squared is independent of the contour chosen indicating that the shape of the population distribution for the high K' levels remains the same as a function of energy but shifts towards higher rotational levels.

5.2.2 $Na^+ + N_2$

For Na^+ excitation, spectra were taken with incident ion energies in the range 2.5-25 keV. Figure 5.16 shows typical spectra compared to the 10 keV Li^+ spectrum. Comparison of the two spectra at 10 keV reveals that the rotational excitation by Na^+ ions is significantly greater than for Li^+ ions. All spectra were taken at collision chamber pressures of 4 millitorr. The lower pressure was necessary in order to reduce the effects of secondary processes. Figure 5.17 shows the spectra obtained in 9.0 keV Na^+ collisions at collision chamber pressures of 20 millitorr and 2 millitorr. At the lower pressure, the intensity reversal is clearly observed. However, at high pressure the intensities of the lines are reversed with the even K" lines being stronger. The effect

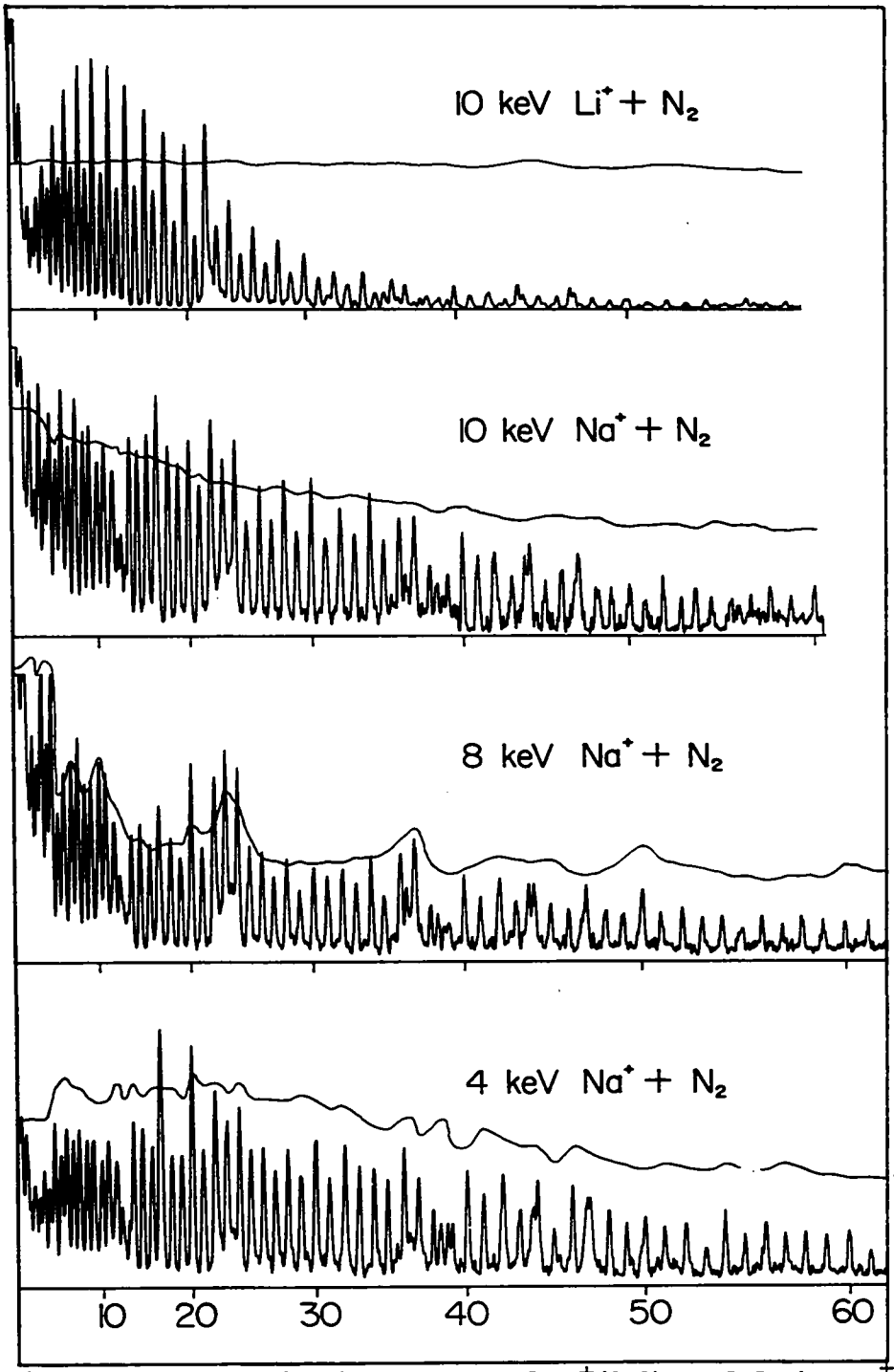

Figure 5.16. Rotational Structure of $N_2^+(0,0)$ Band during Na^+ excitation. Beam current indicated by lines above spectra.

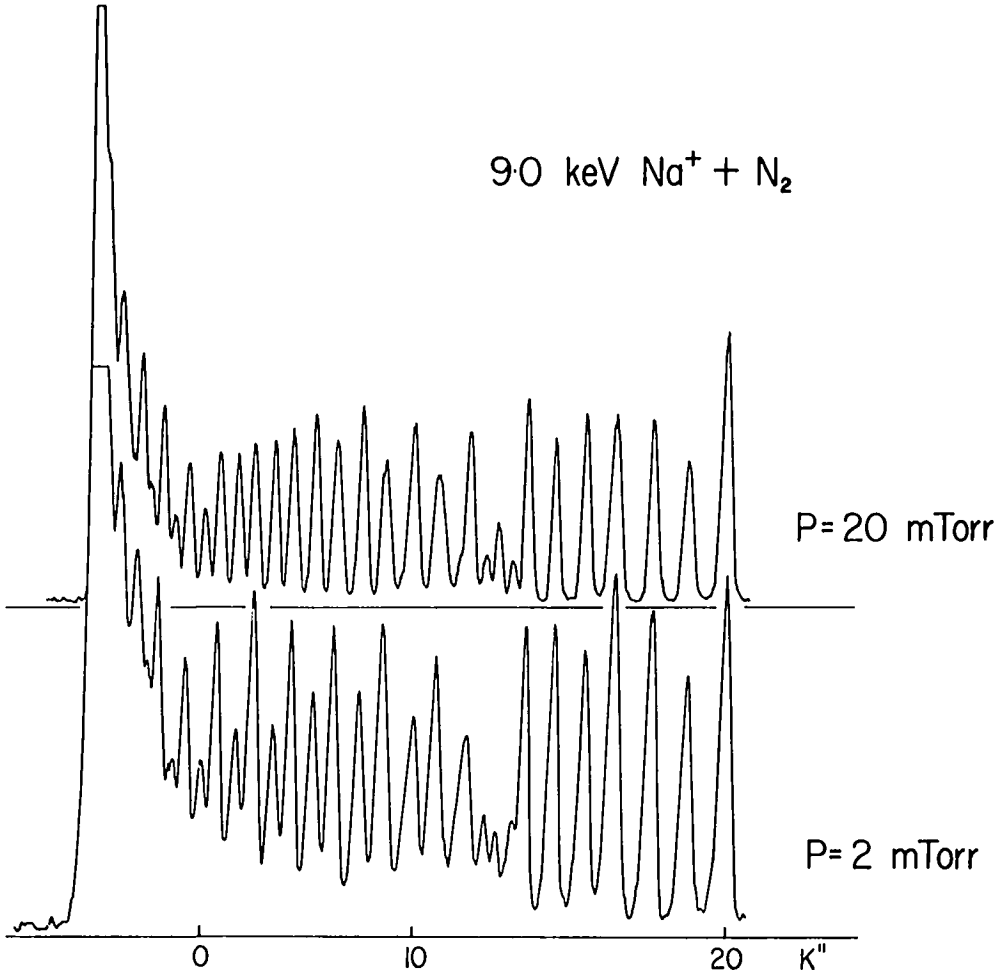

Figure 5.17. Effect of pressure on observed rotational structure of $N_2^+(0,0)$ band during Na^+ excitation.

is characteristic of secondary electron excitation of N_2 producing a Boltzmann distribution at ambient temperature in the N_2^+B state (Moore and Doering (1969)) superimposed on the ion produced spectrum at much higher temperature.

Due to the smaller cross-section of the N_2^+B ($v'= 0$) state for Na^+ than for Li^+ excitation and the need to work at low pressures, a larger spectral slit width ($0.55A^o$) was necessary at lower energies in order to obtain a usable signal to noise ratio. The first 20 lines of the spectrum were not analysed at lower energies (<10 keV) due to the lack of resolution and the possibility of secondary electron contributions. The results are given in figures 5.18 - 5.21. As with Li^+ excitation, non-linearity was observed in the "Boltzmann plots" for the more energetic incident Na^+ ions. However in this case, the non-linearity occurred at energies greater than those observed in the Li^+ data. At energies between 10-7 keV, the curvature is slight while distributions at lower energies could be fitted by a straight line. From a Boltzmann fit of the 2.5 keV Na^+ data a rotational temperature close to 9500^oK was obtained. At these lower energies, the spectra did not extend to high enough K" to determine if deviations from a Boltzmann distribution occurred as were observed for the 1.5 keV Li^+ data. Contributions due to $N_2^+(1,1)$ overlapping were again subtracted. Since no work was done on the vibrational excitation in Na^+ collisions, the

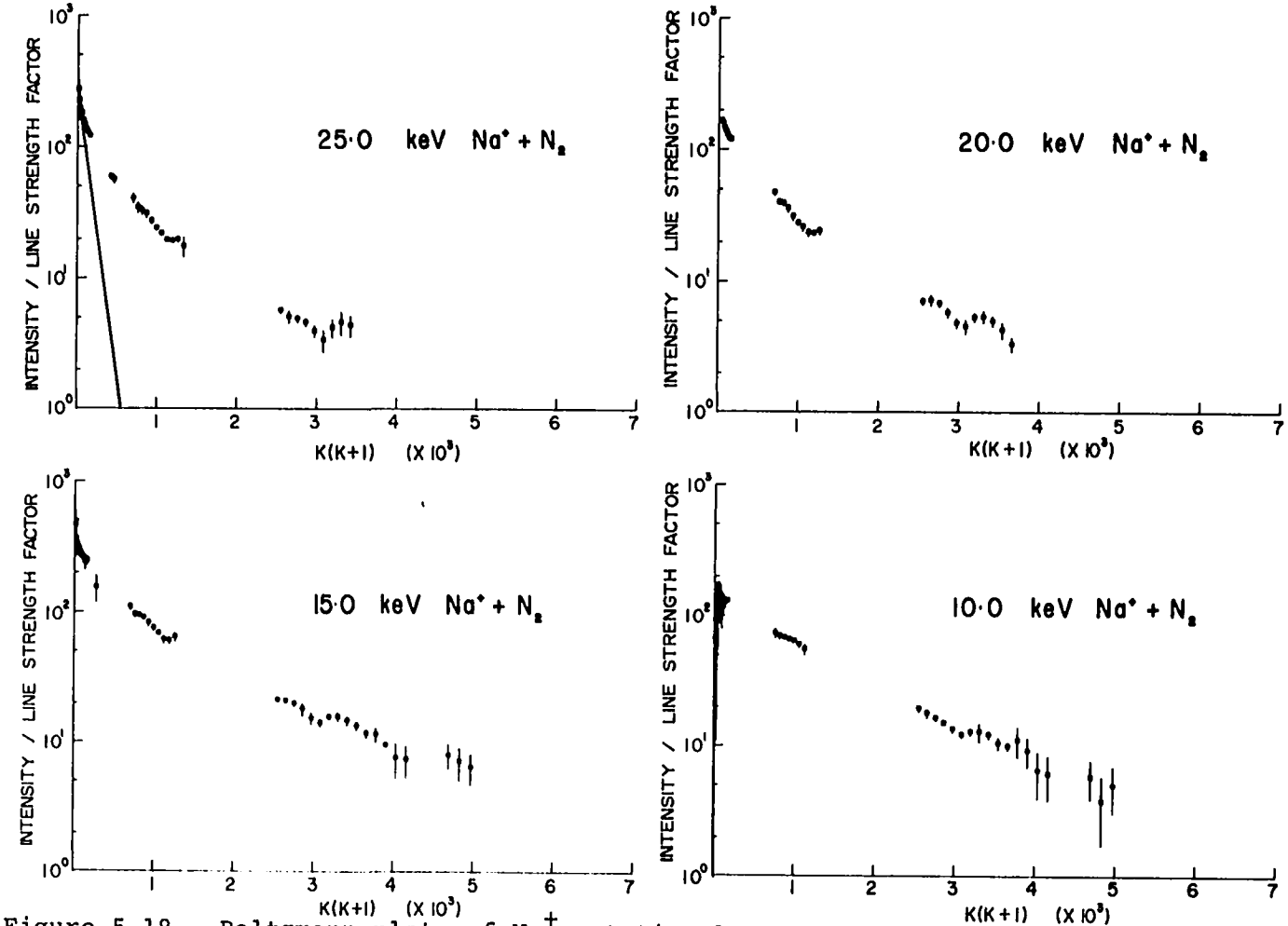

Figure 5.18. Boltzmann plots of N_2^+ rotational populations observed during 25.-10. keV Na^+ excitation. Boltzmann plot for 300 K distribution is indicated by solid line in 25. keV $Na^+ + N_2$ graph.

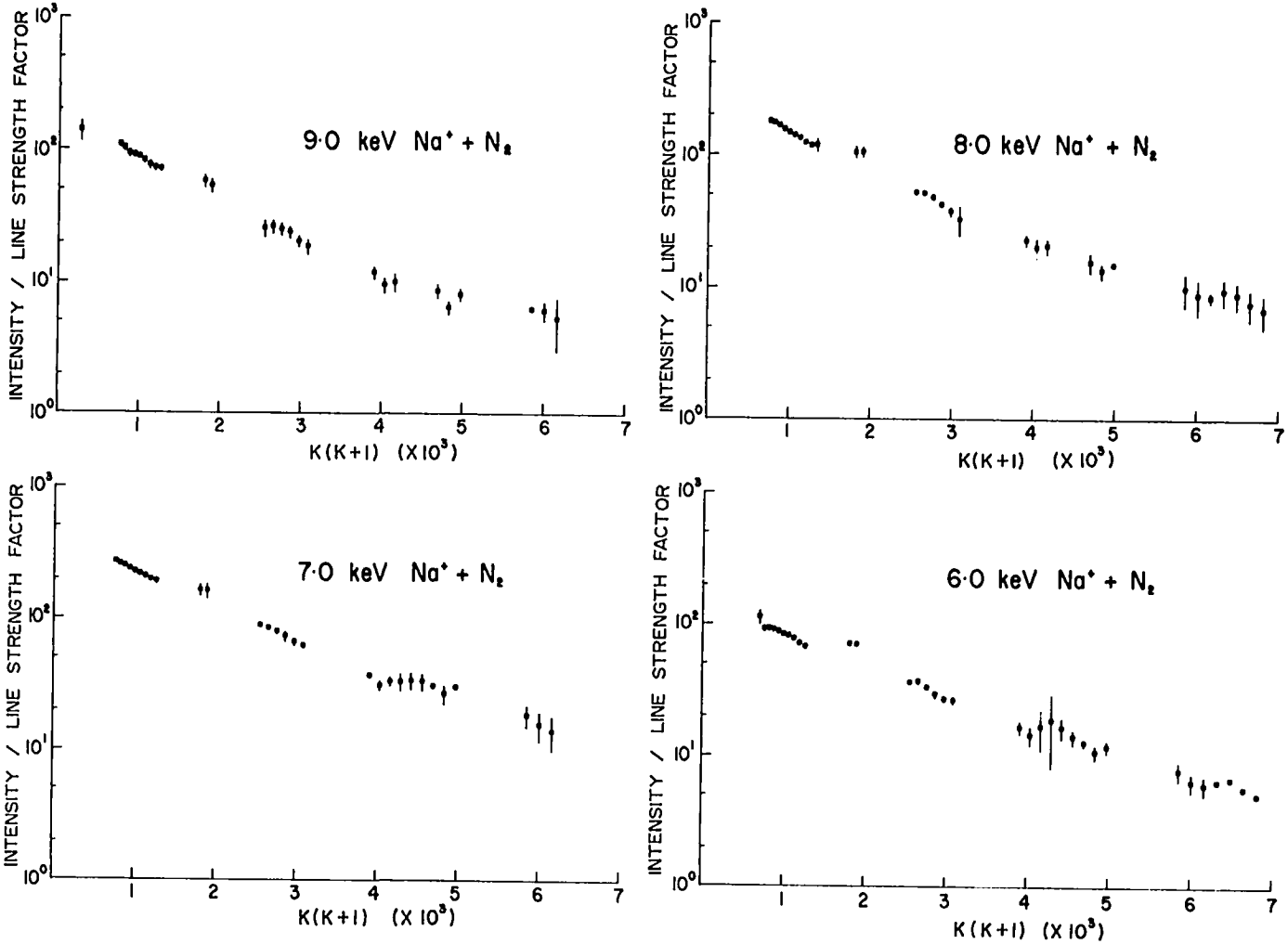

Figure 5.19 Boltzmann plots of N_2^+ rotational populations observed during 9.-6. keV Na^+ excitation.

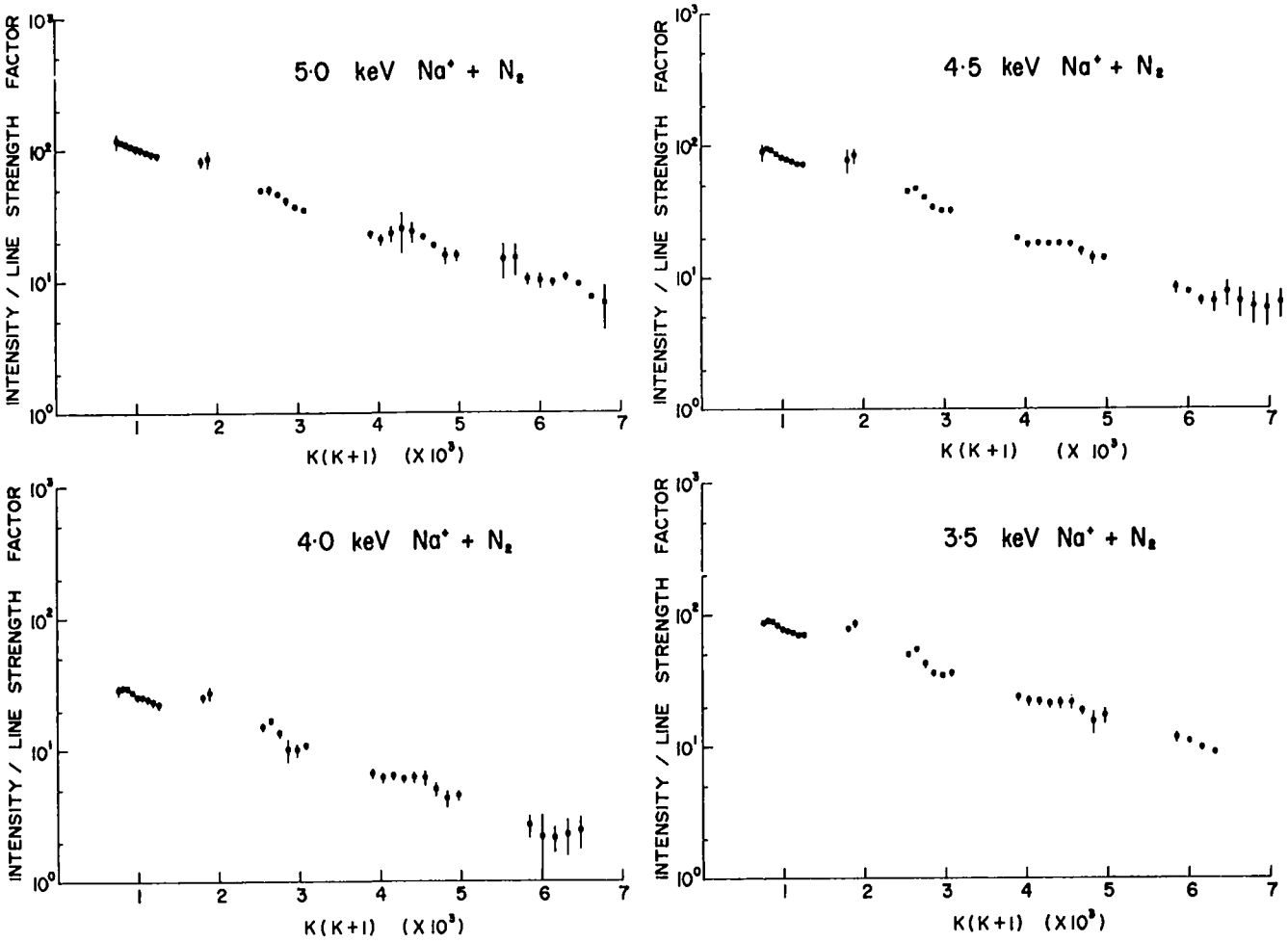

Figure 5.20 Boltzmann plots of N_2^+ rotational populations observed during 5.-3.5 keV Na^+ excitation.

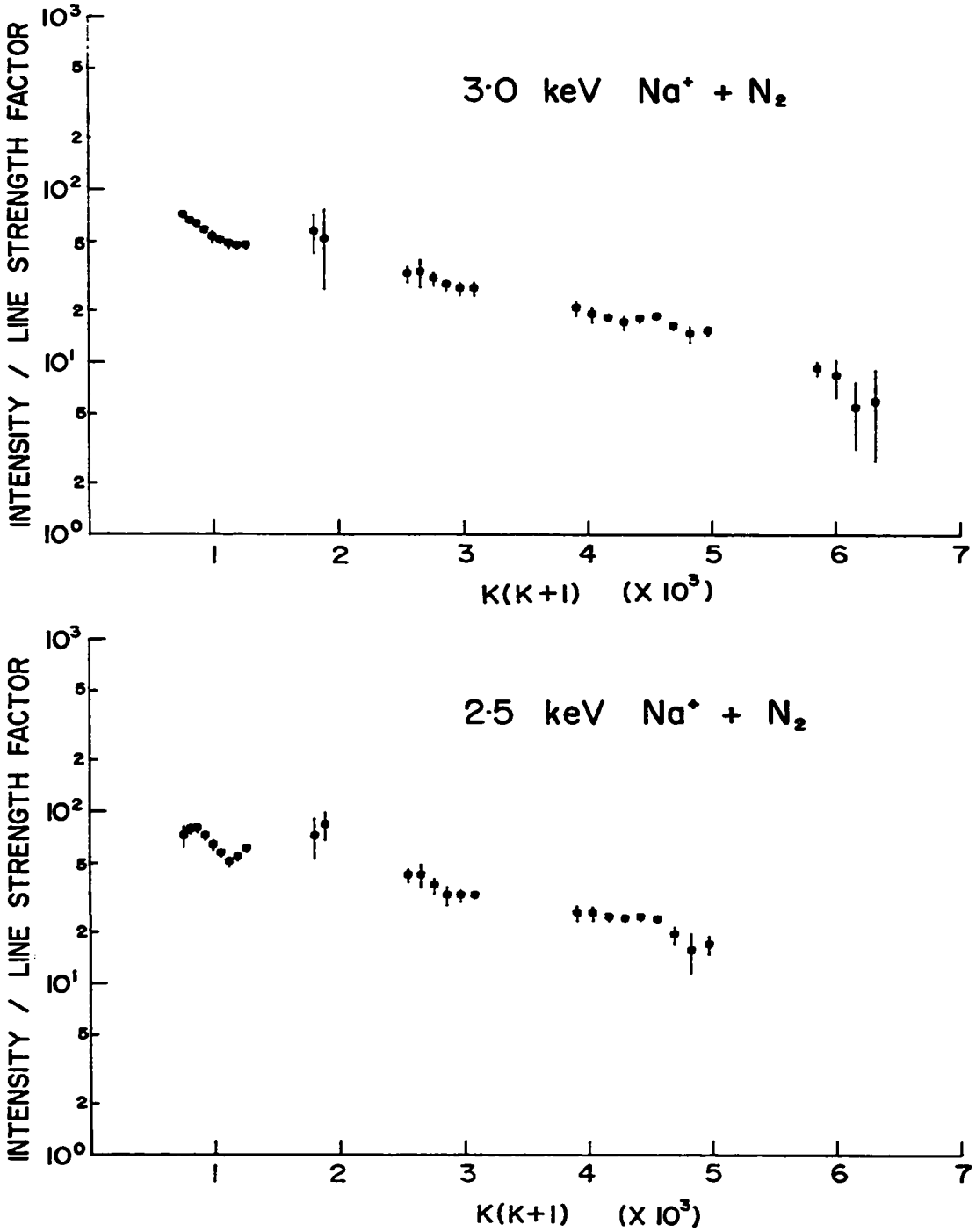

Figure 5.21. Boltzmann plots of N_2^+ rotational populations observed during 3.-2.5 keV Na^+ excitation.

corrections were based on the vibrational excitation in Li^+ collisions at the same laboratory velocity (Moore and Doering (1969)).

The results of the "Boltzmann plots" for all energies at which spectra were taken are summarized in the contour plot presented in figure 5.22. The data for the lower rotational levels were obtained from the extension of a smooth curve representing the distribution at each energy. The contour lines represent the relative populations of these levels compared with the maximum population of the particular distribution. For Na^+ ions, the rotational excitation increases smoothly as the energy of the incident ion decreases. At low energies, the rate of increase of rotational excitation with inverse velocity squared is not as great as at high energies. This change in the trend of the relative populations towards higher rotational levels occurs at an ion energy of 6 keV. Over the full energy range, the shift in relative populations for the higher rotational levels as a function of inverse velocity squared follows the general trend of the maximum population.

5.2.3 $K^+ + N_2$

For K^+ ions, spectra were taken only at energies of 4 and 7 keV. Due to secondary electron excitation, these experiments were done at low pressures and the

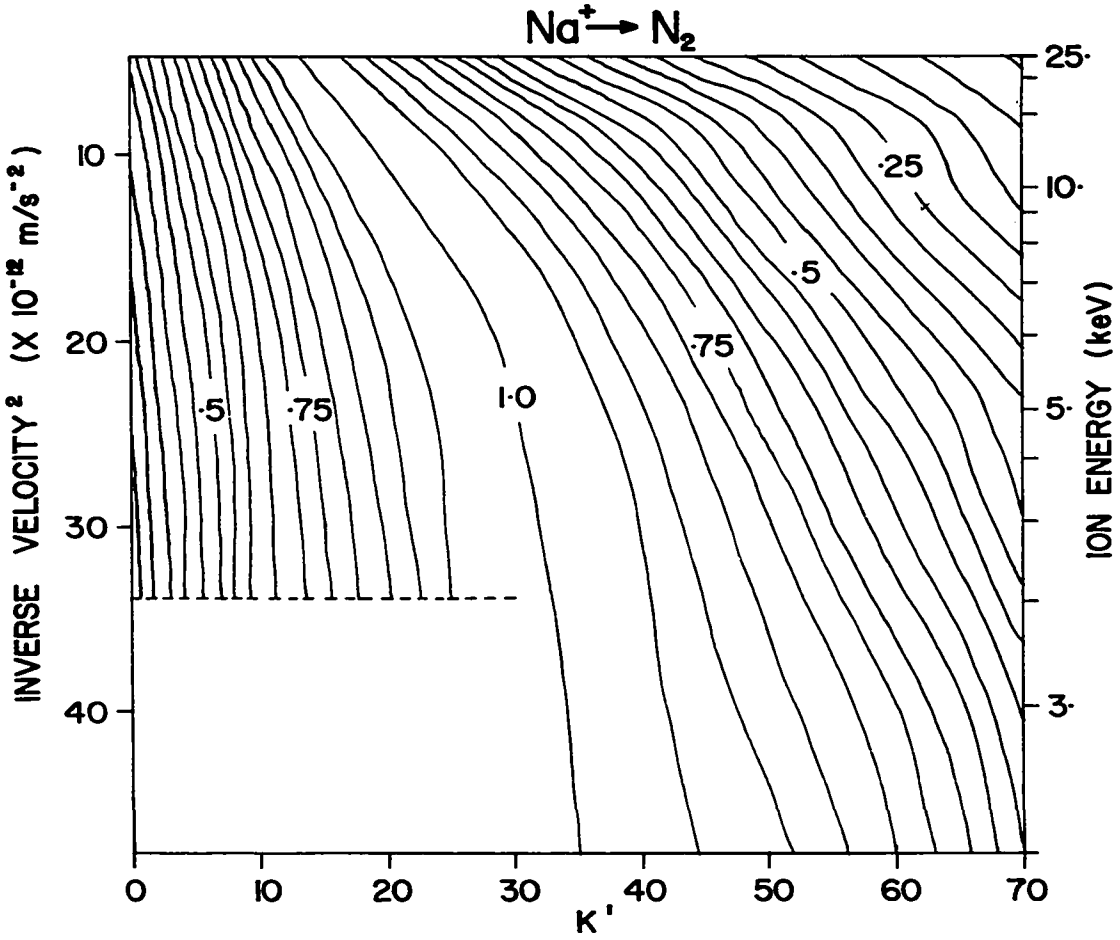

Figure 5.22. Rotational development of $N_2^+B(v'= 0)$ state as a function of reciprocal velocity for Na^+ excitation. Contour lines give the relative population of each level referenced to the maximum population of the distribution at a particular energy.

resulting low light levels necessitated a large spectral slit width (0.55A°). Most of the band was not usable due to overlapping of K II lines so that only a few points were obtained for each Boltzmann plot (figure 5.23). However from these points, it is apparent that extensive rotational excitation of the B state occurs during K^+ ion excitation, contrary to the results of Lowe (1966).

5.3 Vibrational and Rotational Excitation of v'= 1 State

5.3.1 $Li^+ + N_2$

Similtaneous vibrational and rotational excitation were studied by observing the (1,1) band of the First Negative system of N_2^+. A typical high resolution (spectral slit width 0.11A°) spectrum is given in figure 5.24 where the R and P branches of the (0,0) and (1,1) bands have been labelled separately. There is a gain change of 2.5 times for K_1'' greater than 20. The effect of a perturbation on the rotational levels of the v'= 1 state by the $A^2\Pi$ state can be seen by the splitting of the spin doublets around K_1'' equal to 13. The wavelengths and numbering of the (1,1) band rotational lines were determined using the work of Fassbender (1924). Wavelengths of lines with K_1'' greater than 28 were determined by iteration using the wavelengths of the (0,0) band for calibration (Childs (1932)). Since the spectra of the (1,1) band were of sufficiently high resolution, the rotational populations of the upper states were determined directly from

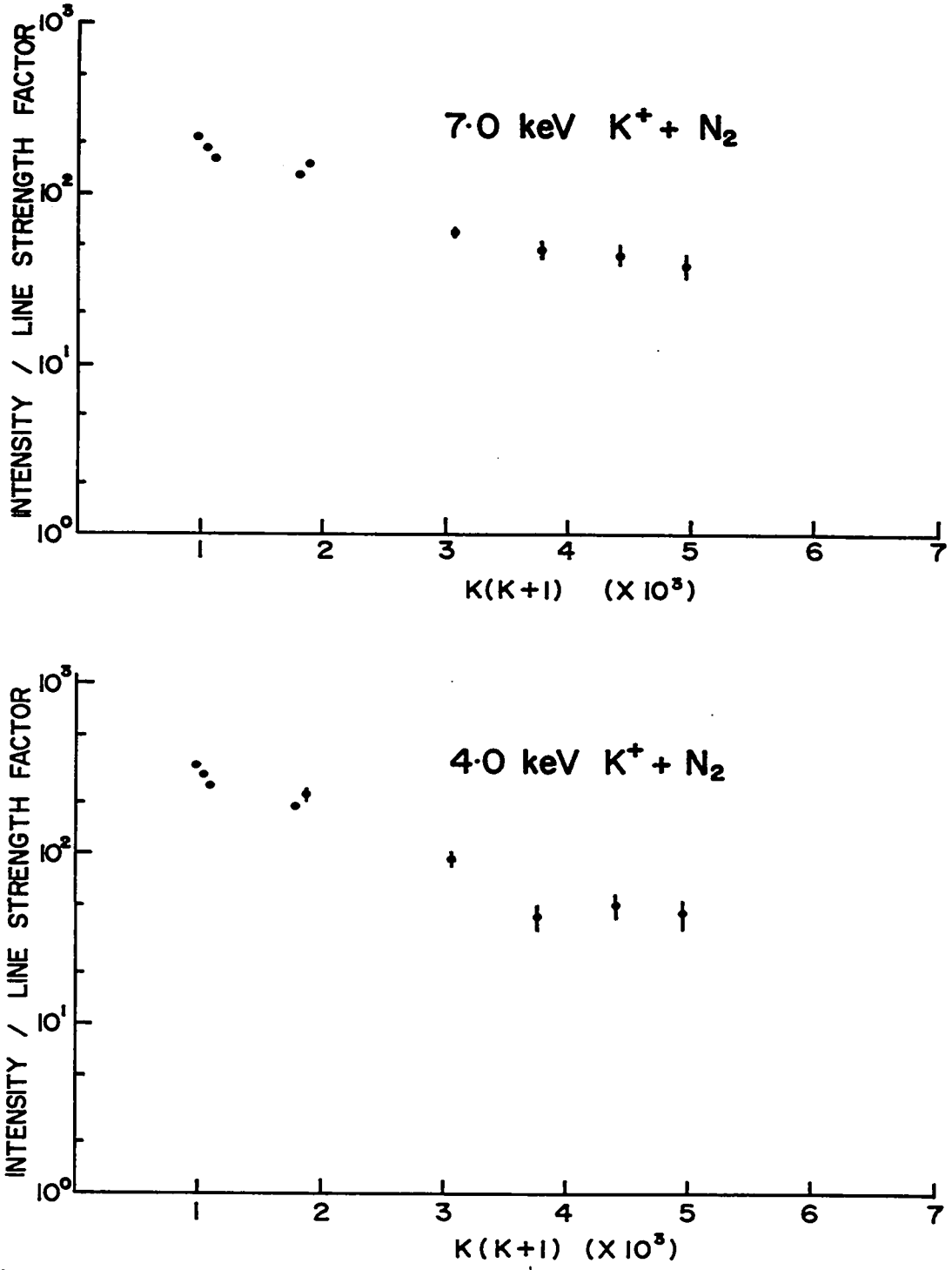

Figure 5.23. Boltzmann plots of N_2^+ rotational populations observed during 7.0 keV and 4.0 keV K^+ excitation

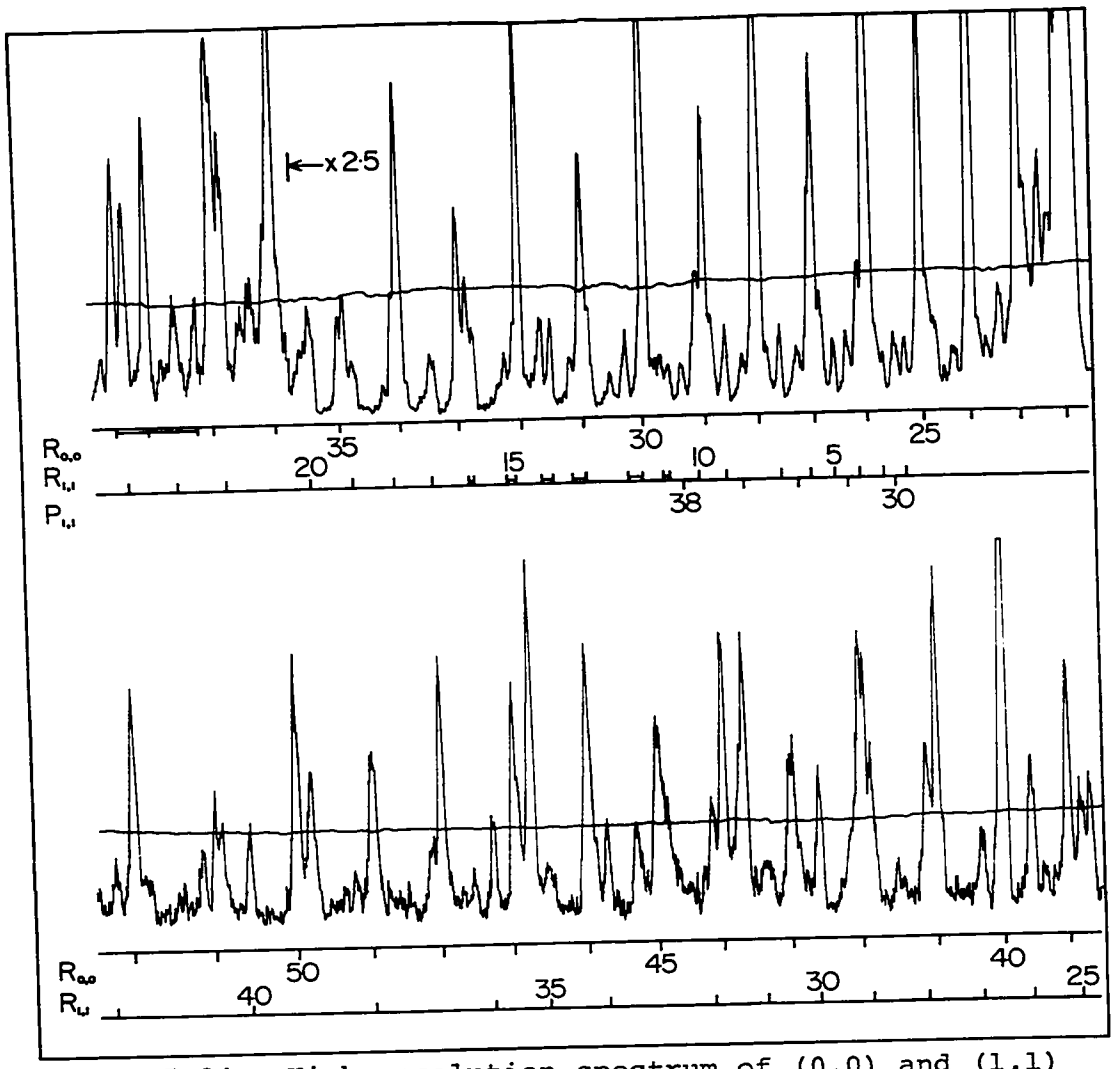

Figure 5.24. High resolution spectrum of (0,0) and (1,1) Bands of First Negative System of N_2^+ excited by 8.0 keV Li^+ ions. Beam current is displayed above spectrum. R-and P-branch lines of (0,0) and (1,1) bands are numbered separately.

equation (5.1).

5.3.2 Rotational Excitation

The graphs of log $(I(J',J")/\upsilon^4 S(J',J"))$ as a function of upper state rotational energy are presented in figures 5.25 and 5.26 for Li^+ excitation at energies of 10-4 keV. The distributions for both the v'= 0 and v'= 1 levels are plotted with the smooth curve representing the v'= 0 data also being drawn through the v'= 1 data. The ratio of the two curves indicates the relative populations of the two levels from which the vibrational excitation can be determined. The rotational development in both levels is similar with a slight deviation from the smooth curve occurring in the v'= 1 state at the higher ion impact energies. This deviation may be due to an incorrect choice of the background level since the signal to noise ratio for the latter points was 1:1.

5.3.3 Vibrational Excitation

For electron excitation of N_2^+, the vibrational distribution of the excited electronic states is well described by the Franck - Condon principle if the electron energy is greater than 100 eV (Fan (1956), Culp and Stair (1967), Moore and Doering (1968)). In this case, if the process involves the excitation of the molecule from the ground state ($N_2X(v"= 0)$) to a particular electronic state ($N_2^+B(v'= i)$) then the ratio of the population of the ith

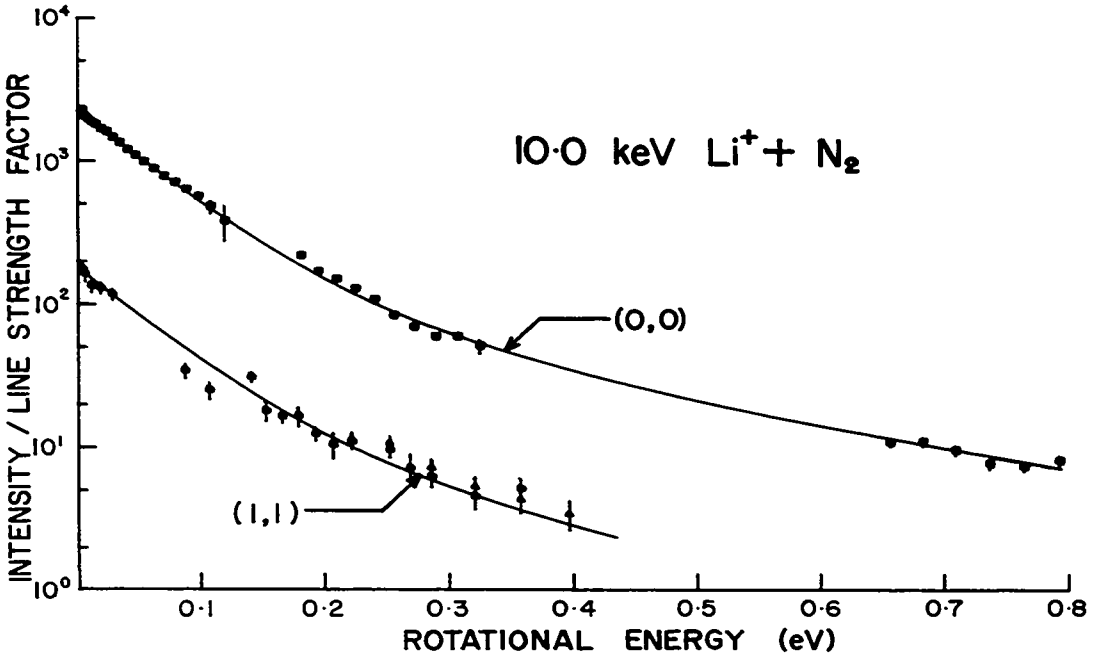

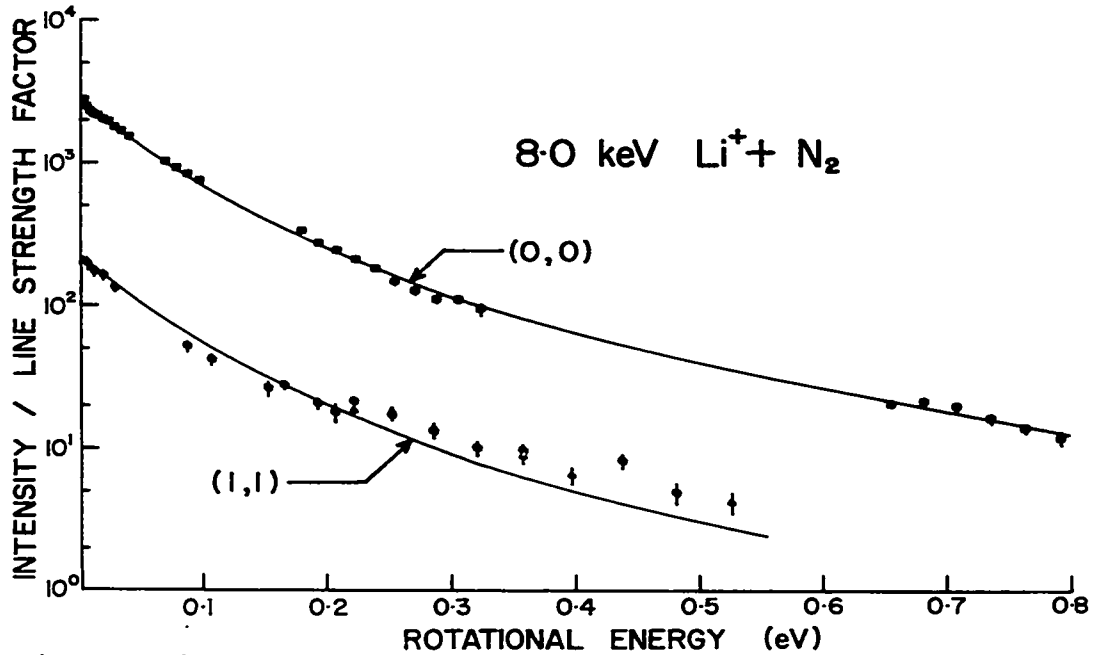

Figure 5.25. Boltzmann plots of rotational populations in v'= 0, 1 levels of N_2^+B state excited by Li^+ ions. The smooth fit of the (0,0) data is also drawn through the (1,1) data.

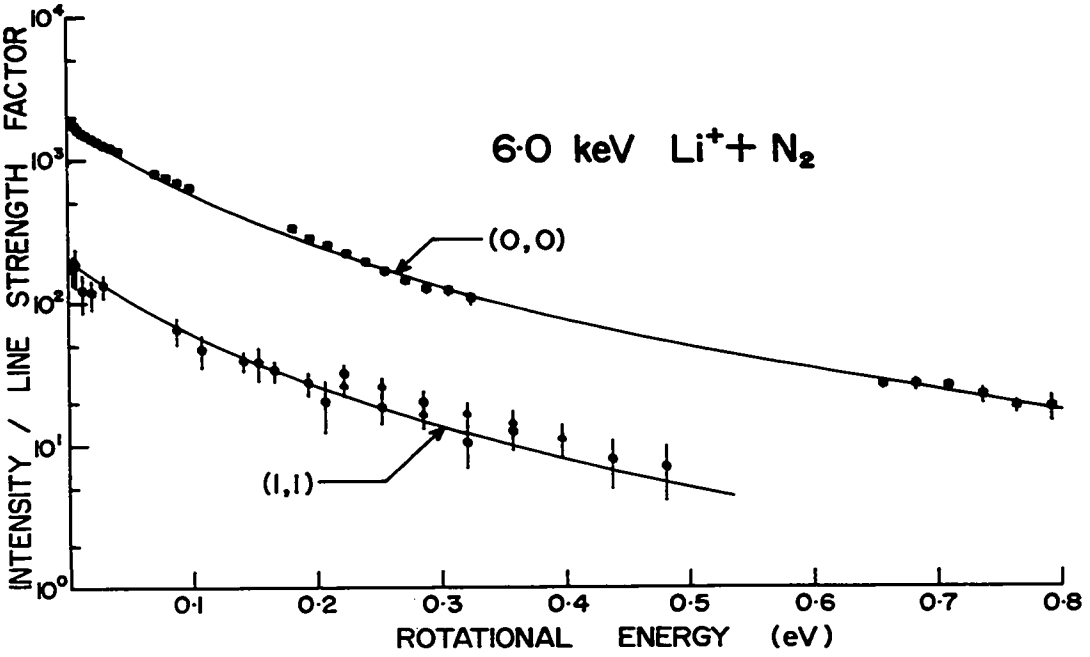

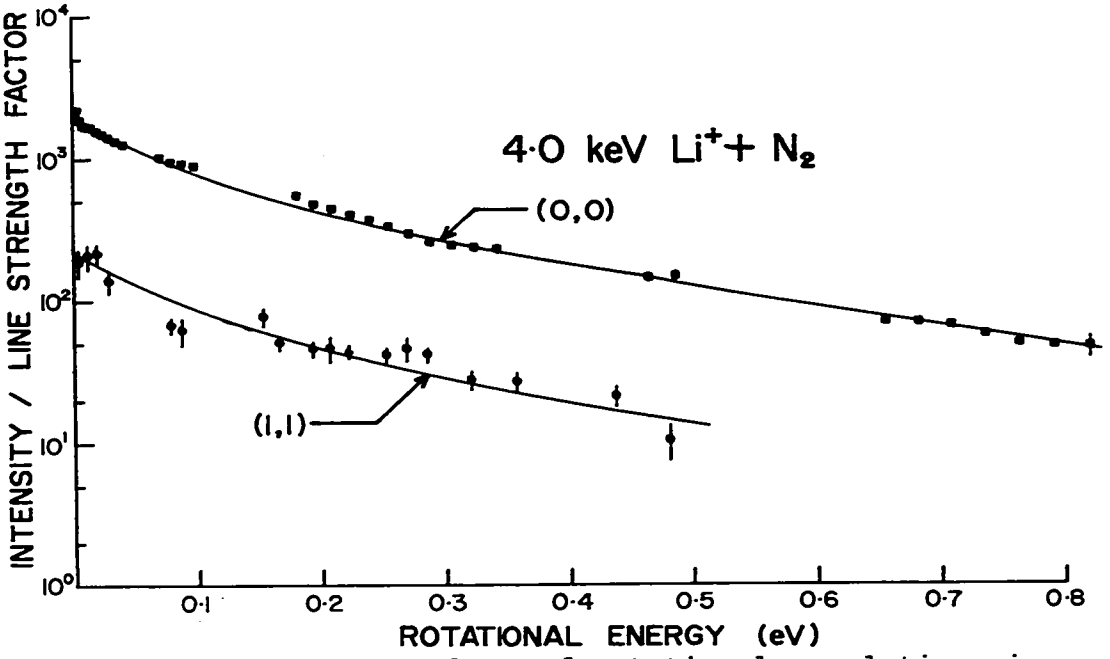

Figure 5.26. Boltzmann plots of rotational populations in v'= 0, 1 levels of N_2^+B state excited by Li^+ ions. The smooth fit of the (0,0) data is also drawn through the (1,1) data.

vibrational state to the v'= 0 state is just the ratio of the Franck-Condon factors for the two transitions

$$\frac{N_i}{N_o} = \frac{q_i^{X \rightarrow B}}{q_o^{X \rightarrow B}} \qquad (5.2)$$

If emissions are observed spectroscopically in a particular sequence, the ratios of the two bands within the sequence is

$$\frac{I(i,i-\Delta v)}{I(j,j-\Delta v)} = \frac{N_i}{N_j}\left[\frac{q_{i,i-\Delta v}}{q_{j,j-\Delta v}}\right]\left\{\frac{\lambda_{j,j-\Delta v}}{\lambda_{i,i-\Delta v}}\right\}^4 \qquad (5.3)$$

where $\lambda_{i,i-\Delta v}$ is the wavelength of the emission from state B to X and $q_{i,i-\Delta v}$ is the Franck-Condon factor for the transition. If during the collision, the vibrational wave function was perturbed, the ratio of the vibrational populations would differ from those predicted by the Franck-Condon factors.

In this work, the vibrational measurements were made using the rotational line intensities directly rather than comparing the intensities of band heads. The latter process assumes the same number of rotational lines contribute to each head and that each vibrational level has the same rotational development.

Using the Franck-Condon factors computed by Nicholls (1962) for the

$$N_2 X^1\Sigma_g^+ \rightarrow N_2^+ B^2\Sigma_u^+$$

and $N_2^+ B^2\Sigma_u^+ \rightarrow N_2^+ X^2\Sigma_g^+$

transitions, the predicted ratio for I(1,1)/I(0,0) is 4.23×10^{-2}. From the spectrum produced by 1.0 keV electrons a Boltzmann plot (figure 5.27) was prepared. Integration of the rotational line intensities for the two bands gave a ratio of 4.2×10^{-2} in good agreement with the calculated value. The vibrational excitation of N_2^+ by Li^+ ions was determined from the intensity ratios of the rotational lines within each band, the results being plotted in figure 5.28. The trend observed by Moore and Doering (1969) for a group of ions is represented by the solid line while the range in values of the ratio for the various ions is indicated by the dotted lines. The results of Polyakova et al (1968) for Li^+ excitation of N_2 are also presented. The ratios obtained in this work are consistently greater than the trend obtained by Moore and Doering. Within the velocity range, the ratio was found to increase monotonically with no suggestion of the maximum found by Polyakova et al at a velocity of 2×10^7cm/sec.

Using the vibrational information of figure 5.28 and the wavelengths of the rotational lines of the (1,1) band, corrections to the intensities of the (0,0) band lines were made. In this way, contributions to the rotational line intensities of the (0,0) band due to insufficient resolution were eliminated.

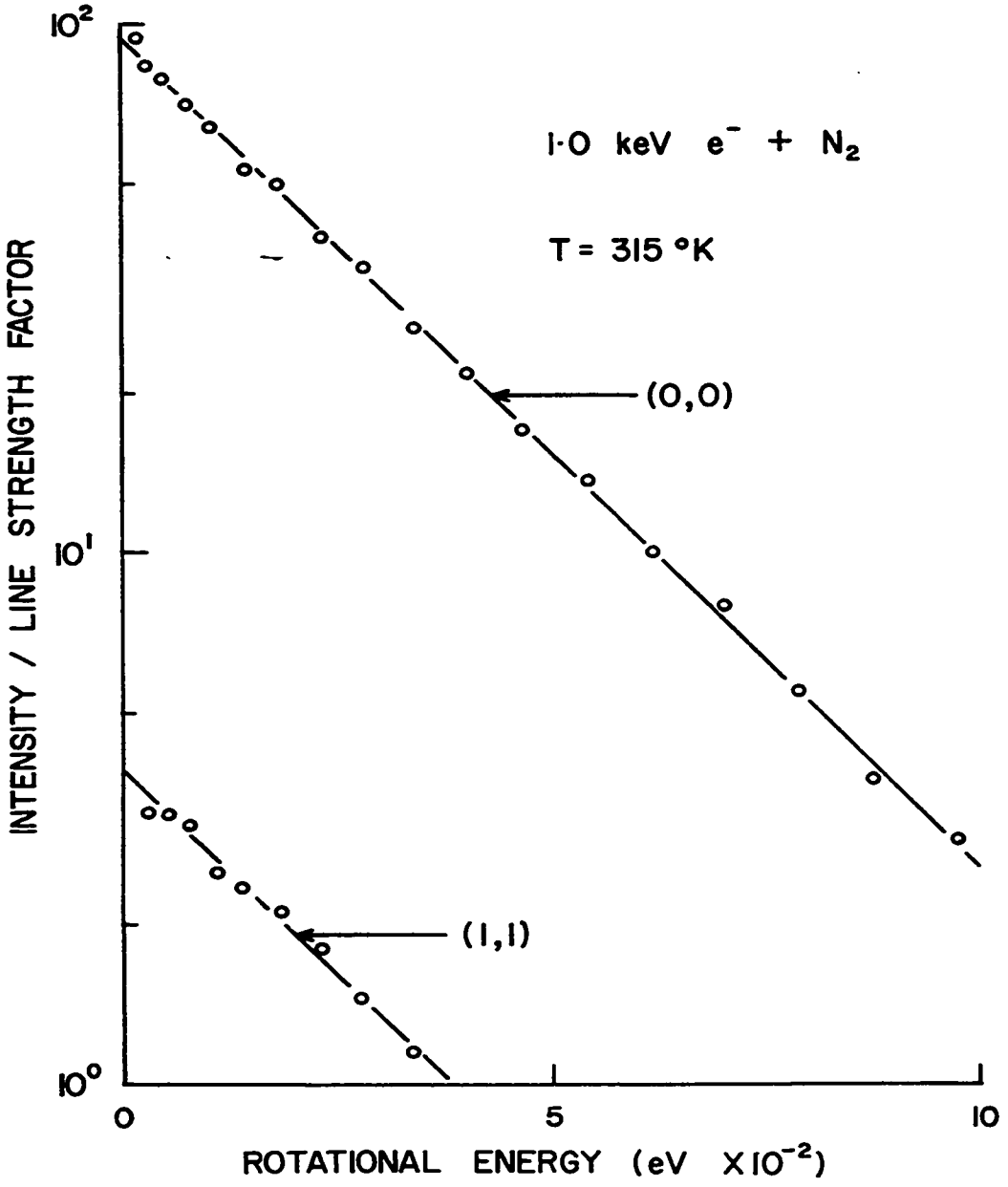

Figure 5.27. Boltzmann plots for $N_2^+B(v'= 0, 1)$ states excited by 1.0 keV electrons.

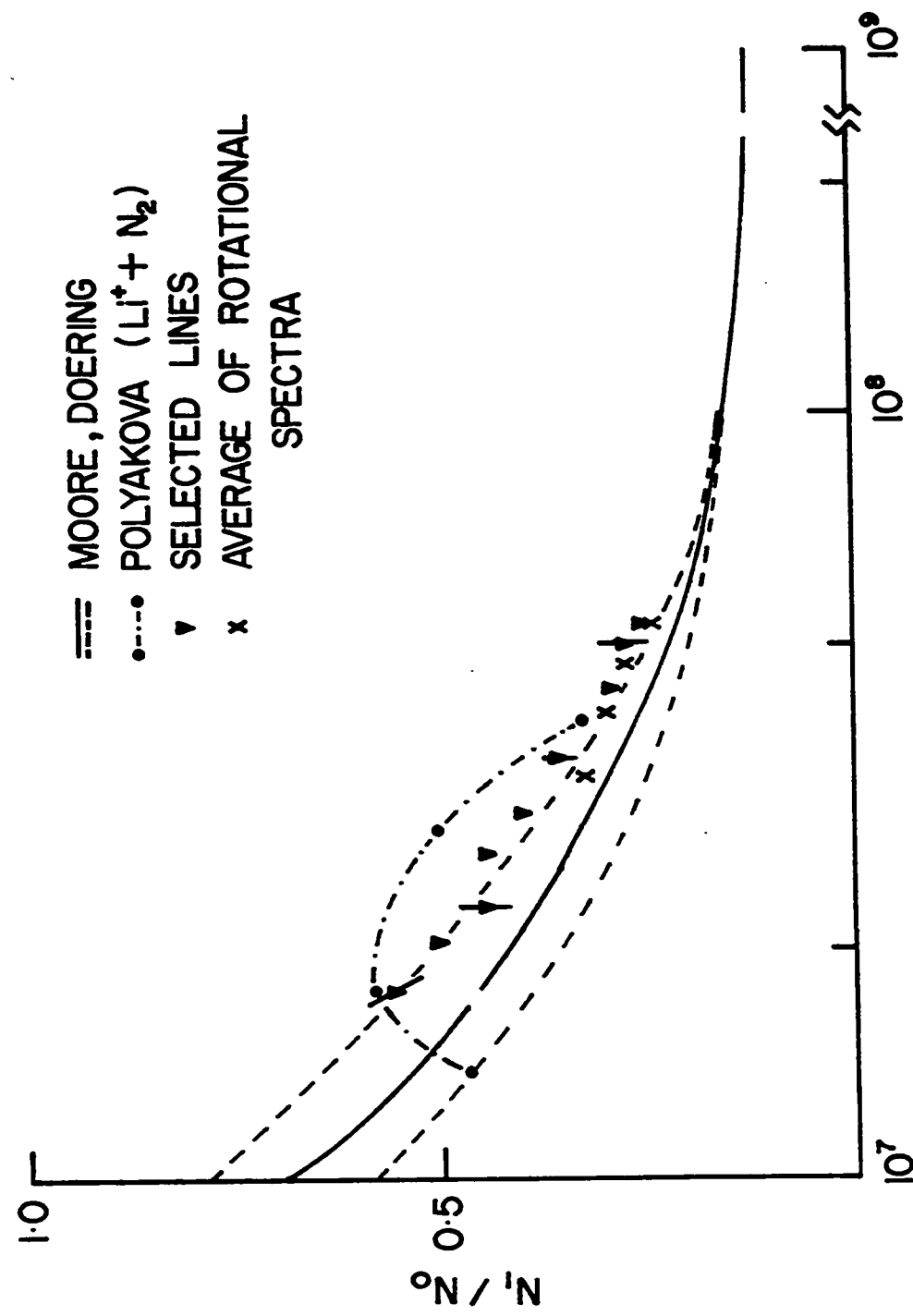

Figure 5.28. Vibrational excitation of $N_2^+B(v'= 1)$ state by Li^+ ions.

5.4 Discussion of Rotational Distributions

In the excitation of N_2^+ by fast Li^+ ions, the upper levels of the B state are rotationally excited to a greater degree than given by a Boltzmann fit to the lower levels. This non-equilibrium in the rotational distribution may be due to a second process which either redistributes the energy prior to the molecule emitting or which produces a Boltzmann distribution at a higher rotational temperature.

A least squares fit of the 8.0 keV $Li^+ + N_2$ data (figure 5.29) to the sum of two Boltzmann distributions suggests that the observed rotational distribution may be due to the sum of two distributions at rotational temperatures of 900°K and 4900°K. The 900°K temperature is slightly lower than that obtained by Lowe and Ferguson (1971) at the same energy; the difference being due to the contribution of the second distribution. The excitation of nitrogen by beam impurities, or by neutrals as possible origins of the 4900°K Boltzmann distribution are discussed in the following section.

5.4.1 Excitation by Beam Impurities

In the survey spectrum of N_2^+ excited in Li^+ collisions, impurities such as sodium which were present due to a lack of momentum analysis, were identified. In section 5.2 Na^+ ions were found to produce a higher degree

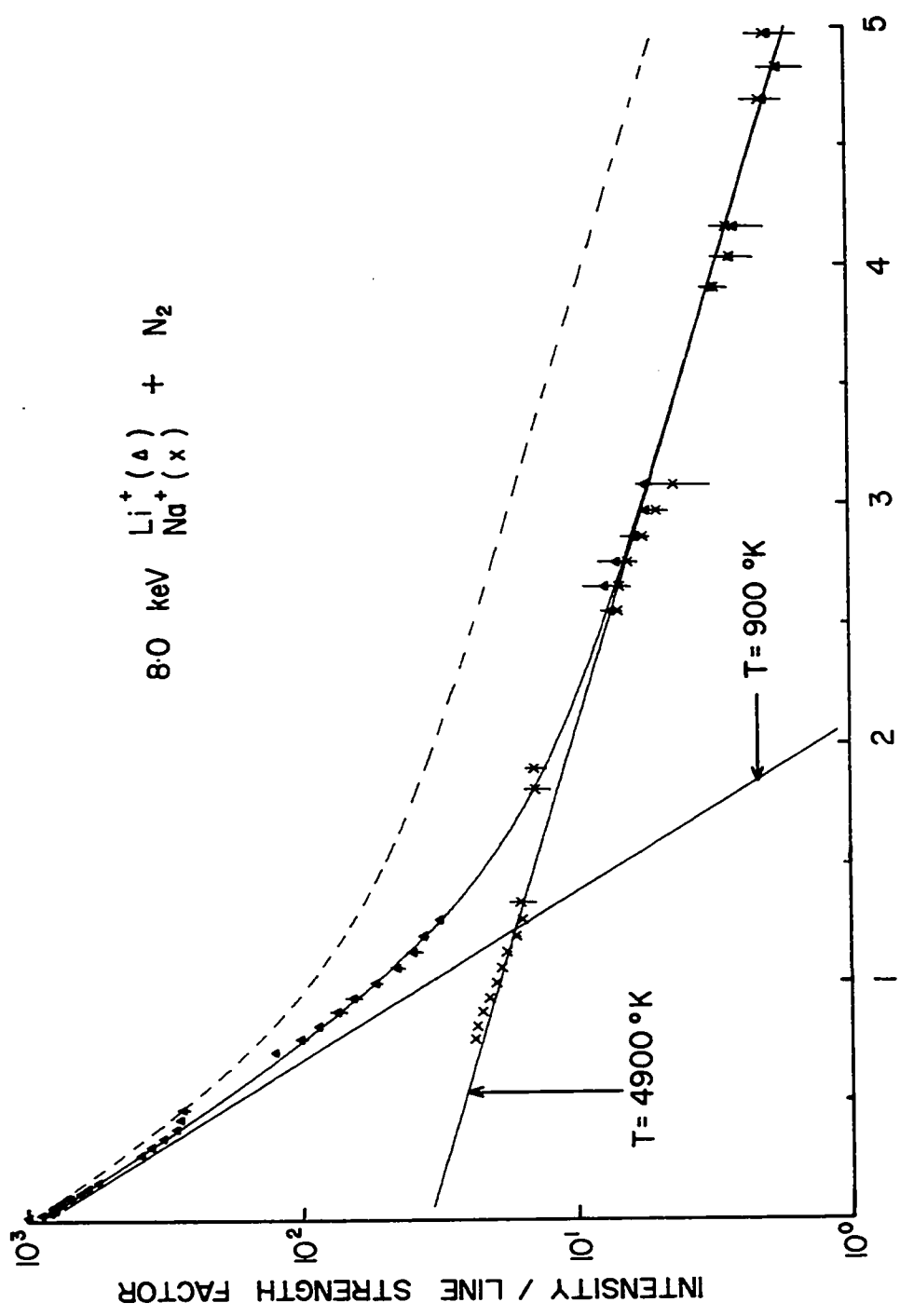

Figure 5.29. Rotational distribution excited by 8 keV Li^+ ions fitted to the sum of two Boltzmann distributions. (---) distribution expected if atomic excitation is significant.

of rotational excitation than Li^+ ions at the same energy. In figure 5.29, the distribution obtained from 8.0 keV Na^+ excitation has been plotted with considerable agreement between it and the 4900°K Boltzmann distribution to which it was normalized. Using the excitation cross-section of the NaD and Li I 6707 lines, the intensity ratio of the two lines during Li^+ excitation indicates that less than 1% of the beam consists of Na^+ ions. Assuming the 900°K Boltzmann distribution is due to Li^+ excitation while the second distribution is due to Na^+ excitation, and using the emission cross-sections of $N_2^+(0,0)$ during Li^+ and Na^+ excitation, a 25% Na^+ content in the beam would be necessary in order to produce the contribution of the 4900°K distribution to the observed intensities. Therefore despite the agreement in the 4900°K distribution with the rotational excitation of N_2^+ by 8.0 keV Na^+ ions, the small fraction of Na^+ ions in the beam is insufficient to account for the non-Boltzmann nature of the distribution.

5.4.2 Excitation by Beam Neutrals

At the same velocity, noble gas atoms produce greater rotational excitation in N_2^+ than the equivalent ions (Polyakova et al (1969)). Since the cross-section for gas ionization by atoms (Kikiani et al (1966))

$$Li + N_2 \rightarrow Li + N_2^+ + e^-$$

is greater than the charge-exchange cross-section (Ogurtsov

et al (1966))

$$Li^+ + N_2 \rightarrow Li + N_2^+$$

the possibility of atoms producing the high temperature distribution was investigated. If the same fraction of N_2^+ molecules were left in the B state (v'= 0) in both cases, the ratio of the above total cross-sections indicates that a neutral content of 5% could produce the observed high temperature distribution.

Since the experimental equipment did not permit the use of a neutralizing cell and deflector plates to produce a neutral beam, two alternate techniques were used to alter the atomic content of the beam so as to observe any changes in the rotational distribution. In the first experiment, a second gas (Ar) was mixed with the nitrogen. The fraction of ions at a distance l into the chamber is

$$I^+(l) = I^+(0)\left\{a + (1-a)\exp\left(-\sum_j [N]^j (\sigma_{10} + \sigma_{01})^j l\right)\right\} \qquad (5.4)$$

where

$$a = \frac{\sum_j [N]^j \sigma_{01}^j}{\sum_j [N]^j (\sigma_{10} + \sigma_{01})^j}$$

and the superscript j refers to the particular gases used. If only one gas were in the system, equation (5.4) is equivalent to equation (2.7). The Ar gas was added in such quantities that the neutral content of the beam would be

doubled, according to equation (5.4). In the second experiment, the pressure along the beam path in the region before it enters the collision chamber was changed sufficiently by widening the chamber slits and closing the diffusion pump to the centre chamber to change the neutral content at the bottom of the collision chamber by a factor of three. The distribution expected to be observed under these new conditions is indicated by the dashed curve in figure 5.29.

Since the nitrogen pressure in the upper chamber was kept constant for both experiments and no changes were observed in the spectra, it is assumed that the non-Boltzmann nature of the rotational distributions is not due to the excitation of nitrogen by atoms.

5.4.3 Redistribution of Rotational Energy

Rotational redistribution after the primary collision but prior to emission could be important if the recoiling molecule underwent a sufficient number of collisions to convert some of the translational energy to rotational energy. Because of the small amount of energy required to excite rotation, the adiabatic criterion predicts that rotational energy is readily exchanged with translational energy at gas kinetic velocities. From a classical treatment of charge transfer collisions, Fan (1956) has shown that the minimum recoil energy is given by

$$E = \frac{M_1}{M} \left| \Delta E + \frac{1}{2} m_e u^2 \right| \qquad (5.5)$$

where M_1 is the mass of the incident ion, M the total mass of the colliding particles, ΔE the energy defect of the process, m_e the mass of the electron transfered and u the relative velocity of the colliding particles. For Li^+ ions on N_2 the recoiling N_2^+ molecule could have a few eV of translational energy which if converted to rotational energy of the molecule might explain the rotational excitation. However it is also necessary to consider if the time between collisions is short enough compared to the radiative half life of the state to make rotational relaxation prior to emission important. The radiative half life of the $N_2^+ B^2\Sigma_u^+$ state is $61.3 \pm 1.6 \times 10^{-9}$ seconds (Gray et al (1971)) while the time between collisions at 300°K and a pressure of 20 millitorr is 7×10^{-6} seconds so that the probability of a gas kinetic collision during a radiative half life is only 10^{-2}. For 10 keV incident Li^+ ions, a minimum recoil energy of 4 eV would increase the probability to 10^{-1}.

From chemiluminescence experiments, an average of 1-10 collisions at gas kinetic energies have been found sufficient to bring about rotational to translational energy transfer in N_2 (Polanyi and Woodall (1972)). The model used to explain the relaxation incorporated

unrestricted ΔJ changes and ascribed a much lower probability of rotational deactivation to the higher J levels. Previously, fluorescence experiments in NO (Broida and Carrington (1963)) had indicated ΔJ changes up to ± 5. The above model suggests that a nonthermal rotational distribution peaked initially at high J would relax to a thermal distribution without generating a peak at intermediate J. Relaxation of the rotational distribution of HCl was adequately described by the above model at each pressure for which the rotational population were observed.

To ascertain if rotational redistribution was occurring, spectra of N_2^+ excited in 8.0 keV Li^+ collisions were observed at pressures of 2 to 30 millitorr. No change in the shape of the distribution was observed indicating the lack of redistribution prior to emission.

5.4 Rotational Excitation in Charge Transfer and Ionization Collisions

From previous arguments, the observed rotational excitation is predominantly a result of primary collisions. Two distinct primary processes may be occurring which lead to rotational excitation: charge transfer and ionization. Coincidence experiments for protons on N_2 at 30 keV (Wehrenberg and Clark (1971)) have indicated that the $N_2^+B(v'= 0)$ state is produced twice as often by charge exchange as by ionization collisions. According to the

classical model of conservation of angular momentum (Lowe (1966), Liu (1971)), ionization interactions should produce significantly greater rotational excitation of the molecule due to the larger energy defect (ΔE= 18.75 eV) than in charge exchanging interactions (ΔE= 5.15 eV) provided the impact parameters are similar. For 30 keV protons, the model suggests mean angular momentum changes of $\hbar$ for charge exchange while ionization would produce changes of $3\hbar$ for the same mean impact parameter ($2A^{o}$). Using the relative cross-sections for $N_2^{+}B$ state excitation by the two primary processes, the classical model suggests a distribution resembling the thermal distribution due to charge exchanging collisions with the upper levels being populated to a greater extent due to the contribution of ionization collisions. Such a result has been observed for 30 keV protons (Polyakova et al (1966)) with the distribution deviating from thermal for K' greater than 15.

As noted previously (figure 5.29), the observed rotational distribution produced in 8.0 keV Li^{+} excitation of nitrogen can be characterized by the sum of two Boltzmann distributions with widely differing rotational development. A similar result (figure 5.30) is obtained for the 1.5 keV Li^{+} excitation of N_2 with measurement of the rotational structure extended to K'= 100. For the 8.0 keV Li^{+} data, integration over the two distributions suggests that if the Boltzmann distribution at high

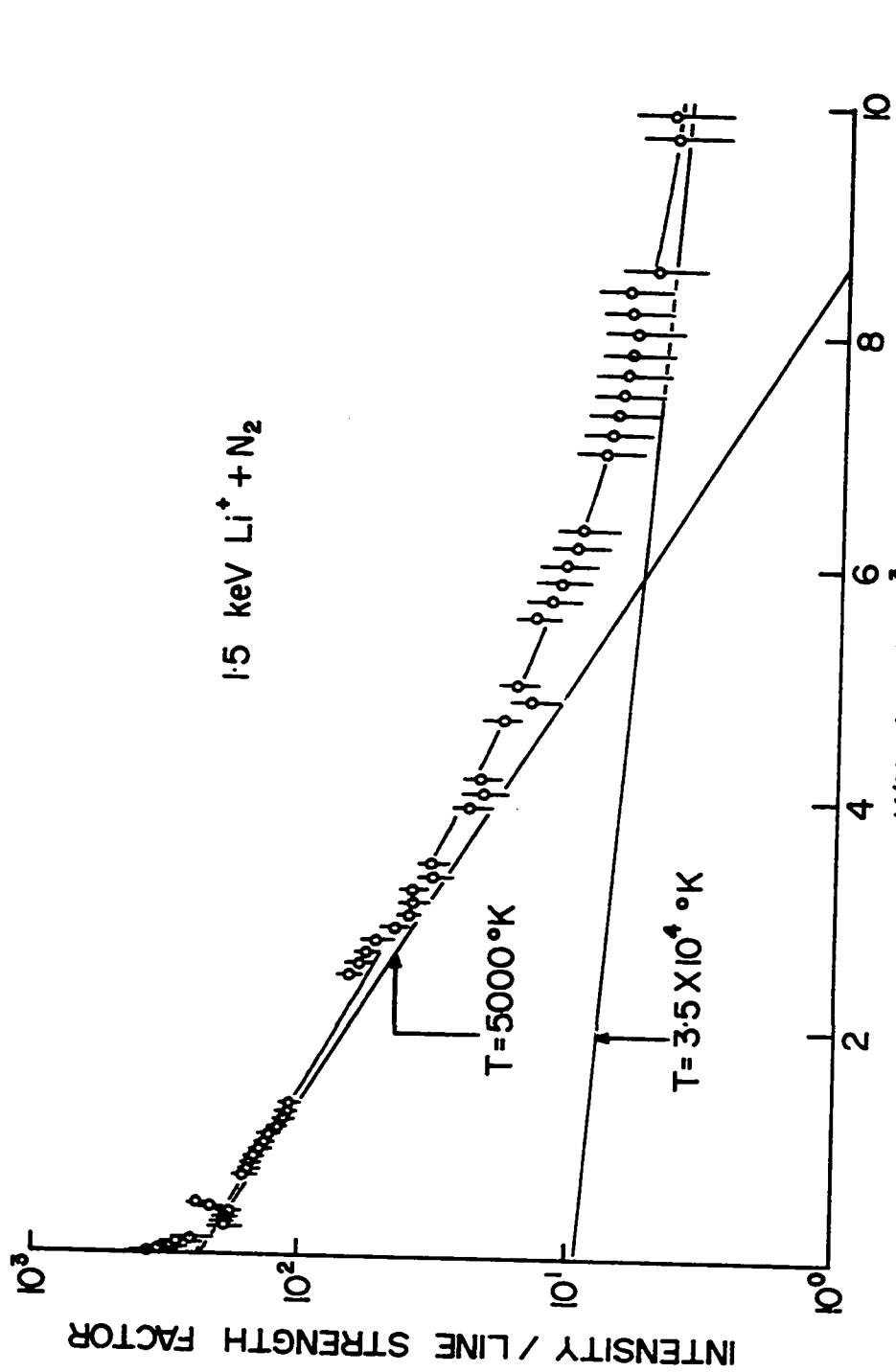

Figure 5.30. Rotational distribution excited by 1.5 keV Li^+ ions fitted to the sum of two Boltzmann distributions.

temperature is due to an ionization process, then

$$\frac{\sigma_c (N_2^+ B(v'=0))}{\sigma_i (N_2^+ B(v'=0))} = 3.5 \qquad (5.6)$$

At 1.5 keV a similar integration suggests that ionization processes would be relatively more important with the ratio being 2.5. A similar result (Wehrenberg and Clark (1971)) for the coincidence experiments involving protons indicated that ionization processes became relatively more important at energies less than 30 keV.

5.5 Rotational Development of N_2^+ State During Li^+ and Na^+ Excitation

Comparison of the rotational development of the N_2^+B state due to Li^+ and Na^+ excitation at decreasing energies can be made using figures 5.15 and 5.22 which for convenience have been reproduced in figure 5.31 Comparison of the two contour plots indicates that the velocity rather than the energy of the incident ion is the dominant variable characterizing the distributions produced in alkali ion excitation. However, the rotational distributions and their development with velocity are also ion dependent. At velocities greater than 2.2×10^5 m/s ($1/v^2 = 20 \times 10^{-12}$ (s/m)^2) development of the lower rotational levels is similar in both Li^+ and Na^+ ion excitation. In the same velocity range, the maxima of the distributions due to Na^+ excitation consistently occur at higher levels

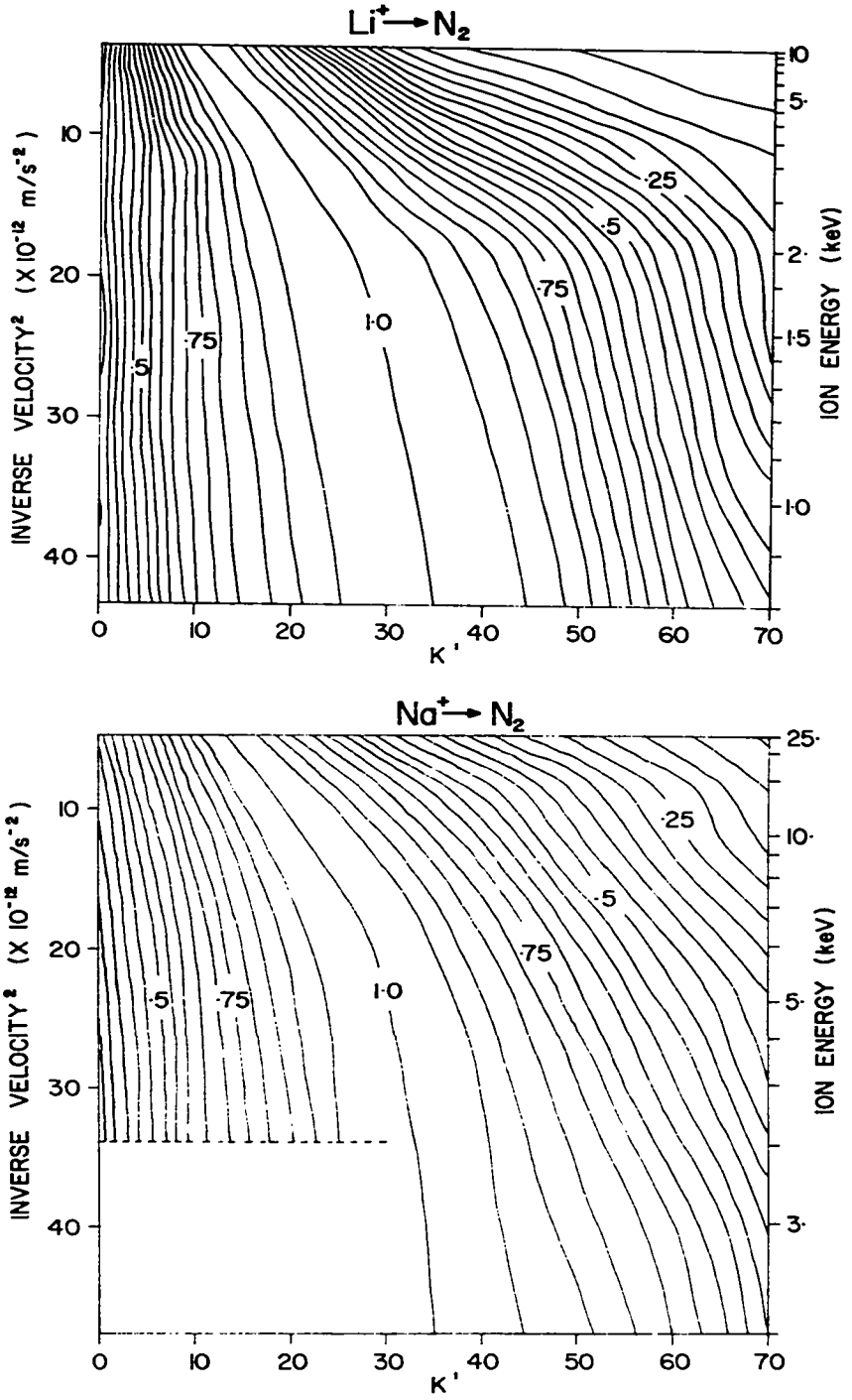

Figure 5.31. Development of rotational populations of $N_2^+B(v'=0)$ state during Li^+ and Na^+ excitation. Disbributions are plotted as a function of inverse velocity.

than for Li^+ excitation. However excitation of the upper levels is significantly greater during Na^+ collisions although at velocities of 2.2×10^5m/s the distributions are comparable due to the faster rate of populating the upper levels during Li^+ collisions. At lower velocities, this rate at which the upper states are populated in Li^+ collisions changes abruptly while for Na^+ excitation the trend of the relative populations towards higher rotational levels slowly decreases.

Information on the general nature of the collisions can be obtained from comparison of the average angular momentum of the N_2^+B state during Li^+ and Na^+ excitation. Comparison with the average momentum transfer predicted by the classical model (Lowe (1966), Liu (1971) cannot be made directly. According to the classical model, for each impact parameter a particular change in angular momentum may occur

$$\Delta L = \frac{b\Delta E}{v} \tag{5.7}$$

so that the angular momentum in the final state K' is given by

$$\overline{K'} = \overline{K''} + \overline{\Delta L} \tag{5.8}$$

However, neither the probability for angular momentum changes associated with each impact parameter nor the effect of the initial state on the probability of an

increase in the angular momentum are known. Attempts to synthesize observed distributions have led Moore and Doering (1969) to suggest that the transition probability is a function of both variables. The lower set of curves in figure 5.32 indicates the average angular momentum of the upper state using the first 70 levels of the observed distributions such that

$$\langle K' \rangle = \frac{\sum_{K'} K' N_{K'}}{\sum_{K'} N_{K'}} \qquad (5.9)$$

However, the contours of relative population (figure 5.31) indicate that at low energies the rotational levels with K'>70 are significantly populated which would cause the above average to be low. The upper set of curves indicate the average angular momentum calculated when the observed rotational distributions are characterized by the sum of two Boltzmann distributions. At high velocities the rotational excitation of the N_2^+B state by Na^+ ions is substantially greater than for Li^+ excitation due to the significant populations in the upper levels. Both increase nonlinearly until at velocities of 2×10^5m/s, the rotational excitation by both ions is comparable. At still lower velocities, the average angular momentum of the upper state continues to increase but at a much slower rate than for the higher velocities. At velocities greater that 10^6m/s, rotational excitation has been found to be non-existent (Moore and Doering (1969)) suggesting that a

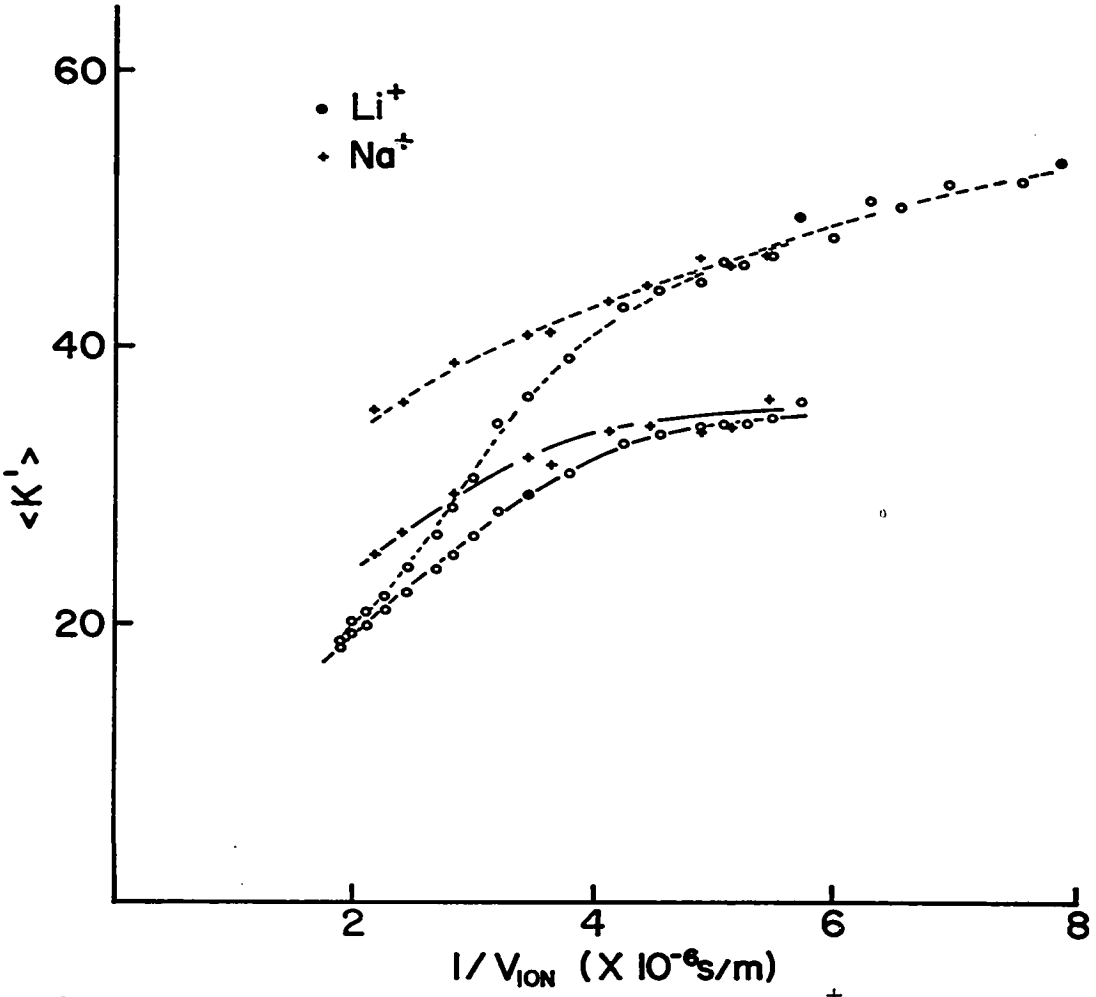

Figure 5.32. Average angular momentum of $N_2^+B(v'= 0)$ state for Li^+ and Na^+ excitation. (——) determined from first 70 rotational levels of state. (---) determined from fit of distribution to the sum of two Boltzmann distributions.

sharp break in the rotational excitation by Na^+ ions similar to that observed for Li^+ excitation will occur at energies greater than 25 keV.

A significantly different result is observed when the relative populations are plotted as a function of velocity (figure 5.33). For Na^+ excitation the contours of relative population increase smoothly towards higher rotational levels as the velocity of the incident ion decreases. For Li^+, the same general trend is observed. The sharp change in the contours previously observed at 2 keV (figure 5.31) now appears as a shift of the populations towards higher rotational levels in the energy range around 2 keV. Results from charge changing interactions of Kr^+ ions on N_2 (Kassal and Fishburne (1971)) indicate that little rotational excitation of the $N_2^+B(v'= 0)$ state occurs during thermal energy collisions suggesting that the relative population contours will peak as the velocity of the ion decreases.

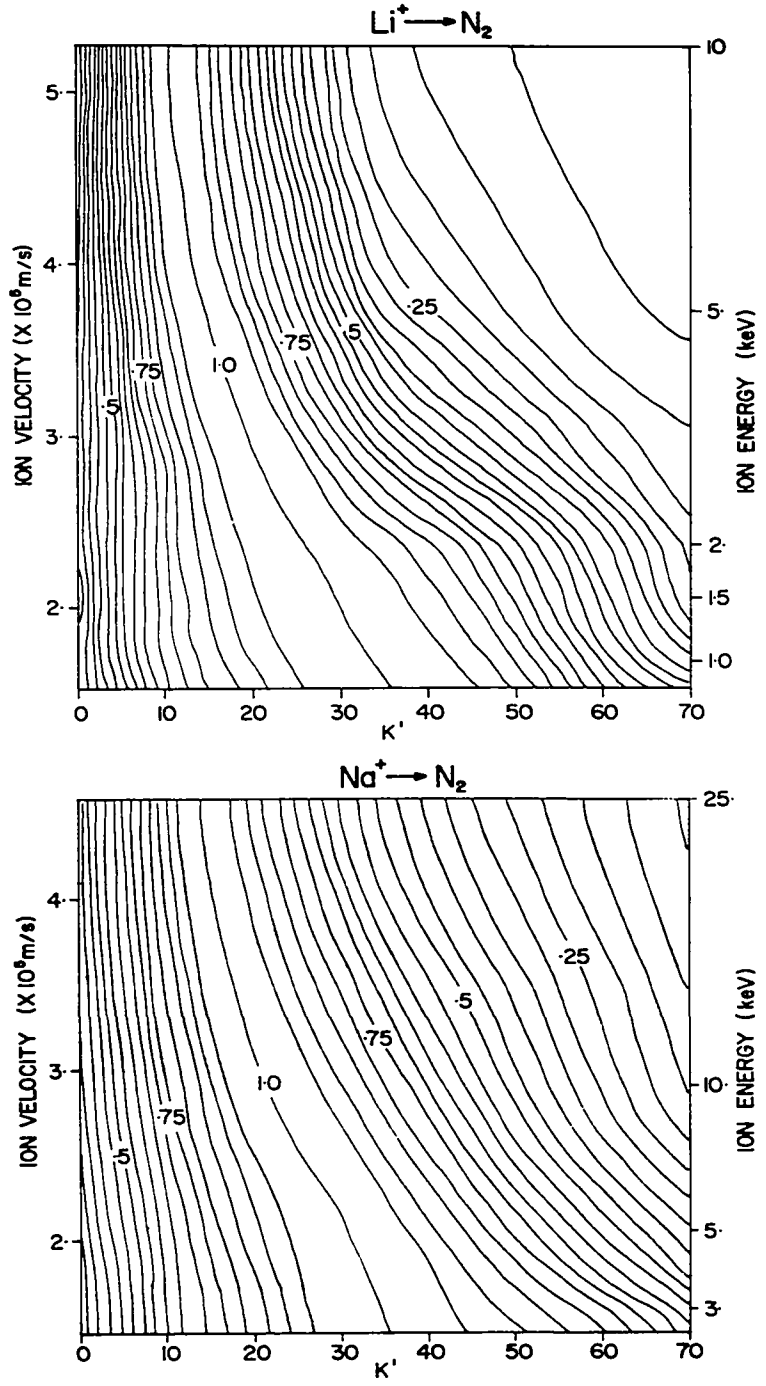

Figure 5.33. Comparison of rotational development of $N_2^+B(v'= 0)$ state for Na^+ and Li^+ excitation. Data plotted as a function of velocity.

CHAPTER VI

CONCLUSIONS

6.1 Review of Results

Better efficiency of the recording equipment has permitted measurements to be made at much lower light levels than previously observed. With this increased sensitivity, rotational spectra of the (0,0) band of the First Negative system of N_2^+ were observed at energies as low as 600 eV and the range of rotational lines observed was extended to K"= 100. High resolution spectra were taken with the R and P branch lines being resolved and with the rotational structure of the N_2^+(1,1) band being observed. Further, experiments were performed at pressures typically less than 5 millitorr where the effects of secondary collisions were greatly reduced.

Survey spectra for the excitation of nitrogen by alkali ion bombardment have indicated that one of the main processes occurring is dissociation of the molecule. Other processes are charge exchange and direct excitation of the alkalis with the former apparently dominant for the lighter alkalis since the main emissions are from the excited atom. However, for potassium the majority of the spectral features arise from simple excitation of the ion. The molecular features observed are the First Negative

bands of the N_2^+ molecule. The less intense Second Positive bands of N_2 indicate that secondary processes are not an important excitation mechanism.

Relative emission cross-sections corrected for instrumental sensitivity were normalized to measurements of the electron excitation of N_2^+ (Borst and Zipf (1970)). The largest cross-sections for excitation of N_2 by the alkalis were those for the resonance lines indicating that approximately one quarter of the charge transfer collisions left the atom in its lowest excited state. In the energy range of 1 to 10 keV, only the alkali lines tended towards maxima. Structure in the total cross-sections of the ^2P-^2D Li I transitions suggested interference effects between nearly degenerate energy levels of the system (Tolk et al (1971)). The shape of the $N_2^+(0,0)$ cross-sections closely resemble the total charge exchanging cross-sections (Ogurtsov et al (1966)) suggesting the importance of charge exchange in exciting the N_2^+B state. Absolute cross-sections indicate that close to 10% of the charge exchanging collisions leave the N_2^+ in the $B(v'= 0)$ state. The relatively large cross-sections for dissociative excitation products imply that dissociation of the molecule is frequent despite the large energy defect involved. The adiabatic criterion suggests that the different shapes of the N I and N II cross-section data are due to the former being produced through direct dissociation collisions

rather than charge transfer collisions with dissociation as in the latter case. Cross-sections for the dissociation products followed the adiabatic exponential form with mean interaction distances much less than 7A°.

Observations of rotational excitation of the N_2^+ molecule by Li^+ and Na^+ collisions have conclusively shown that the rotational distributions cannot be adequately described by a Boltzmann distribution as previously reported. As the energy of the incident ion decreases, the break from a Boltzmann distribution occurs at higher K' values while the rotational excitation of the molecule increases. Qualifying experiments have ruled out the non-Boltzmann nature being due to excitation by neutrals or impurities in the beam. Rotational relaxation and polarization effects have also been eliminated as possible sources. On the other hand, excitation by ionization as well as charge exchange have been suggested as possible processes producing the observed rotational distributions. Distributions have been found to be ion dependent with Na^+ ions producing greater rotational excitation of the N_2^+ molecule than Li^+ ions at the same velocity.

Vibrational excitation of the N_2^+ molecule by Li^+ ions was found to be significant in the energy range of 1-10 keV. As the energy decreased, the relative population of the first to zeroth vibrational level increased monotonically from 2.5 to 5 times the ratio

predicted by the Franck-Condon principle. At low energies the approach to a maximum observed by Polyakova et al (1968, 1969) was not apparent. The ratios were consistently greater than those obtained by Moore and Doering (1969) for other ions of similar velocity suggesting that vibrational excitation is also ion dependent.

Simultaneous vibrational and rotational excitation of the N_2^+ molecule were observed using the (1,1) band of the First Negative system. Rotational excitation was found to be unaffected by simultaneous vibrational excitation with the distributions in the first vibrational level being the same within experimental precision as the rotational development of the zeroth vibrational level.

6.2 Suggestions for Further Experiments

As is usually the case with an experimental programme, several avenues appear which may be expected to lead to further clarification of the work.

Experiments involving Li^+ ions have indicated that a maximum in the rotational excitation cross-section may occur at energies less than 600 eV. The present ion-collision apparatus suffers from a severe loss of beam current at projectile energies less than 1 keV possibly due to space-charge effects which make it impossible to extract an intense beam from the source and convey it to the collision chamber. Along with decreasing excitation

cross-sections of the $N_2^+B(v'= 0)$ state, usable spectra were thus limited to energies greater than 580 eV. However a multistage apparatus in which the ions from the source are conveyed through the apparatus at a high energy (10 keV) and then decelerated to the final energy as they enter the collision chamber could result in an increase of the beam current at low energies (Moore and Doering (1968)). Since a factor of 30 or greater in beam current available at the collision chamber now occurs between energies of 0.6 and 10 keV, an order of magnitude increase in beam current at the lower energy would not seem impossible. Measurements could then be made at lower energies than presently attainable.

Rotational excitation by ions at thermal energies could also be studied. Using a similar technique to Kassal and Fishburne (1971) rotational excitation of the $v'= 0,1$ levels of N_2^+ by metastables could be ascertained. With the present apparatus the rotational structure of the (0,0) and (1,1) bands can be fully resolved during low energy electron excitation. Enhancement of the observed intensities due to collisions of the second kind between N_2 and metastable inert gas atoms and ions would permit direct measurement of the rotational structure rather than measurements of the band envelope (Kassal et al (1971)).

To date, all experiments involving rotational

excitation have been concerned with the rotational distribution produced by various ions and atoms at various energies. These distributions have then been generally characterized as to velocity and energy defect dependence. However no attempt has been made to observe the final distribution as a function of initial rotational distribution or energy associated with the angular momentum change. Attempts (Moore and Doering (1969)) to synthesize observed spectra have suggested that the transition probability is a function of K" as well as ΔK. The effect of the initial rotational state on the transition probability could be determined by observing the final distribution at a particular ion energy as a function of the ambient gas temperature in the collision chamber. Results from two separate experiments (Moore and Doering (1968, 1969)) suggest that for 3 keV $H_2^+ + N_2$ collisions, the lower K' levels of the upper state are populated relatively more when the initial distribution is at a lower temperature. For larger momentum transfers (i.e. large K' in the upper state) the two distributions tend towards each other. However absolute changes in the final state cannot be calculated from the presented data. The effect of the upper state (i.e. rotational energy change involved in a given angular momentum change) could be examined by using two molecules with significantly different rotational constants. HCl at $650^{\circ}K$ has the same rotational development as N_2 at $130^{\circ}K$. For 2 keV

Li^+ excitation of N_2, ΔJ changes of 20 have been observed representing a 0.15 eV increase in the rotational energy of the molecule for a transition from the level of maximum population in the ground state. For HCl a similar change in angular momentum represents rotational energy changes of 0.53 eV. Experiments involving HCl initially in low temperature distributions could also be useful in determining the probability of ΔK changes. At gas kinetic temperatures of 130°K, the rotational distribution for HCl peaks near K"= 1 so that the final distribution would give directly the probability for a given ΔK change from the K"= 1 level. Once again by changing the temperature of the gas, the dependence of the final distribution on initial K" could be studied.

Rotational redistribution due to collisions prior to emission could be studied using molecules with sufficiently long lived excited states. A particularly good molecule for such a study is CO^+. The $^2\Sigma$ state (First Negative system) having a radiative lifetime of 39.5 x 10^{-9} seconds (Lawrence (1965)) has a low probability (5 x 10^{-3} at 20 millitorr) for collision prior to radiating. The observed distribution would therefore be due to the primary collision. However, the $^2\Pi_i$ state (Comet-Tail System) of CO^+ having a radiative lifetime of 2.6 x 10^{-6} seconds (Bennett and Dalby (1960)) has a probability of .3 of undergoing a collision prior to emission under the

same conditions. By changing the pressure in the collision chamber and therefore the number of secondary collisions prior to emission, rotational relaxation of the molecule could be studied.

Previous results have suggested that the non-Boltzmann nature of the observed rotational distributions may be due to the effects of two primary processes: charge transfer and ionization. Protons on N_2 results (Wehrenberg and Clark (1971)) have shown that both processes are significant in producing $N_2^+(0,0)$ radiation. Ionizing collisions by atoms have been found to produce significantly higher rotational excitation than the ions at the same velocity (Polyakova et al (1969)). The importance of charge transfer collisions in the rotational excitation of N_2^+ by alkali ions could be studied using photon-photon coincidence techniques. From the measured cross-sections (Chapter IV) of the alkali lines, one quarter of the charge exchanging collisions leave the Li atom in its lowest excited state from which the 6707A° emission is observed. Using this emission as an indication of a charge transfer event, photon-photon coincidence with the $N_2^+(3914A^\circ)$ emission could be used to ascertain the relative importance of charge transfer collisions producing rotational excitation. Comparison of the coincidence measurements to the total emission for various sections of the band would indicate if the non-Boltzmann

nature of the distribution was due to ionization. A more direct technique for obtaining the same results would be photon-particle coincidence measurements where the ionization and charge-changing contributions could be determined directly without necessitating a recalibration using the Li I 6707 excitation cross-section.

APPENDIX I

TECHNIQUE FOR DETERMINING ROTATIONAL DISTRIBUTIONS

In Chapter V, a modified version of the technique of Wink et al (1971) was used to determine the distributions from analysis of the rotational line intensities. Wink et al assumed that R(K") and P(K" + 27) coincided exactly in wavelength and ignored the doublet splitting. The modification discussed below corrects for these assumptions. In addition, the observed intensities had to be corrected for (1,1) band overlapping and the transmission function of the monochromator. This Appendix describes the method used to treat the data.

I.1 Effect of Transmission Function of the Monochromator

The transmission function of the monochromator was assumed to be triangular so that two lines of intensity A and B separated in wavelength by $\Delta\lambda$ would produce a peak intensity of

$$C = A + (1 - \frac{\Delta\lambda}{h})B \qquad (I.1)$$

if A>B and $\Delta\lambda$<h, the half width of the transmission function. In the $N_2^+(0,0)$ band, P(K" + 27) closely overlaps R(K") (Childs (1932)) so that if the intensity of R(K")>P(K" + 27), then the resultant peak intensity would be given by

$$I = \tfrac{1}{2} R(K'')\left(2 - \frac{\Delta\lambda'(K'')}{h}\right) + \tfrac{1}{2} P(K''+27)\left(2 - \frac{2\Delta\lambda + \Delta\lambda''(K''+27)}{h}\right) \quad (I.2)$$

and when $P(K'' + 27) > R(K'')$

$$I = \tfrac{1}{2} P(K''+27)\left(2 - \frac{\Delta\lambda''(K''+27)}{h}\right) + \tfrac{1}{2} R(K'')\left(2 - \frac{2\Delta\lambda + \Delta\lambda'(K'')}{h}\right) . \quad (I.3)$$

$\Delta\lambda'(K'')$ and $\Delta\lambda''(K'' + 27)$ are the wavelength separations of the spin doublets in the R- and P- branch lines while $\Delta\lambda$ is the least separation of the R(K") and P(K" + 27) lines.

I.2 Modifications to Wink's Method

Using Wink's method for determining the rotational distributions, a series of three consecutive line intensities must be observed in order to determine the intensity contributions of the R- and P- branch lines to the central line of the triplet. If the observed lines are such that the centre line of the triplet is an even K" valued line then the rotational lines of the band will consist of the following combination

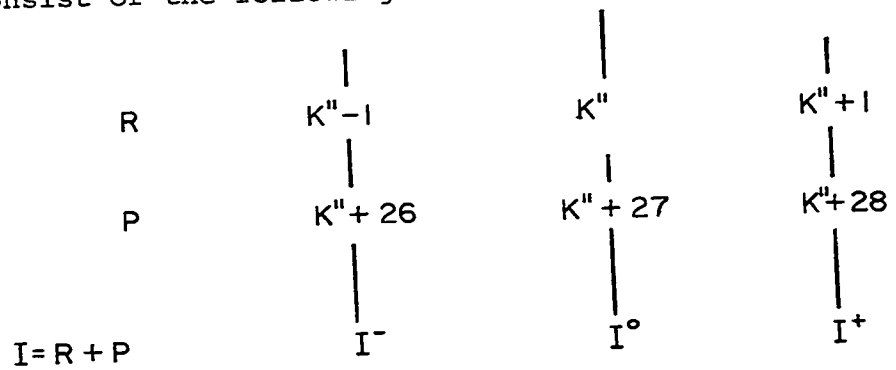

where a strong R- branch line is overlapped by a weak P- branch line.

Taking account of the doublet and R- and P- branch separations, the observed intensities would be given by

$$I^- = k_R^- R(K'' - 1) + k_P^- P(K'' + 26) \quad (I.4)$$

$$I^o = k_R^o R(K'') + k_P^o P(K'' + 27) \quad (I.5)$$

$$I^+ = k_R^+ R(K'' + 1) + k_P^+ P(K'' + 28) \quad (I.6)$$

where the k_R and k_P values are the correction factors determined from equation I.2 or I.3. Using the same approximation as Wink et al (1971), the R and P lines in the triplets can be related by

$$R(K'') = R(K'' - 1) + R(K'' + 1) \quad (I.7)$$

$$\text{and } 4P(K'' + 27) = P(K'' + 26) + P(K'' + 28) \quad (I.8)$$

For Boltzmann distributions at 300°K, the above approximations are valid within 2% with the error decreasing to less than 1% at rotational temperatures greater than 1000°K. Solutions of equations I.4 - I.6 using equations I.7 and I.8 give

$$R(K'') = \left\{ \frac{I^-}{k_P^-} + \frac{I^+}{k_P^+} - \frac{4I^o}{k_P^o} \right\} \Big/ \left\{ \frac{k_R^+}{2k_P^+} + \frac{k_R^-}{2k_P^-} - \frac{4k_R^o}{k_P^o} \right\}$$

if

$$\delta_1 \left\{ \frac{k_R^-}{k_P^-} - \frac{k_R^+}{k_P^+} \right\} << \left\{ \frac{I^-}{k_P^-} + \frac{I^+}{k_P^+} - \frac{4I^o}{k_P^o} \right\} \quad (I.9)$$

where

$$R(K''-1) = \tfrac{1}{2} R(K'') + \delta_1$$

and (I.10)

$$P(K''+27)=\left\{\frac{I^{+}}{k_R^{+}}+\frac{I^{-}}{k_R^{-}}-\frac{I^{\circ}}{k_R^{\circ}}\right\}/\left\{\frac{2k_P^{+}}{k_R^{+}}+\frac{2k_P^{-}}{k_R^{-}}-\frac{k_P^{\circ}}{k_R^{\circ}}\right\}$$

if

$$\delta_2\left\{\frac{k_P^{-}}{k_R^{-}}-\frac{k_P^{+}}{k_R^{+}}\right\} \ll \left\{\frac{I^{+}}{k_R^{+}}+\frac{I^{-}}{k_R^{-}}-\frac{I^{\circ}}{k_R^{\circ}}\right\}$$

where

$$P(K''+26)=2P(K''+27)+\delta_2$$

Due to the slow change in wavelength separation over a triplet compared to the spectral slit width

$$\frac{k_P^{-}}{k_R^{-}} \simeq \frac{k_P^{+}}{k_R^{+}}$$

while the change in intensity δ is much less than the intensities of the lines involved. For Boltzmann distributions at temperatures greater than 500°K, omission of the δ term involves errors of less than 1% in the calculated R- and P- branch line intensities. A similar argument can be used for K" odd.

A first order calculation, using the method of Wink et al, was made to ascertain if R(K") was greater than or less than P(K" + 27) in order to obtain the proper equation for the correction factors (k_P and k_R). Having determined R(K") and P(K" + 27) using equations I.9 and I.10, a check was made to determine if the same relation resulted as previously obtained. If not, the correction factors were recalculated and R(K") and P(K" + 27)

redetermined.

Having obtained the intensities of the R- and P- branch lines in the (0,0) band, corrections for overlapping by the (1,1) band of N_2^+ were made to those lines with K" greater than 22. Using the results of the vibrational excitation of the v'= 1 state, the wavelengths of the rotational lines (Fassbender (1924)) and assuming the rotational development of the v'= 1 state was similar to the v'= 0 level, the contributions to the observed line intensities of the (0,0) band by (1,1) band overlap were subtracted taking account of the line separations and the transmission function of the monochromator. These corrected intensities were then used to redetermine the R- and P- branch line intensities using the technique given above.

REFERENCES

Bennett, R.G. and Dalby, E.W. (1960). In The Band Spectrum of Carbon Monoxide. ed. P.H. Krupenie. National Bureau of Standards, 5.

Borst, W.L. and Zipf, E.C. (1970). Phys. Rev. A 1, 834.

Broida, H.P. and Carrington, T. (1962). J. Chem. Phys. 38, 136.

Carleton, N.P. (1957). Phys. Rev. 107, 110.

Childs, W.H.J. (1932). Proc. Roy. Soc. 137, 641.

Culp, G. and Stair, Jr., A.T. (1967). J. Chim. Phys. 64, 57.

de Heer, F.J. (1966). In Advances in Atomic and Molecular Physics Vol. 2. ed. D.R. Bates. Academic Press, London.

de Heer, F.J., Shutten, J. and Moustafa, H. (1966). Physica 32, 1766.

de Heer, F.J. and Aarts, J.F.M. (1970). Physica 48, 620.

Dufay, M., Desesquelles, J., Druetta, M. and Eidelsberg, M. (1966). Ann. Geophys. 22, 614.

Fan, Y.F. (1956). Phys. Rev. 103, 1740.

Fassbender, M. (1924). Z. Physik 30, 73.

Flaks, I.P., Kikiani, B.I. and Ogurtsov, G.N. (1966). Sov. Phys.-Tech. Phys. 10, 1590.

Fournier, P.C., Govers, T.R., van de Runstraat, C.A., Schopman, J. and Los, J. (1971). Seventh Intern. Conf. on the Phys. of Electronic and Atomic Collisions: Abstracts of Papers pg. 433, Amsterdam. North-Holland Publ. Co., Amsterdam.

Gray, D.D., Roberts, T.D. and Morack, J.L. (1971). Phys. Lett. A (Neth) 37, 25.

Handbook of Chemistry and Physics (1961). 40th edition. Chemical Rubber Publishing Company, Cleveland.

Hasted, J.B. (1962). In Atomic and Molecular Processes. D.R. Bates ed. Academic Press, New York.

Hasted, J.B. and Lee, A.R. (1962). Proc. Phys. Soc. 79, 702.

Hasted, J.B. (1964). Physics of Atomic Collisions. Butterworth, London.

Haugh, M.J. and Bayes, K.D. (1970). Phys. Rev. A 2, 1778.

Kassal, T.T. and Fishburne, E.S. (1970). J. Chem. Phys. 54, 1363.

Kikiani, B.I., Ogurtsov, G.N., Fedorenko, N.V. and Flaks, I.P. (1966). Sov. Phys.-JETP 22, 264.

Latimer, C.J., Browning, R. and Gilbody, H.B. (1971). Seventh Int. Conf. on the Phys. of Electronic and Atomic Collisions: Abstracts of Papers pg. 372, Amsterdam. North-Holland Publ. Co., Amsterdam.

Latypov, Z.Z. and Shaporenko, A.A. (1970). JETP Letters 12, 123.

Lawrence, G.M. (1965). In The Band Spectrum of Carbon Monoxide. ed. P.H. Krupenie. National Bureau of Standards, 5.

Liu, C. (1970). J. Chem. Phys. 53, 1295.

Lowe, R.P. and Ferguson, H.I.S. (1965). Proc. Phys. Soc. 85, 813.

Lowe, R.P. (1966). Ph.D. Thesis. University of Western Ontario.

Lowe, R.P. and Ferguson, H.I.S. (1971). Can. J. Phys. 49, 1680.

Massey, H.S.W. (1949). Rep. Prog. Phys. 12, 284.

Maurer, W. (1939). Phys. Zeits. 40, 161.

M.I.T. Wavelength Tables (1939). John Wiley and Sons, Inc. New York.

Moore, C.E. (1959). A Multiplet Table of Astrophysical Interest. National Bureau of Standards (US) Tech. Note 36.

Moore, Jr., J.H. and Doering, J.P. (1968). Phys. Rev. 174, 178.

Moore, Jr., J.H. and Doering, J.P. (1969). J. Chem. Phys. 50, 1487.

Moore, Jr., J.H. and Doering, J.P. (1969). Phys. Rev. 177, 218.

Moran, T.F., Petty, T. and Turner, G.S. (1971). Chem. Phys. Letters 9, 379.

Neff, S.H. (1963). Ph.D. Thesis. Harvard University.

Nicholls, R.W. (1962). J. Quant. Spectr. Rad. Trans. 2, 433.

Ogurtsov, G.N., Kikiani, B.I., and Flaks, I.P. (1966). Sov. Phys.-Tech. Phys. 11, 362.

Pearse, R.W.B. and Gaydon, A.G. (1963). The Indentification of Molecular Spectra. Third Edition. Chapman and Hall, Ltd., London.

Philpot, J.L. and Hughes, R.H. (1964). Phys. Rev. 133, A107.

Pierce, J.R. (1940). In Focusing of Charged Particles Vol II. (1967) pg. 31. ed. A. Septier. Academic Press, New York and London.

Pleiter, D. (1956). Ph.D. Thesis. University of Western Ontario.

Polanyi, J.C. and Woodall, K.B. (1972). J. Chem. Phys. 56, 1563.

Polyakova, G.N., Tatus', V.I., Strel'chenko, S., Fogel' Ya.M. and Fridman, V.M. (1966). Sov. Phys.-JETP 23, 973.

Polyakova, G.N., Tatus, V.I. and Fogel', Ya.M. (1967). Sov. Phys.-JETP 25, 430.

Polyakova, G.N., Fogel', Ya.M. and Zats, A.V. (1967). Sov. Phys.-JETP 25, 993.

Polyakova, G.N., Fogel', Ya.M., Erko, V.F., Zats, A.V. and Tolstolutskii, A.G. (1968). Sov. Phys.-JETP 27, 201.

Polyakova, G.N., Erko, V.F., Fogel', Ya.M., Zats, A.V. and Fizgeer, B.M. (1969). Sov. Phys.-JETP 29, 994.

Pop, S.S., Krivskii, I.Yu., Zapescachnyi, I.P. and Baletskaya, M.V. (1970). Sov. Phys.-JETP 31, 434.

Reeves, E.M. (1957). M.Sc. Thesis. University of Western Ontario.

Reeves, E.M. (1959). Ph.D. Thesis. University of Western Ontario.

Reeves, E.M. and Nicholls, R.W. (1961). Proc. Phys. Soc. 78, 588.

Sheridan, J.R. and Clark, K.C. (1965). Phys. Rev. 140, A1033.

Thomas, E.W., Bent, G.D. and Edwards, J.L. (1968). Phys. Rev. 165, 32.

Tolk, N.H., White, C.W., Dworetsky, S.H. and Simms, D.L. (1971). Seventh Int. Conference on the Phys. of Electronic and Atomic Collisions: Abstracts of Papers pg. 584, Amsterdam. North-Holland Publ. Co., Amsterdam.

Wehrenberg, P.J. and Clark, K.C. (1971). Seventh Int. Conf. on the Phys. of Electronic and Atomic Collisions: Abstracts of Papers pg. 387, Amsterdam. North-Holland Publ. Co., Amsterdam.

Wiese, W.L., Smith, M.W. and Glennon, B.M. (1966). Atomic Transition Probabilities Volume I. National Bureau of Standards, 4.

Wiese, W.L., Smith, M.W. and Miles, B.M. (1969). Atomic Transition Probabilities. Volume II. National Bureau of Standards (US), 22.

Wink, R.D. (1970). M.Sc. Thesis. University of Western Ontario.

Wink, R.D., Ferguson, H.I.S. and Lowe, R.P. (1971). J. Quant. Spect. Rad. Trans. 11, 1147.